RAS EXPRESSION IN NORMAL AND ABNORMAL BREAST TISSUE

by James Jensen Going

Department of Pathology, Edinburgh University
Medical School

Thesis submitted to the University of Edinburgh
for the degree of Doctor of Philosophy
in the Faculty of Medicine
1989

Abstract

Unfixed human breast tissue obtained prospectively from biopsy and mastectomy specimens was supravitally stained with methylene blue to select areas of altered parenchyma in which ras expression was studied by immunohistochemistry. The monoclonal antibody Y13-259 binds to an epitope common to all three p21 ras proteins. Y13-259 immunoreactivity did not survive formaldehyde fixation and paraffin embedding but fixatives periodate-lysine-paraformaldehyde (PLP) and its dichromate derivative (PLPD) preserved immunoreactivity and good morphology in paraffin sections. Rodent fibroblasts (CHL cells) and derived cells expressing abundant p21 ras (FHO5T1 cells) provided negative and positive controls for avidin-biotin-complex immunostaining. A semi-quantitative score was devised and validated to express and compare immunostaining results for 99 women with carcinoma and 72 women with benign changes.

Expression of p21 ras was the same in large ducts, small ducts and terminal duct lobular units (TDLU). Intensity and extent of epithelial immunostaining for p21 ras increased in the sequence normal - ductal hyperplasia without atypia - atypical hyperplasia - ductal carcinoma in situ. Lobular hyperplasias showed a similar increase. There was no difference in p21 ras expression between non-invasive and invasive carcinomas. In normal parenchymal epithelium, p21 ras score was the same in women with cancer and women with benign changes only, but decreased with age. 20 carcinomas with vascular invasion showed stronger p21 ras immunostaining of carcinoma cells surrounded by stroma than carcinoma cells within vascular lumina. This may reflect interaction between malignant and stromal cells. There were no differences between p21

ras scores of carcinomas with vascular invasion or lymph node metastasis and those without. Membrane staining of FHO5T1 cells in culture or growing as tumours in mice contrasted with cytoplasmic staining in optimally fixed and processed human material. Human carcinomas may therefore express abundant cytoplasmic p21 *ras*.

References

The reference list (chapter 10) is arranged and numbered in alphabetical order. All authors are given unless there are more than six, in which case the first three only are given in full, with '*et al*'. Citations in the main text use the reference number only.

Declaration

I am the author of this thesis and have performed the work descibed in it except as acknowledged. Some of the work described here has been presented [49,50] and published [48,51] previously. Full references appear in the reference list.

James Jensen Going 10th January 1989

Acknowledgements

I am indebted to my supervisors, Dr Thomas Anderson and Dr Andrew Wyllie, for support and advice. I am also grateful to Dr Alistair Williams and Dr Sharon Battersby for discussion, and Dr Alec McLean for statistical help. Dr Demetrios Spandidos provided FHO5T1 and hybridoma cells, as well as advice and encouragement. The help of Mr. Alan Smith, Mr. Derek Bishop, Mrs. Joyce Nicol, Mrs. Linda Ferrigan and Mr. Douglas Campbell has been indispensible for processing cells and tissues for light microscopy, and Mrs. Lorraine Allison for electron microscopy. Mr. David Elliot printed the photographs. Mr. Robert Morris has provided support in the field of cell culture. Dr. CM Steel and Ms Liz Foster provided the immune-deprived CBA mice in which FHO5T1 tumours were grown. Surgical and theatre staff in the Breast Unit at Longmore hospital have been unfailingly helpful. Dr RA Hawkins and Miss Anne Tesdale have kindly made available oestrogen receptor data. I am grateful to Professor Sir Alastair Currie and Professor Colin Bird who as successive Heads of Department have provided every encouragement as well as making available departmental facilities. This work would not have been possible without the support of the Medical Research Council, which awarded me a Training Fellowship and provided grants to Dr Anderson for video equipment and a dissecting microscope. The Melville Trust of Edinburgh University also provided financial assistance. The unstinting encouragement of my wife, Dr Sheila Going, has been inestimably valuable.

Contents

Abbreviations

ABC	Avidin-biotin complex
ADH	Atypical ductal hyperplasia
ALA	Atypical lobules, type A
ALB	Atypical lobules, type B
ALH	Atypical lobular hyperplasia
BSA	Bovine serum albumen
CHL	Chinese hamster lung cell line
DAB	Diaminobenzidine
DCIS	Ductal carcinoma *in situ*
DDW	Deionized distilled water
DNA	Deoxyribonucleic acid
EGF	Epidermal growth factor
EM	Electron microscopy
FH	Family history
FHO5T1	Cell line expressing mutated p21 *ras*
Ha-*ras*	Harvey *ras* gene
IGS	Immunogold-silver
Ki-*ras*	Kirsten *ras* gene
LCIS	Lobular carcinoma *in situ*
MTV	Mouse mammary tumour virus
MW	Molecular weight
NP	Nonproliferative
N-*ras*	Neuroblastoma *ras* gene
OCT	Embedding medium for cryotomy
OR	Oestrogen receptor
RNA	Ribonucleic acid
SPB	Sörensen's phosphate buffer
TDLU	Terminal duct lobular unit
TRIS	Tris(hydroxymethyl)aminomethane

Figures

4.10 PLPD fixed FHO5T1 tumour. Y13-259 50µg/ml, IGS detection.

5.1 Breast carcinoma, Y13-259 50µg/ml, ABC detection, PLPD fixation.

5.2 Same carcinoma and immunostaining, Carson's fixation.

5.3 PLPD-fixed lobular carcinoma in situ showing membrane staining. Y13-259 50µg/ml, ABC detection.

5.4 Comparison of repeated scoring of p21 ras immunostaining.

5.5 Comparison of scoring in PLP and PLPD fixed tissue.

5.6 Scores for p21 ras in normal epithelial and myoepithelial cells (large ducts, small ducts and TDLU.

5.7 Cumulative scores for p21 ras in large ducts, illustrating Kolmogorov-Smirnov statistic.

5.8 Cumulative scores for p21 ras. Same data as figure 5.6.

5.9 Scores for p21 ras in normal TDLU, hyperplastic and atypical epithelium, DCIS and invasive carcinoma.

5.10 Cumulative scores for p21 ras in normal TDLU, hyperplastic and atypical epithelium, DCIS and invasive carcinoma.

5.11 Graphs of separate extent and intensity immunostaining scores for normal TDLU, hyperplastic and atypical epithelium, DCIS and invasive carcinoma.

5.12 Breast carcinoma. Lack of Y13-259 immunoreactivity in areas of coagulative necrosis. PLPD fixation.

5.13 Breast carcinoma. Lack of Y13-259 immunoreactivity in apoptotic cells. PLPD fixation.

5.14 Cumulative scores for p21 ras in epithelium of normal TDLU for 83 women with cancer and 72 women with benign changes.

5.15 Cumulative scores for p21 ras in 20 carcinomas with vascular invasion comparing cells in vessels with those outside.

5.16 Cumulative scores for p21 ras in 29 carcinomas having vascular invasion compared with 56 lacking vascular invasion.

5.17 Cumulative scores for p21 ras in node-negative and node-positive carcinomas.

5.18 Cumulative scores for p21 ras in carcinomas by number of involved nodes.

5.19 Diameter of primary carcinoma plotted against p21 ras score

5.20 Carcinoma OR content plotted against p21 ras score.

5.21 Cumulated scores for p21 ras in normal TDLU, ALH, LCIS and invasive lobular carcinoma.

5.22 PLPD-fixed breast tissue, Y13-259 50 µg/ml, ABC detection. Positivity in myoepithelial cells and vascular smooth muscle.

5.23 PLPD-fixed breast tissue, Y13-259 50 µg/ml, ABC detection. Positivity in vascular smooth muscle.

5.24 Cumulative scores for p21 ras in epithelial and stromal cells of carcinomas.

5.25 PLPD-fixed breast tissue, Y13-259 50 µg/ml, ABC detection. Basal immunoreactivity in apocrine cells.

5.26 PLPD-fixed breast tissue, Y13-259 50 µg/ml, ABC detection. Apical immunoreactivity in apocrine cells.

5.27 PLPD-fixed breast tissue, Y13-259 50 µg/ml, ABC detection. No immunoreactivity in flattened cells.

5.28 Cumulative scores for p21 ras in normal TDLU of women younger than 45, and 45 or older.

7.1 PLPD-fixed paraffin-embedded FHO5T1 tumour. Y13-259 50µg/ml, IGS detection, reprocessed for EM. Plasma membrane signal.

7.2 PLPD-fixed paraffin-embedded FHO5T1 tumour. Y13-259 50µg/ml, IGS detection, reprocessed for EM. Cytoplasmic signal.

7.3 Indirect EM-immunogold labelling of FHO5T1 on cover slips.

7.4 Indirect immunogold-silver labelling of FHO5T1 cells on cover slips. Y13-259 50µg/ml, IGS detection.

7.5 Negative control for 7.4, omitting primary antibody.

7.6 Breast carcinoma. Cryostat section. Y13-259 50µg/ml, ABC detection, osmicated and processed for electron microscopy.

7.7 Negative control for figure 7.6, omitting Y13-259.

Tables

CHAPTER 1 GENERAL INTRODUCTION

Breast carcinomas develop by unknown mechanisms from small epithelial lesions. Oncogene abnormalities have been found in human carcinomas and while experiments with cell lines and transgenic animals are very fruitful in suggesting hypotheses about human cancer, it is only by examining human material that these hypotheses can be tested directly. The present studies are concerned exclusively with human breast tissue and in particular with putative precursor lesions in which oncogene expression may correlate with abnormal morphology to illuminate the processes by which carcinomas evolve. An attempt has been made to develop methods for isolation and study of such lesions, in which expression of the products of the ras proto-oncogene family has been examined in detail.

In general, the identification of precursor lesions rests upon their morphological similarities with carcinoma, co-occurrence with carcinoma, and on the increased risk of subsequent breast carcinoma among women shown by biopsy to have these alterations in the absence of demonstrated carcinoma. Before considering these lesions in detail, it is helpful to review the normal anatomy of the adult female breast, from which these lesions deviate. The nomenclature for different parts of the parenchymal tree varies between authors but that given below is essentially that used by Dawson [26] and Wellings and Jensen [151].

1.1 Normal breast anatomy

Between a dozen and a score of major ducts reach the nipple and each engenders a complex hierarchy of smaller

ducts ramifying throughout the breast. The terminal ducts are distal to the last duct bifurcation but proximal to the lobules. Lobules are the individual glandular elements of the breast and are composed of branching ductules embedded in specialized myxoid stroma. Ductules and terminal ducts share the ability to undergo secretory differentiation and can be considered together as terminal duct lobular units (TDLU).

These relationships are illustrated in figure 1.1a, a schematic section through breast and nipple. Only four major ducts are shown reaching the nipple but an enlarged section (figure 1.1b) through the nipple perpendicular to the ducts depicts a representative number. The branching duct system arising from one large duct is illustrated down to the lobules, represented by small ellipses joined to the ductal tree by terminal ducts. The ducts tend to radiate from the nipple, but the breast is not segmental and duct territories overlap. The parenchymal elements (ducts and lobules) are supported by collagenous stromal connective tissue which is physically continuous with fascia deep to the breast and attached to skin by the suspensory ligaments of Astley Cooper. The remainder of the breast is fat. Ratios of parenchyma, collagenous and adipose connective tissue vary from woman to woman and with age. Figures 1.1c and 1.1d show the arrangement of a duct, terminal duct and lobule composed of numerous ductules. Figure 1.1c shows the structure in three dimensions while figure 1.1d shows the appearance characteristic of histological sections in which connections between elements are not apparent.

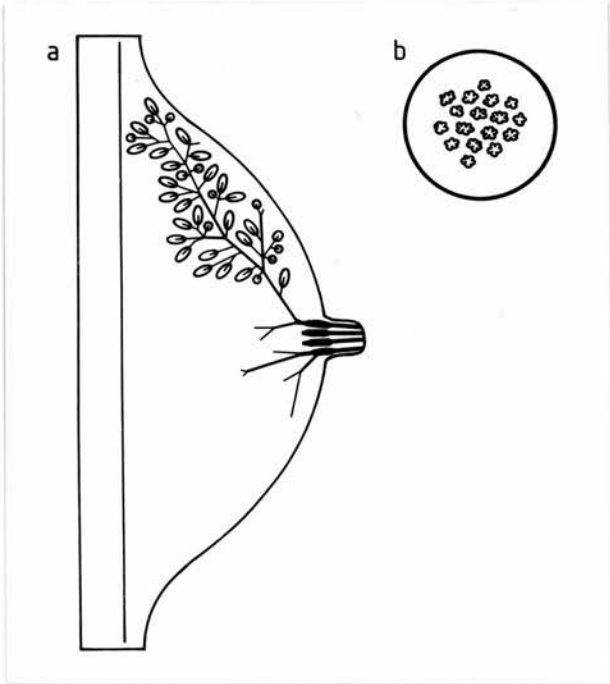

Figures 1.1a and b. Diagrammatic section through adult female breast and section through nipple showing arrangement of major ducts.

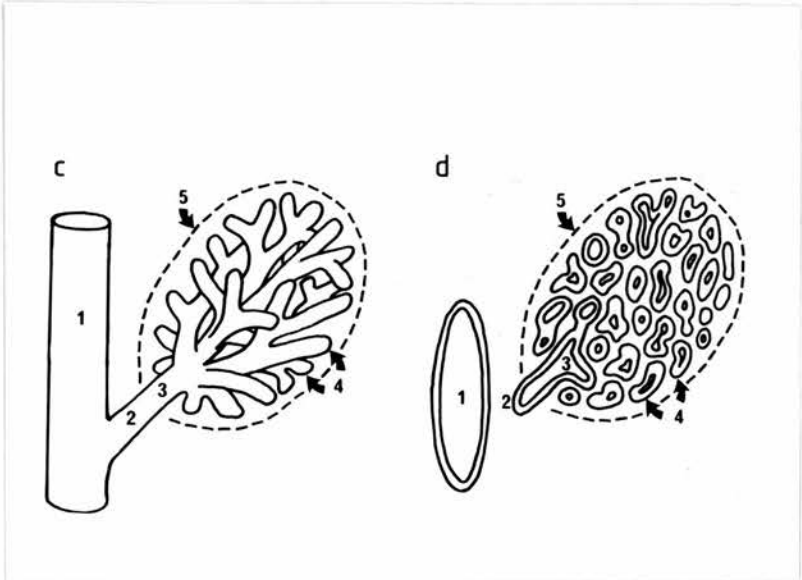

Figure 1.1c. Three-dimensional structure of terminal duct lobular unit. 1, large duct. 2 and 3, extra- and intra-lobular terminal ducts. 4, ductules. 5, boundary of specialized lobular connective tissue. Figure 1.1d. Terminal duct lobular unit in histological section.

1.2 Histogenesis of breast carcinoma

The evolution of carcinoma from breast epithelium remains mysterious. Even such concrete matters as the morphological stages passed through, which alterations in the breast are associated with increased risk of breast carcinoma, and which lesions are authentic precursors of carcinoma are uncertain. The chief reasons for this doubt are the multiplicity of alterations, the impossibility of studying the temporal evolution of a particular lesion in a particular breast, and the destruction by invasive carcinomas of surrounding tissues, obliterating earlier stages of the evolutionary process. Despite these difficulties, much has been learned, and in the next sections available evidence will be reviewed to provide the foundations for the studies to be described subsequently.

1.3 'Fibrocystic disease' and carcinoma

For long the relation between carcinoma and the complex of morphological alterations known among other names as 'fibrocystic disease' has been debated, and strongly opposed views held. Authors have approached this question in various ways, and some of these approaches are discussed in the following sections.

1.3.1 Histological transitions between benign and malignant epithelium

Transitions between non-malignant and malignant epithelium could theoretically provide direct evidence for the origin of carcinoma in the breast, but for several reasons such transitions have not been convincingly demonstrated. As already noted, invasive

carcinomas destroy tissues, and cover their traces. An invasive carcinoma five millimetres in diameter, tiny in clinical terms, may already be many times larger than the parent lesion in which it developed. Secondly, non-invasive carcinomas colonise benign parenchymal elements, displacing and replacing original populations of epithelial cells, hence malignant cells may lie in locations far from their origin, in contact with populations of cells which had nothing to do with their genesis. It is a rare 'transition' that on morphological grounds alone can be distinguished from a collision of disparate elements.

A different type of transition would exist if a morphological continuum could be shown between normal parenchyma, through a range of alterations sharing structural features with malignant lesions, one blending imperceptibly into the next, until unequivocally malignant lesions are reached. Wellings, Jensen and their colleagues have constructed two models of the evolution of different types of breast cancer [106,134,151]. They define five grades of 'atypical lobule type A' (ALA I-V), grade V being ductal carcinoma in situ (DCIS), and five grades of 'atypical lobule type B', grade V being lobular carcinoma in situ (LCIS). But the impossibility of extrapolating from static to dynamic description is a drawback, and not all authors accept that these morphological alterations represent an authentic biological continuum. Azzopardi, for instance, denies that ALA III and ALA IV are similar enough to establish a continuum [3]. The morphological definitions of these lesions will be discussed in 1.4, where their relationship to alternative classifications will be considered in the light of evidence reviewed in the next two sections.

1.3.2 Retrospective studies

In an attempt to discover whether breast carcinoma was preceded by significant pathology, Foote and Stewart [38] determined the frequency of earlier breast operations in 1200 women with breast cancer. 2.4 per cent of women with breast cancer had a recorded breast operation for benign changes, an incidence 2.2 times that for women with other, non-mammary cancers. But when questioned, four per cent of the women with breast cancer recalled previous breast operations. This discrepancy illustrates one of the weaknesses of retrospective studies. Haagensen believed that it was impossible to determine accurate information from such studies [58]. Steinhoff and Black [126] attempted to rectify this defect by reviewing the original benign biopsies of thirty women who later developed breast cancer and comparing the findings with those of thirty age-matched controls, but such small-scale studies do not yield convincing results.

1.3.3 Prospective studies

In reviewing a number of prospective studies, Azzopardi [3] noted that many are best described as 'prospective observational studies done in retrospect'. The subsequent fate of women who have had benign biopsies in the past is determined. Modern diagnostic criteria can be applied to the review of available pathological material, but the selection of material for examination, fixation and processing are of course immutable. It is assumed that the excised tissue is representative of pathological changes in the breast but does not necessarily include all pathological tissue present in the breasts. Nevertheless such studies currently provide the best assessments of the cancer risks associated with

different morphological alterations in the breast. Many older studies predate precise criteria distinguishing epithelial hyperplasia from carcinoma *in situ* and even the recognition of lobular carcinoma *in situ*, which was described in 1941 by Foote and Stewart [39]. These difficulties effectively disqualify, for example, the studies by Warren in 1940 [148] and Clagett *et al* in 1944 [20], and lobular carcinoma *in situ* was rarely recognised by 1954 when Kiaer [72] published his studies. Against this background exhaustive recent studies of the component parts of the 'fibrocystic disease' complex by Page *et al* [33,97], using modern criteria, have given particularly valuable information and it is appropriate to review their findings in some detail.

Page *et al* [33] studied 10,366 consecutive breast biopsies done at three Nashville hospitals up to 1968. These yielded a group of 2408 biopsies showing proliferative changes or carcinoma *in situ*, but not invasive carcinoma, with 2011 control biopsies lacking such changes. These 4419 biopsies were from 3318 women for whom adequate material for pathological reassessment and follow-up for a minimum of seventeen years were available. The 'proliferative' group were divided into the diagnostic categories in table 1.1.

'Non-proliferative' diagnostic categories included mild hyperplasia of usual type, cysts, parenchymal microcalcification, fibroadenoma, and papillary apocrine metaplasia. The morphological criteria used are those of McDivett [84] for *in situ* carcinoma, and similar to those of Jensen *et al* [67], Wellings *et al* [150], and Black and Chabon [10] for other lesions. The findings are summarised in table 1.2 which gives the cancer risk associated with various proliferative morphological

Ductal carcinoma *in situ* (DCIS)
Lobular carcinoma *in situ* (LCIS)
Atypical ductal hyperplasia (ADH)
Atypical lobular hyperplasia (ALH)
Moderate and florid hyperplasia of usual type
Papillomas
Ductal involvement with cells of ADH
Sclerosing adenosis

Table 1.1. Diagnostic categories used by Page *et al* [33,97].

	Relative risk
Proliferative disease without atypia	1.9 (1.2-2.9)
typical hyperplasia, overall	5.3 (3.1-8.8)
Atypical hyperplasia, no FH	4.3 (2.4-7.8)
Atypical hyperplasia, with FH	8.4 (2.6-27)

Table 1.2. Risks of subsequent carcinoma in women with various hyperplastic states in the breast relative to women without proliferative changes on breast biopsy. From [33]. Bracketed figures are 95% confidence limits.

alterations relative to the risk for women with nonproliferative (NP) changes only. The 95% confidence intervals for these estimates are also given.

In a more detailed analysis [97], atypical ductal hyperplasia (ADH) was separated from atypical lobular hyperplasia (ALH), and the effects of family history (FH) were considered, to give the relative risks shown in table 1.3.

In summary, for women with ADH or ALH the risk of subsequent breast cancer was about five times that for women without proliferative changes, in whom the risk was the same as in the general population. If there was a history of breast cancer in a first degree relative, that risk doubled, and was almost the same as the risk associated with in situ carcinoma, which for DCIS and LCIS is eleven-fold that of the general population [57,98,104]. A point worth noting is that the lesions designated 'atypical' in these studies have distinct morphological resemblances to carcinomas in situ. Others have used 'atypical' for all hyperplasias [10,150] and it is important to appreciate this. Women with proliferative changes but no atypia had about twice the cancer risk of the general population.

Haagensen [58] has considered that 'gross cystic disease' is a risk factor for subsequent carcinoma. The studies just discussed did not find that cysts were an independent risk factor but were associated with doubled risk in women with a positive family history.

Numerator	Denominator	Relative risk
ADH	NP	4.7 (2.5-8.9)
ADH, no FH	NP, no FH	3.9 (1.9-8.3)
ADH with FH	NP with FH	7.2 (1.9-27)
ADH with FH	NP, no FH	9.7 (3.7-25)
ALH	NP	5.8 (3.0-11)
ALH, no FH	NP, no FH	4.8 (2.3-10)
ALH with FH	NP with FH	9.3 (2.4-35)
ALH with FH	NP, no FH	13 (4.8-35)

Table 1.3. Risks of subsequent carcinoma in women with various hyperplastic states in the breast relative to women without proliferative changes on breast biopsy and including the effects of family history of carcinoma. From [97]. Bracketed figures are 95% confidence limits.

1.4 Evolution of carcinoma: Subgross studies

The comprehensive studies by Wellings, Jensen and their colleagues also provide valuable evidence concerning the evolution of breast carcinoma [151]. They examined nearly two hundred intact fixed mastectomy and autopsy breasts sliced at 2mm intervals, stained with haematoxylin and cleared in methyl salicylate. All areas where the parenchyma departed from the normal 'background' lobular morphology were photographed and processed for paraffin histology. They considered that this approach identified all parenchymal lesions and permitted their histological examination in 5-500 paraffin blocks per breast.

The most significant finding was that most parenchymal alterations in the breast arose in terminal duct lobular units (TDLU) or the lobules themselves. The only exception was intraduct papilloma developing in large ducts. As well as benign changes such as cyst formation they identified two series of atypical lobules, type A and type B. It is important to note that 'atypical' is being used here in a sense different to that used by Page et al, but similar to the usage of Black and Chabon [10], meaning any lobular alteration. Atypical lobules type A (ALA) were commoner in the breasts of women with breast cancer and could be arranged morphologically in a continuum with DCIS. As DCIS was approached atypical lobules expanded and 'unfolded' to give the false impression that DCIS was a ductal lesion (figure 1.2a-d). These morphological findings were taken to support the hypothesis that 'ALA' were premalignant lesions. The atypical lobule type B (ALB) continuum was based on relatively few cases, but stood in the same relation to LCIS as ALA to DCIS. The work of Jensen and her

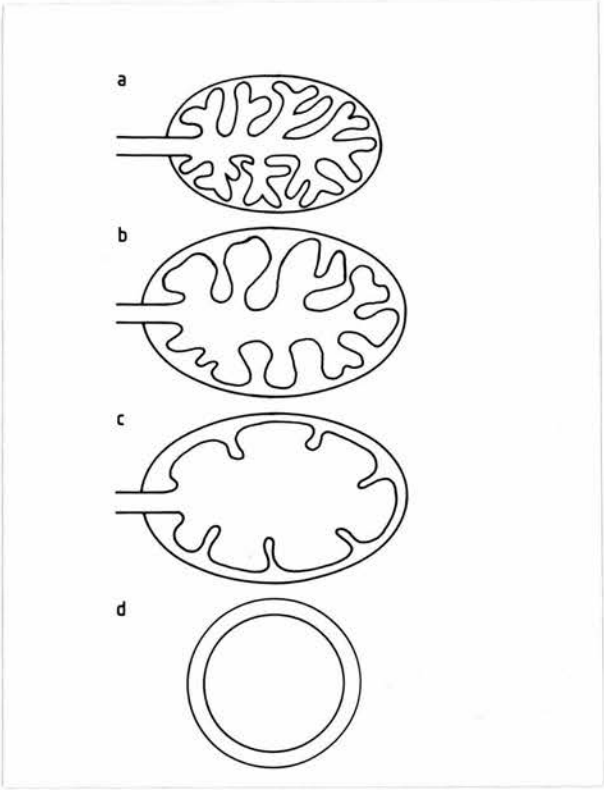

Figure 1.2. 'Unfolding' of a lobule to simulate a ductal structure. The ductules are progressively dilated and coarsened until finally they are lost. If the plane of histological section no longer identifies a terminal duct (d) the illusion is complete. These morphological changes occur in association with diverse cellular pathology.

colleagues represents the most determined attempt to establish the precursors of human breast cancer by morphological criteria. While the detailed histological series (ALA I-V and ALB I-V) have not been universally accepted and indeed this nomenclature was later abandoned by Alpers and Wellings [1], proof of the origin of breast carcinoma in lobules was of paramount significance.

Differences concerning what constitutes *in situ* carcinoma certainly exist between authors. Azzopardi [3] was unconvinced that a continuum had been demonstrated and considered that ALA grade IV represented ductal carcinoma *in situ*. He was reluctant to accept the concept of atypical hyperplasia. Differences in the incidence of ostensibly identical lesions in studies by different authors certainly suggest differences in interpretation. It is interesting to contrast the findings of Nielsen *et al* [93] who processed for histology all breast tissue from 110 medico-legal autopsies of women aged 20-54. Their blocks were 5mm thick and their identification of small lesions may have been less sensitive but using the criteria of Azzopardi [3] they found DCIS in 15, LCIS in 4, and DCIS and LCIS in one of their cases. A further two women had invasive carcinoma. Only one of the women was known during life to have breast cancer. In contrast to this overall 20 per cent incidence of carcinoma, Alpers and Wellings' most recent publication [1] documents ALA grade V (i.e. DCIS) in 5 of 88 women aged 20-59, an incidence of 5.7 per cent. Only two more women had lesions of ALA grade IV. These 7 women represent 7.9 per cent compared with the 14.5 percent with DCIS of the women studied by Nielsen *et al*. Either there is a large difference in the incidence between Denmark and California, or interpretative and methodological differences apply.

Fortunately, the studies of Page et al [33,97] provide a morphological formulation of proven prognostic significance. Azzopardi's reservations concerning atypical hyperplasia as a concept are answered by the demonstration of intermediate risk associated with it, and a continuum of risk, if not of evolution, was demonstrated. The histological criteria of Page et al [33,97] were adopted in this thesis and are reviewed in the next sections.

1.5 Histopathological criteria for the diagnosis of breast hyperplasia, atypia and neoplasia

This thesis is concerned with the relationship between expression of the ras proto-oncogene and the evolution of breast carcinoma. As discussed above there is no certain way of identifying the stages of this evolution, although the importance of lobular epithelium has been stressed. Because of its proven association with prognosis, and clearly illustrated diagnostic criteria, I have adopted the formulation of Page et al [33,97], recently expanded by Page and Anderson [96]. Ensuing sections describe the key elements of this classification (table 1.4) some illustrations of which will be provided in chapter 3.

In normal breast parenchyma there are two cells between basement membrane and lumen. Hyperplasia exists when this number is exceeded. Abnormally numerous glandular elements composed of cells retaining the usual relation to the basement membrane constitute adenosis, a separate entity. Mild epithelial hyperplasia begins when an increased number of cells is present. Sectioning artefacts may mimic this appearance and the whole unit must be assessed, not single ductules. More florid examples show many more cells and may expand the elements

1. 'Lobular' changes
   - Atypical lobular hyperplasia (ALH)
   - Ductal involvement by cells of ALH
   - Lobular carcinoma in situ (LCIS)

2. 'Ductal' changes
   - Hyperplasia without atypia
   - Atypical ductal hyperplasia (ADH)
   - Ductal carcinoma in situ (DCIS)

3. Apocrine metaplasia
   - Papillary apocrine change

4. Invasive carcinoma including special types

Table 1.4. Hyperplastic, atypical and neoplastic alterations of breast parenchyma. This is not an exhaustive list but includes the lesions on which this thesis concentrates, in relation to ras expression and cancer risk.

containing them. In this formulation, 'atypia' implies morphological features similar to those of non-invasive carcinoma while not completely satisfying the criteria for that latter diagnosis.

1.6 Epithelial hyperplasias without and with atypia

1.6.1 Epithelial hyperplasia of usual type ('Ductal')

Historical precedent has applied the 'ductal' label to these hyperplasias which affect terminal ducts and lobular units. They are 'usual' in the sense of being the most commonly observed hyperplasias in breast while lacking specific apocrine features or features of atypical ductal or lobular hyperplasias. Mild hyperplasia of usual type does not expand parenchymal elements or bridge or solidly occupy lumina. This change is present in up to 50 per cent of premenopausal biopsies and carries no increased carcinoma risk. Moderate and florid hyperplasias of usual type may occur in 20 per cent of biopsies. Expansion and luminal bridging are present and may coexist with 'columnar alteration of lobules', a change in which the epithelial cells are abnormally tall, sometimes with secretory snouts, but hyperplasia is absent by definition because the epithelium remains two cells thick. The patterns in moderate and florid hyperplasia of usual type are very varied. In more florid examples, 'swirling' or 'streaming' of the cells, slit-like spaces, tapering cellular arches composed of cells elongated parallel to the arch, cell-to-cell nuclear variability representing heterogeneous cellular differentiation (but lacking cytologic features of malignancy) all point to benign proliferation.

1.6.2 Atypical ductal hyperplasia

This diagnosis implies architectural or cytological features of ductal carcinoma *in situ* but not fulfilling all criteria for its diagnosis. The most important features are monotony of cells, smooth geometric spaces between cells (unlike the irregular slit-like spaces of benign hyperplasia), and nuclear hyperchromasia. The swirling pattern is absent. Partial involvement of a space by cells of DCIS does not qualify for DCIS; Page *et al* [97] adopted a rule that two whole spaces should show the changes of DCIS to secure that diagnosis. Complex patterns are seen and this area is one of diagnostic difficulty.

1.6.3 Atypical lobular hyperplasia

Unlike atypical ductal hyperplasia, there is no corresponding non-atypical lesion, despite the attempt by Jensen and her colleagues to define such a series, which was quoted above (section 1.4). As with the definition of ADH given above there is the possibility of a simple definition, but some inconsistencies exist in the literature. The cytological appearance of the cells in ALH is the same as the cells of LCIS. Page and Anderson [96] state that when the characteristic cells occupy or expand less than half of the ductules in a parenchymal unit, ALH is the diagnosis, not LCIS. Page *et al* [97] say that the features of LCIS must be present 'throughout the major portion' of a lobular unit in order for LCIS to be diagnosed. Stated criteria vary in emphasis even within the writings of the same authors, and for the purposes of this thesis complete replacement of the normal epithelium in a parenchymal unit by the characteristic cells is taken as necessary and sufficient

for a diagnosis of LCIS. Preservation of the original lumen or partial retention of the original cell population is the usual way in which full criteria for LCIS are not met. Intracytoplasmic lumina are found in ALH and LCIS and do not discriminate between these lesions. Uniform, evenly spaced, small round cells are characteristic. Pagetoid spread by these cells may be seen and termed 'ductal involvement by ALH'.

1.7 Carcinoma *in situ*

1.7.1 Ductal carcinoma *in situ*

Under this heading three separate patterns are recognised. Micropapillary and cribriform ductal carcinoma *in situ* frequently occur together and transitions between the two forms are found. Unlike them, comedonecrotic DCIS is notable for cellular pleomorphism. Occasionally all three patterns are present. Lesions vary from less than a millimetre to massive involvement in all quadrants of the breast. Solid [2] and signet-ring [36] patterns of DCIS may be identified but their biological potential is ill-characterised. To what extent types behave differently is unclear.

Diagnostic features of the non-comedonecrotic lesions have been referred to above but for completeness some details may be added. Micropapillary DCIS is characterised by regular cellular projections, often broader at tip than base, lacking a fibrovascular core (unlike papillary non-invasive carcinomas). Cytology of both micropapillary and cribriform DCIS is uniform, with regular punched-out spaces in the latter. Necrosis is not usually conspicuous in these variants, but is of

course characteristic of comedonecrotic DCIS. Although the increased risk of invasive breast carcinoma associated with DCIS is about tenfold that of the general population, this risk may be confined to the ipselateral breast [149], and the prognosis for DCIS without evidence of invasion after adequate sampling is excellent [12].

1.7.2 Lobular carcinoma *in situ*

Lobular carcinoma *in situ* is impalpable and usually invisible in gross specimens. It was more recently recognised than DCIS and appears to be associated with equal risk of subsequent invasive carcinoma to either breast. The characteristic cells have been described above in section 1.6.3 (atypical lobular hyperplasia) with the criteria distinguishing it from ALH. LCIS is characteristically multicentric and lacks necrosis and may be associated with pagetoid colonisation of duct epithelium. The ductal lesions associated with ALH or LCIS are identical and the differential diagnosis can only be resolved on lobular morphology. Colonization by cells of DCIS within lobules retaining their usual archetecture must be differentiated from LCIS. Greater cellular pleomorphism in this case is usually distinct from the monotony of the cells of LCIS.

1.8 Invasive carcinomas

Breast carcinomas are histologically diverse, and a number of characteristic special types are recognised, but the majority do not possess such features and are known as ductal carcinomas or carcinomas of 'no special type'. Recognised special types include lobular, medullary, mucoid, tubular, tubulo-lobular, cribriform, and papillary invasive carcinomas.

1.8.1 Invasive carcinoma (no special type)

Ductal invasive carcinoma is typically composed of irregular islands of pleomorphic malignant cells in a fibrous stroma. Glandular differentiation may be present but features of special types of carcinoma are not prominent. A carcinoma in which more than half the section area belongs to no special type should be regarded as being of no special type overall. These carcinomas are diverse in appearance and diagnosis rests on the lack of features belonging to special type lesions.

1.8.2 Special types of invasive carcinoma

Lobular invasive carcinomas, like LCIS, were first reported by Foote and Stewart [37]. They are characterised by cytological and infiltrative pattern and a number of variants have been described. The classical infiltrating lobular carcinoma has small, non-cohesive, regular cells with round nuclei. These cells invade widely in enfilades. Solid and alveolar variants lack this infiltrative pattern but retain characteristic cytology. The mixed variant mingles features of these types while the diffusely infiltrative pleomorphic variant lacks cytological regularity. Lobular invasive carcinoma is often found with LCIS, which cytologically it resembles.

Despite its capacity for diffuse infiltration, classic invasive lobular carcinoma has a better prognosis than carcinoma of no special type, and so do the other special type carcinomas, one or two of which have a particularly good outlook. Tubular and cribriform invasive carcinomas, both characterised by regular nuclear

morphology and archetecture, belong to this favourable group. It is curious that medullary carcinoma of breast, characterised by extreme cellular pleomorphism, also has a relatively favourable outlook. It is unnecessary to go into detail about the histological features of these relatively rare types of carcinoma, but a subjective element to their assessment should be appreciated, reflected in the different frequecies with which special types are recorded in various series.

It is into this morphological framework that this thesis seeks to fit observations on the expression of genes of the ras family.

1.9 Ras genes

The remainder of this introduction reviews the biology of ras genes, in general and as they relate to the breast, before discussing briefly other oncogenes relevant to breast neoplasia and ways in which oncogene expression in breast may be studied. A distinction is observed between proto-oncogenes and oncogenes. Proto-oncogenes are normal cellular genes while oncogenes are abnormal forms of these genes activated by diverse mechanisms including point mutation. This usage will be observed as far as possible.

1.9.1 Biochemistry of ras products

Ras genes are responsible for the acutely transforming activity of the Harvey and Kirsten strains of murine sarcoma virus. These viral oncogenes (v-Ha-ras, v-Ki-ras) have four normal homologues in all mammals: The genes c-Ha-ras1 and c-Ki-ras2 and pseudogenes c-Ha-ras2 and c-Ki-ras1. The mammalian N-ras gene was discovered

by transfection of neuroblastoma DNA into NIH3T3 cells [112] and has not been found in the genome of a retrovirus [54]. Analogous genes are found in lower organisms.

The products of the three ras genes are proteins of molecular weight 21,000, conventionally known as "p21 ras" proteins. They are closely associated with the inner face of the plasma membrane, and indeed are difficult to dislodge from that location [54]. Certain biochemical activities are constant features of p21 ras proteins: notably GTP and GDP binding [108,111,130,135] and weak GTPase activity [46,83,86,128,135]. These activities are important for physiology of normal ras proto-oncogene products and for the transforming properties of ras oncogenes [22,34,155]. It appears that GTP bound to p21 ras activates it while the GDP-bound form is inactive.

Evidence for the importance of guanine nucleotide binding and hydrolysis of GTP to the transforming activities of ras proteins includes reversion of the transformed phenotype in NIH3T3 cells transformed by ras genes when injected with antibodies which inhibit guanine nucleotide binding [22,34]. Mutant ras proteins incapable of guanine nucleotide binding are incapable of transforming NIH3T3 cells [76,155], and transforming mutant ras genes encode proteins deficient in GTPase activity [46,83,86,128,135].

The physiological roles of p21 ras proteins remain unclear [6]. Evidence connects them with cell division [66,77,80,90] but also with differentiation [5,19,42,55,94]. Microinjection of cultured cells with ras oncogene products stimulates transient cellular

proliferation and morphological transformation [35,65,125], and cells engineered to express constitutively supranormal quantities of p21 ras proto-oncogene [18,30,88,100] and oncogene [18,100,120,122] proteins have a transformed phenotype and will form aggressive malignant tumours in immune deprived mice [122,156]. In general the oncogenes induce more floridly malignant phenotypes than the proto-oncogenes [6].

Direct and indirect evidence link growth factors with p21 ras expression. NIH3T3 cells into which an inducible N-ras proto-oncogene had been inserted had normal basal levels of inositol phospholipid turnover but increased N-ras expression was associated with a supranormal increase in turnover of inositol phospholipids in response to bombesin and bradykinin but not to EGF or PDGF [145]. Other ras genes may be associated with increased turnover in response to other growth factors such as serotonin or PDGF. Unlike ras proto-oncogenes, overexpressed ras oncogenes are associated with increased basal turnover of inositol phospholipids [145], apparently because the GTP-bound, active form of p21 ras predominates.

There is no clear correlation between ras expression and cellular proliferation in a variety of tissues [19]. Although regenerating rat liver expresses up to eight times as much p21 ras as normal liver [53], the rat tissue expressing most p21 ras is brain [131], while in mice the tissue richest in p21 ras is cardiac muscle [120]. The PC12 phaeochromocytoma cell line provides another link with differentiation. In this line p21 ras microinjection induces neuronal differentiation [5,55,94], and neuronal differentiation induced by nerve growth factor is blocked by microinjection of monoclonal antibody Y13-259 [59]. Human immunocytochemical studies

have demonstrated p21 ras in various terminally differentiated cells [19,42]. Discovery of GTPase activating protein, GAP, [14] points towards understanding of ras protein physiology but many questions remain.

Abnormally expressed ras genes are common in human carcinomas, but it is not clear where these abnormalities occur along the stages that lead to the emergence of a fully malignant cell , and even how important they are in spontaneous tumours. The enthusiasm engendered by initial reports of transforming genes in human tumours [31,99,106] and the subsequent demonstration of point mutations in ras genes, apparently responsible for these transforming properties [102,129,134], was followed by a more cautious phase [24,116] but since then more refined genetic analysis has shown that in some locations, such as colo-rectal and pancreatic carcinomas, ras gene mutations are frequent [11,40].

1.9.2 Ras genes and experimental neoplasia

Experimental tumour research defines areas significant for spontaneous human cancer as well as for experimental lesions. Some significant experiments will be described here, before considering ras genes and other oncogenes in their specific relationship to the breast. Spandidos and Wilkie [122] showed that the mutated Ha-ras gene was capable of engendering full malignant transformation in low passage rodent cells, if introduced into those cells along with transcriptional enhancers. These cells had the transformed phenotype in vitro and were tumorigenic in nude mice. They also showed that, while not causing the transformed phenotype, primary cultures of rodent

cells were protected from senescence ('immortalised') by the introduction of either normal ras gene with enhancers to ensure its expression at high levels, or by the mutated ras gene without such enhancers. This blurs the customary distinction between immortalizing and transforming genes, suggesting that the same gene can be both under appropriate conditions.

On the basis of what they found in these experiments, Spandidos and Wilkie [122] proposed a role for ras in earlier stages of carcinogenesis than had been suggested previously. Balmain et al [4] noted that papillomas induced on the skin of mice by repeated application of chemical carcinogens could contain cellular Ha-ras DNA capable of transforming NIH 3T3 cells [61]. A specific mutation is frequently induced by a particular carcinogenic hydrocarbon [101]. Adenomatous polyps of colon have elevated ras transcripts [121] and expression of p21 ras [153]. Wyllie et al showed [156] that cell lines expressing ras and myc genes both engendered metastasizing fibrosarcomas when injected into nude mice, and some interesting differences came to light in this study. Ras-expressing cells engendered more aggressive tumours than myc expressing ones and non-mutated Ha-ras1 was capable of inducing metastasizing fibrosarcomas in an aneuploid rat fibroblast cell line. Cell death by apoptosis was more frequent in cells transformed by myc than ras genes, which is of interest in that cell death by apoptosis can be very conspicuous in human cancers. Another observation was that c-abl and c-fos were strongly expressed in cells transformed by Ha-ras or myc genes, implying widespread alterations in metabolic activity and raising the possibility of co-activation of complementary oncogene groups [78,87]. It was unclear whether altered expression of c-fos and c-abl was a

direct consequence of altered myc or ras expression, given that other genetic abnormalities might have accumulated during the selection process by which these cells were generated, and the transformed cells derived from primary cultures of chinese hamster lung (CHL) cells were aneuploid, while their parent cells were not. On the other hand microinjection of p21 ras also increased the expression of these other oncogene products, which would be in keeping with a direct effect. While not directly defining a role for oncogenes in the evolution of spontaneous human malignancies, such experiments do support a role for these oncogenea and their products.

Interesting results have been obtained with transgenic animals. Oncogenes have been inserted with promoter sequences into the genome of such animals and the tissue effects have been studied. Stewart et al [127] created strains of mice in which the myc gene was coupled to hormonally-inducible promoters from mouse mammary tumour virus (MTV). These MTV/myc genes were associated with mammary adenocarcinomas which developed in a stochastic fashion during pregnancy. More recently Sinn et al [115] have mated MTV/myc and MTV/v-Ha-ras transgenic mice to create dual carrier mice in which potent synergism of myc and ras genes was demonstrated, but even in these animals mammary adenocarcinomas developed stochastically, indicating that a further event was needed before malignant transformation was completed. But transgenic mice bearing MTV/c-neu (c-erbB2) fusion genes develop synchronous polyclonal malignant transformation indicating that overexpression of c-neu activated by mutation is sufficient for single-step malignant transformation [91]. The contrast is striking.

1.10 Ras and breast carcinoma

Evidence relating ras genes and their expression to human breast carcinoma derives from several lines of enquiry. Published studies have examined the genes themselves, the RNA they encode, and their p21 protein products. Researchers have sought gene amplification [9,136], gene rearrangement [136], quantitative differences in ras RNA expression between putatively normal breast and carcinomas [119,152], and activating mutations in ras genes of carcinomas, by transfection into NIH 3T3 cells or by generation of restriction endonuclease cleavage fragments characteristic of particular mutations [9,136]. The p21 ras proteins in breast extracts have been studied in immunoblots [21,27,132,136], by radioimmunoassay [95] and immunocytochemically using diverse antibodies including RAP-5 [41,45,64] and Y13-259 [15,64,95]. Some consistent themes emerge from these studies but contradictions abound and the role of ras genes in the evolution of breast cancer remains unclear. The results of these and other studies will be reviewed in the next three parts of this subsection under headings DNA, RNA, and protein. Table 1.5 summarises the findings of fourteen studies which included at least some breast cancers. No clear picture of ras expression emerges and major differences between the findings of different studies are hard to interpret. Some of these issues will be addressed in the next subsections.

1.10.1 DNA: ras genes

Studies of ras genes have sought rearrangement, amplification, mutation, rare alleles and allelic loss. Biunno et al [9] examined all three ras genes in 65 carcinomas and found no rearrangements. One case only

showed a fifty-fold c-Ha-ras amplification absent from white blood cells of the same patient but this carcinoma did not overexpress c-Ha-ras mRNA. Biunno et al sought altered restriction enzyme cleavage fragment sizes which could have disclosed mutations at position 12 of c-Ha-ras and c-Ki-ras, and found none.

Transfection assays on the same cases were also negative. Theillet et al [136] found no mutations of codon 12 of c-Ha-ras and c-Ki-ras genes of 32 and 64 carcinomas respectively, using similar analytic methods but not a transfection assay. The contrast with colorectal carcinoma is striking, for there a high incidence of mutation, particularly at codon 12 of the c-Ki-ras gene, has been documented, albeit by other techniques [11,40]. Some at least of this difference may reflect the sensitivity of the methods used. Bos et al [11] probed amplified DNA with oligomeric probes while Forrester et al [40] used RNAase A mismatch cleavage analysis. These methods may detect mutations that other methods would not. Slight degradation of tumour DNA could negate transfection assays especially for large genes such as c-Ki-ras which has more than 45,000 base pairs. Codon-12 mutated c-Ha-ras genes were detected in two of 24 carcinomas by Spandidos [123] and in a cell line derived from a breast "carcinosarcoma" [74] but the evidence remains against a high frequency of transforming mutations in breast cancer.

Krontiris et al [75] have suggested that rare alleles of c-Ha-ras are more frequent in DNA from normal cells and tumours in patients with diverse malignancies including some breast cancers, and that the possession of such rare alleles might reflect an inherited susceptibility to cancer. Their study was based on a polymorphism of BamHI

Study	A	B	C	D	E	F	G	H	I	J	K	L	M	N
Cancers	43	54	10	16	100	104	104	100	12	30	22	53	20	23
Controls	9	-	CL	-	100	WC	WC	WC	12	21	25	46	8	27
DNA analysis	-	-	-	-	+	+	+	+	-	-	-	-	-	-
Allelic loss	-	-	-	-	14/65	14/51	-	3/6	-	-	-	-	-	-
Rare alleles	-	-	-	-	7/200	-	86/208	-	-	-	-	-	-	-
Mutations	-	-	-	-	-	-	0/64	-	0/65	-	-	-	-	-
RNA analysis	-	-	-	-	-	+	-	+	+	-	-	-	-	+
p21 analysis	+	+	+	+	-	+	-	-	-	+	+	+	-	-
Western blots	+	+	+	-	-	+	-	-	-	-	-	-	-	-
Immunohisto-chemistry	-	-	-	+	-	-	-	-	-	+	+	-	+	-
Antibodies	Y	Y	PC	R	_	Y	_	_	_	R	R	RY	Y	-
p21 or ras RNA	^^	^^	D	>	-	D	-	D	^^	^	>	^	>	>

Table 1.5. Studies of ras expression in breast. Studies F and G refer to the same 104 patients. Numbers refer to benign cases except for study G (benign tissue from the cancer cases). WC implies comparison with normal white cells, CL with cultured cell lines. Y is monoclonal antibody Y13-259, R is RAP-5. PC represents polyclonal antisera. ^^ implies p21 or ras RNA elevated at least 5 times in carcinomas relative to normal tissue from the same or other cases; ^, lesser but elevated levels; > , detection without elevation; D, detection without data for comparison with normal tissue. These are the references: A=[27] B=[21] C=[132] D=[41] E=[82] F=[136] G=[79] H=[9] I=[119] J=[64] K=[45] L=[95] M=[15] N=[152].

restriction fragment size reflecting variable tandem reiteration of a 28-base-pair sequence adjacent to the c-Ha-*ras*1 gene itself [16]. There are four common alleles designated A1, A2, A3, and A4. Experimental support for Krontiris' hypothesis has only been forthcoming in the study of breast carcinoma by Lidereau *et al* [79]. The controls in this study were lymphocytes from people without cancer themselves or in close relatives but it is not clear that demographic comparability was assured. No excess of rare alleles was found in one hundred carcinomas from Edinburgh [82]. In that study placentae from women delivering infants in Edinburgh were appropriate controls. McGee's group in Oxford have come to the same conclusion [85]. There is doubt, therefore, whether rare *ras* alleles do relate to increased cancer risk. The recent demonstration that a single nucleotide substitution in the 4th intron of the T24/EJ Ha-*ras* oncogene increases *ras* expression tenfold provides a basis for believing that rare alleles could be important [23].

More definite is the finding of *ras* homozygosity in carcinomas arising in patients heterozygous for *ras* in lymphocytes, presumably due to the deletion of a larger or smaller portion of the short arm of chromosome 11. MacKay *et al* [82] and Theillet *et al* [136] found comparable rates for the evolution of homozygosity in heterozygotes, fourteen of sixty-five and fourteen of fifty-one respectively. Lower rates have been reported [9]. The significance of allelic loss is unclear. According to Theillet *et al* [136] such loss is commoner in oestrogen-receptor negative, high-grade tumours. MacKay *et al* found the same relationship to receptor status and that larger tumours were more likely to show loss. The relatively frequent occurrence of a deletion

on the short arm of chromosome 11, site of human c-Ha-*ras*1, may reflect participation not by that gene itself but by an adjacent anti-oncogene lost during the evolution of breast carcinoma. *Ras* allelic loss in such a case might mark the deletion. The Wilms tumour anti-oncogene is located on the short arm of chromosome 11, although there is no specific evidence linking this locus with breast cancer.

1.10.2 RNA: *ras* transcription

If studies of *ras* genes have not yielded a coherent picture, nor have those of RNA expression. Spandidos and Wilkie [119] reported Ha-*ras*1 mRNA expression in carcinomas at levels 2.5 to fifteen times that in non-neoplastic parenchyma from the same cases, relative to the same quantity of ribosomal RNA. The relative contribution of epithelial and stromal cells in their study cannot be assessed. Sixteen of twenty-two carcinomas examined by Theillet *et al* [136] expressed mRNA complementary to c-Ha-*ras* and not to c-Ki-*ras*, but they did not relate the levels of expression found to those in non-neoplastic breast parenchyma. Biunno *et al* [9] compared twenty carcinomas with white blood cells from the same patients and found elevated transcripts for c-Ha-*ras* in 13, for c-Ki-*ras* in 6, and for c-N-*ras* in 3. The findings of Whittaker *et al* [152] differ in that they found abundant Ha-*ras* mRNA in only one of twenty-three carcinomas while N-*ras* and Ki-*ras* transcripts were not infrequent. These differences may reflect probe specificity and stringency of hybridization and detailed comparisons between studies are compromised by variations of technique.

1.10.3 Protein: ras translation

Neither has a clear picture emerged of ras protein expression in carcinomas. Different studies have used monoclonal [64] and polyclonal [132] antibodies raised against peptide fragments of p21 ras molecules, or monoclonals against cells infected with Harvey murine sarcoma virus [43]. Biochemical and immunocytochemical studies have used different techniques so it is not surprising that varied findings are reported. Nonetheless some of the differences observed are hard to explain even on this basis. Thus four immunocytochemical studies [15,41,45,95] employing the same monoclonal antibodies have reported quite divergent findings. Ohuchi et al [95] used mouse monoclonal RAP-5, from the RAP series generated by immunization with synthetic peptides corresponding to amino acids 10-17 of normal and mutated p21 ras [64]. They showed marked differences between immunoreactivity of normal breast parenchyma, usual and atypical hyperplasias, carcinoma in situ and invasive carcinoma, with a marked trend towards increased expression in the more abnormal epithelial elements. They studied formalin-fixed paraffin-embedded tissues and stated that an identical pattern of staining was obtained on the same material with rat monoclonal Y13-259 [43]. Fromowitz et al recorded strong staining of carcinomas with RAP-5 without staining of normal parenchyma [41]. But, also studying formalin-fixed paraffin-embedded tissue, Ghosh et al [45] employed the same antibody and could detect no differential immunoreactivity between benign and frankly malignant tissues. A similar gulf separates the results of Candlish et al [15], using rat monoclonal Y13-259 on acetone-fixed cryostat sections, who found a pattern similar to that seen by Ghosh et al [45], from those of Ohuchi et al [95] using the same

antibody on formalin-fixed paraffin-embedded tissue. At least a major difference in technique exists in this latter example. Otherwise differences in reactivity make one suspect that different antibodies are being described. Confusion in print between different anti-p21-ras antibodies occurs; in the report by Horan Hand et al [64], in which the RAP antibodies were originally described, detection of p21 ras in paraffin sections is reported with Furth's antibody 'YA6-259', which was not among the eight reported by Furth and may be a confusion of Y13-259 with one of the four YA6 series antibodies. Another paper [54] imprecisely truncates Y13-259 to 'Y259' throughout.

Biochemical evidence from two studies using Western blots with Y13-259 corroborates those immunocytochemical studies which have suggested a large difference in p21 ras expression between benign and malignant breast tissue. De Bortoli et al [27] found a fivefold or greater elevation in p21 ras in 21 of 43 carcinomas relative to benign breast tissue, and Clair et al [21] found a comparable elevation in 21 of 54 carcinomas. Overall, then, the evidence favours elevated expression of a Ha-ras (probably non-mutated) gene in many breast carcinomas.

1.11 Other oncogenes and breast carcinoma

Few studies have addressed other oncogenes and often reports have been concerned with few cases. Thus in the context of a much larger study Slamon et al [117] examined mRNA for a number of oncogenes and were able to demonstrate transcripts of fes, fos, fms, myc, Ha- and K-ras in at least three of four carcinomas, but abl, myb and src not so often. Biunno examined twenty cases for

transcription of eight oncogenes relative to white blood cells and found elevated fos and Ha-ras transcripts in 13 and 15 respectively. They also found c-myc amplification in two of 45 carcinomas examined.

More recently, particular interest has centred on the genes c-erbB1 and c-erbB2. The former is now identified with the epidermal growth factor receptor gene [140]. The latter has 50% sequence homology witn c-erbB1 and is thought to encode a receptor molecule for an as yet uncharacterised ligand [110]. This gene has also been independently discovered in humans and named HER-2 [24] and v-erbB related gene [73] and appears to correspond to rat neu gene [107]. EGF receptor is expressed in breast carcinomas and may be expressed in greater concentration in carcinomas with adverse prognostic features.

Amplification of c-erbB2 was first identified in a breast cancer [73] and the same abnormality has been documented in 15 of 86 carcinomas (17%) examined by Zhou et al [157], and in 2 of the series of 11 by Slamon [116]. Slamon has suggested that c-erbB2 amplification correlates with an adverse prognosis and cautious support for this comes from Zhou et al who found amplification in only one of twenty-one node-negative carcinomas but in eight of thirty-seven node-positive cases. De Vijver et al [141], Venter et al [143], and Gusterson et al [56] showed c-erbB2 amplification associated with increased expression of the encoded protein. The former study contains no clear statement of numbers studied but only two of ten carcinomas with lymph node metastases showed positive staining for c-erbB2 protein in primary or node deposits. A subsequent publication by this group [142] confirmed the close correlation between c-erbB2 amplification and protein expression but did not show a

relationship with relapse-free survival in a series of 187 patients of whom 27 had carcinomas in which c-erbB2 protein immunohistochemistry was positive. Venter et al [143] showed amplification of the gene in 12 of 36 carcinomas. Amplification of c-erbB2 has been shown in a minority of breast carcinomas and although the suggestion that it is related to an adverse outlook is not yet certain this gene and its product certainly merit the attention they currently receive. No other oncogenes show consistent patterns of involvement.

1.12 Approaches to oncogenes in the breast

We have seen from earlier discussion (1.1) that the lesions which are thought to be precursors of breast cancer arise in the terminal duct lobular units (TDLU). As these structures are only one or two millimetres in diameter, biochemical methods appropriate to invasive cancers may not be applicable. In general the methods of DNA, RNA and protein analysis require greater quantities of tissue than are available. Amplification of DNA from single tissue sections, by the polymerase chain reaction, has recently been applied with impressive results, but this method is competent to answer only certain questions about known DNA sequences. Larger quantities of tissue could be analysed but at the expense of precise knowledge of what is being examined. Even if it were possible to examine a representative histological preparation, the heterogeneity of the tissue would remain a problem, as it is unusual for a population of lobules all to show the same abnormality. Widespread ductal carcinoma in situ (DCIS) is not uncommon but is an advanced lesion; the morphological features of carcinoma are already fully developed. Immunohisto-chemistry and in situ hybridization preserve morphology and allow some

assessment of biochemical activities within tissue. Adaptations of these methods do allow some degree of quantitation, which is likely to become a more routine feature of such studies than at present, but there are considerable technical problems.

In their studies of the sub-gross anatomy of breasts from women with breast cancer and of random autopsy material, Jensen and her colleagues showed that the number of atypical lobules varies dramatically. Sometimes one or two lesions are found, while in other cases there are several hundred. In the latter it is not difficult to obtain material for further study while in the former chance plays a part. The method used by Jensen would have limited utility for immunohistochemistry and _in situ_ hybridization studies because the whole breast is fixed. However, Jensen _et al_ proposed a related but simpler and more flexible technique to obtain unfixed altered and atypical units, by staining thin slices of tissue with methylene blue in an ice-cold culture medium and examining the fresh slices under the dissecting microscope; tissue could be selected on the basis of staining. Jensen used this method to obtain altered lobules for experiments on the angiogenic response obtained when these lobules were implanted in the anterior chamber of the eye of the rabbit; and it has been used to obtain morphologically normal lobules for studies of thymidine labelling in normal breast [47]. Compared to the examination of cleared fixed tissue stained with haematoxylin, this method has two disadvantages. One is that the tissue is still viable and excludes dye, thereby preventing appreciation of morphological details. The other disadvanatage is that what staining does occur is confined to the superficial layers of the slice. These considerations

notwithstanding, it was felt that this method offered the best approach to obtaining altered and atypical parenchma which could be examined by immunocytochemistry. The selection of unfixed tissue would make it possible to use cryostat sections with monoclonal antibodies such as the the pan-*ras* reactive rat monoclonal Y13-259, which recognises an epitope which does not survive formalin fixation and paraffin embedding [153].

This thesis concentrates on expression of p21 *ras*. Antibodies which work well in paraffin embedded tissue have only recently become available for certain oncogene products, for example c-*erb*B2. Antibodies which were available, and were evaluated in preliminary work, include anti-*myc* monoclonal antibodies 6E10 and 9E10, antibodies directed against the epidermal growth factor receptor, and monoclonal antibody Ki-67, directed against a proliferation marker. None of these antibodies yielded satisfactory immunostaining in paraffin embedded tissue, whether fixed in conventional formaldehyde-based fixatives, or PLP and PLPD.

CHAPTER 2 SUPRAVITAL STAINING AND TISSUE SELECTION: METHODS

2.1 Patients selected for study

The study population was composed of women with benign and malignant breast conditions treated surgically at Longmore Hospital, Edinburgh. All women with carcinomas received surgery as part of primary therapy; women who had received radiotherapy, chemotherapy, or surgical or medical endocrine manipulations were excluded. Most carcinomas were treated by mastectomy or wide local excision. A few wedge biopsies of advanced carcinomas were included. Cases were selected without defined age limits but there was a bias towards women in their fourth and fifth decades in whom atypical parenchymal lesions were more likely to be present [150]. Some needle localization biopsies were included.

2.2 Collection of tissue

Some benign biopsies were collected unfixed from the operating theatre. Most biopsies and mastectomies from malignant cases were brought unfixed to the department. Almost all cases included in the present study were examined by the author, sectioned, and tissue chosen for diagnosis and other procedures as detailed below. Pathological reporting was supervised by Dr. T.J. Anderson. When particularly fresh tissue was wanted specimen examination and sampling were done at Longmore Hospital as soon as the specimen was available in theatre. In general tissue slicing was performed within an hour of excision.

2.3 Supravital staining

The method of Buhring and Jensen was followed [13]. Fresh tissue was sliced into sheets 3-4mm thick using disposable dermatome blades on a perspex jig. Blocks for conventional histology were selected and remaining tissue immersed in ice-cold nutrient medium or Ringer's solution containing methylene blue with periodic agitation until staining was strong enough to permit appreciation of parenchymal architecture.

2.4 Examination and microdissection

Stained tissue was examined under a Leitz dissecting microscope with a long operating distance and zoom magnification x6 to x50. Areas of interest selected for further examination were either dissected out with ophthalmic scissors and forceps, with which single lobules or stromal strips bearing several lobules were dissected free, or larger, more conventional blocks were selected.

2.5 Cryostat sectioning

Microdissection yielded 1-5mm tissue fragments which were placed in ice-cold nutrient medium or Ringer's solution. When collection was complete, they were floated in OCT embedding medium on a cryostat chuck as a close-packed group in the same plane, and frozen with solid carbon dioxide. A covering of further OCT put on just before complete freezing ensured good support round tissues and facilitated sectioning. 4-5 micron sections collected on gelatin-coated slides were air-dried at room temperature for thirty minutes.

2.6 Fixation of tissues

2.6.1 Composition of fixatives

Almost all tissues were fixed in one of four fixatives. These were Carson's solution [17], which is a buffered formaldehyde-based fixative, periodate-lysine-paraformaldehyde (PLP)[89], its dichromate derivative (PLPD)[63], and acetone. Carson's fixative is our routine fixative for diagnostic paraffin histology and was used for that purpose. Acetone was used initially as a fixative for cryostat sections as it gives good antigenic preservation although morphological preservation is poor. PLP and PLPD were used in an attempt to combine good antigenic and morphological preservation in paraffin embedded tissues. Details of the composition of these fixatives are given in chapter 9.

PLP and PLPD were chosen because published data indicated that these fixatives preserved lymphoid antigens which did not survive well in conventionally fixed paraffin-embedded tissue [63]. Determined attempts were made to exploit Carson's fixed material as success would have given access to a considerable body of archival material. Pre-digestion with pepsin and trypsin for a variety of times (1-24 minutes) and detection systems (including ABC and IGS) were explored unsuccessfully. In addition to PLP and PLPD, half-strength PLP containing 1 per cent rather than two per cent paraformaldehyde gave excellent Y13-259 immunoreactivity but poor morphology, for which reason it was abandoned.

2.6.2 Fixation schedules

After air-drying for 30 minutes, cryostat sections were fixed by immersion in acetone for 10 minutes at room temperature, air-dried and stored in sealed boxes at -70C until needed.

3mm tissue blocks in cassettes were fixed by immersion in freshly prepared PLP and PLPD pre-cooled on ice. Fixation was continued for 24-32 hours in a refrigerator at a checked temperature of 4C. Similar blocks for diagnostic histology were fixed in Carson's fixative for 16-24 hours at room temperature.

Fixation time was determined by practical considerations. Tissues were put into fixative during the day (0900-1700hrs) and washing started at 1700hrs next day. This synchronised blocks for the next processing stage. Longer fixation times up to 72hrs had no adverse effect on immunoreactivity.

2.7 Tissue washing

Blocks fixed in PLP and PLPD were washed overnight (16 hours) in running tap water (average temperature 18C) to remove residual dichromate which can react with alcohol during processing to form an insoluble pigment. PLP-fixed blocks were washed similarly in order to eliminate major processing differences between PLP and PLPD fixed tissues, and to keep blocks from the same case 'in step' during processing.

2.8 Paraffin embedding

Tissues fixed in PLP and PLPD were processed at room temperature (20-24C) on a Histokinette. Dehydration through graded alcohols was followed by clearing in chloroform and xylene followed by impregnation with a paraffin wax (Raymond Lamb) melting at 56C. Measured temperature of the wax bath was 58-60C and blocks were embedded in the same wax.

2.9 Preparation of paraffin sections

All sections were cut on Leitz microtomes at 4um. Initial sections stained with Meyer's heamatoxylin and eosin were assessed to select blocks for immunohistochemistry. Sections from these selected blocks were cut, mounted on gelatin-coated slides, dried at 56C, and stored at room temperature before use.

CHAPTER 3 SUPRAVITAL STAINING AND TISSUE SELECTION: RESULTS

3.1 Supravital staining

Examination of supravitally stained unfixed breast tissue with the dissecting microscope was rewarding in several ways. Unfixed tissue retained its natural texture, which was informative. Small lesions were palpable and diffuse alterations invisible to the eye could be appreciated by touch in a manner impossible in rigid, leathery fixed tissue. Occasionally diffuse infiltration by lobular invasive carcinoma was suspected in tissue which looked normal. Even unstained tissue gave some idea of the number and distribution of lobular units was apparent, because the specialized myxoid stromal tissue surrounding parenchymal units was translucent and appeared darker than the white, opaque, collagenous extralobular stroma.

A property of viable tissue is its ability to exclude vital dyes, and breast tissue was no exception. Parenchymal elements showed little tendency to stain with methylene blue. Colour contrast was subtle and could be difficult to appreciate. Illuminating the tissue through an orange filter increased contrast but the effect was weak by comparison with methylene blue staining of fixed tissue which took up the stain strongly. If the plane of section passed through an unfixed parenchymal unit, the cut surface took up the dye more than if the plane of section was tangential to a unit which retained its integrity.

Some parenchymal alterations were characteristic under the dissecting microscope. Normal lobules could usually be appreciated because they formed a dominant population,

and occasionally the epithelium took up enough dye to make clear that there was no abnormal cellularity. At the other extreme, the cell groups of invasive carcinoma (figure 3.1) sometimes took up dye more readily than benign epithelium and revealed a characteristic streaming, infiltrative pattern, often extending between adipocytes. It was almost always possible to be certain when dealing with invasive carcinoma. Lesions such as sclerosing adenosis, which might have simulated an infiltrative pattern, were usually distinguishable by an organoid nodular pattern. The elastotic centres of radial scars and complex sclerosing lesions, so characteristic histologically, were also prominent under the dissecting microscope, having an ivory hue quite distinct from white collagen. Dye uptake revealed the radial parenchymal distribution while the absence of characteristic streaming distinguished larger lesions from carcinoma. Cysts were conspicuous when larger than one or two millimetres in diameter. Phagocytic cells in lymphatics were an exception to the general reluctance of cells to absorb dye. Lymphatic networks around parenchymal units were often outlined by chains of intensely stained cells, presumably macrophages. This property was useful on occasion as it sometimes revealed the distribution of non-staining epithelial elements within a unit. Red cells in capillaries did not take up dye.

Other parenchymal changes were inapparent or inconspicuous in supravitally stained tissues. The subgross studies of Wellings and Jensen showed that a variety of different cellular processes affecting lobules were attended by similar changes of overall form. Thus distension and coalescence of ductules could be associated with cyst formation, epithelial hyperplasia of

Figure 3.1. Supravitally stained breast tissue showing invasive carcinoma of no special type. The infiltrating pattern is subtle but almost diagnostic. x60.

usual type, atypical hyperplasias of ductal or lobular type, and carcinoma in situ. In supravitally stained tissue these could all appear very similar although distinctive features were sometimes found. Ductal carcinoma in situ of comedonecrotic type was characterised by an abnormally thick epithelial lining with opaque white-to-yellow central necrosis (figure 3.2). Duct ectasia could look similar but lacked thick epithelium and the inspissated luminal content was less solid than the necrotic material in DCIS. Lobular carcinoma in situ was sometimes distinguished by distention of lobular units (figure 3.3) but if distention was absent, as often in atypical lobular hyperplasia, such units were very difficult to tell from normal.

3.2 Tissue selection

The initial approach to tissue selection for further study was microdissection. This was time consuming and yielded relatively few lesions. Lack of specificity was a disadvantage. Frequently an interesting-looking, potentially hyperplastic lobule turned out to be merely a small cluster of interconnected apocrine cysts. This sometimes became obvious when one of the cysts was punctured during dissection and the group collapsed. When it became apparent that good immunocytochemistry could be performed on tissues fixed in PLP or PLPD and embedded in paraffin, the collection strategy was changed. Supravital staining was continued, but instead of selecting individual units for study, larger areas of tissue were selected to include all identifiable tissue changes and 2-12 tissue blocks per case were selected for fixation and paraffin embedding. The final selection of areas for immunohistochemistry could be based on

Figure 3.2. Supravitally stained breast tissue showing ductal carcinoma in situ. Thickened epithelium and opaque necrotic material in the lumen are typical. x10.

Figure 3.3. Supravitally stained breast tissue showing a lobule with ductules expanded by lobular carcinoma in situ. This expansion is the only clue to the pathological process. The epithelium effectively excludes methylene blue. x80.

haematoxylin and eosin stained sections of these blocks, with greatly improved precision over supravital staining alone. The quality of histological preservation is demonstrated in the next section, which also serves to illustrate important morphological changes in breast parenchyma, discussed in the introduction in relation to cancer risk.

3.3 Histology

PLP and PLPD both gave satisfactory morphological preservation of breast parenchyma for critical assessment of histology. The atlas of lesions which follows (figures 3.4-3.13) is confined to material fixed in PLPD, which was the fixative used for immunohistochemical assessment, and serves to illustrate the morphological groupings used in these studies, which have been referred to in the introduction, and to illustrate the good quality of the histology obtained. All photographs are of preparations from which material was selected for immunohistochemical study.

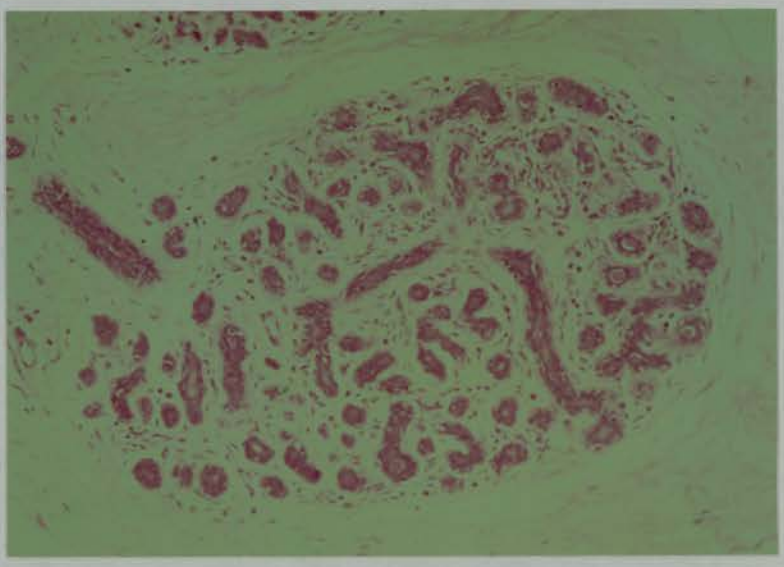

Figure 3.4. Normal lobule. The terminal duct enters the lobule at the 11 o'clock position. x40

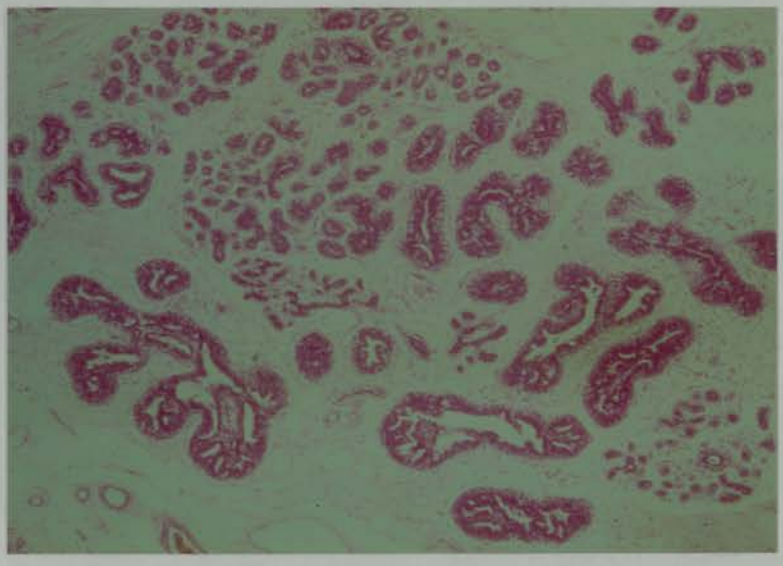

Figure 3.5. Mild hyperplasia of usual type (ductal). Some parenchymal units are expanded, with papillary epithelial proliferation. Normal lobular units are also present. x25

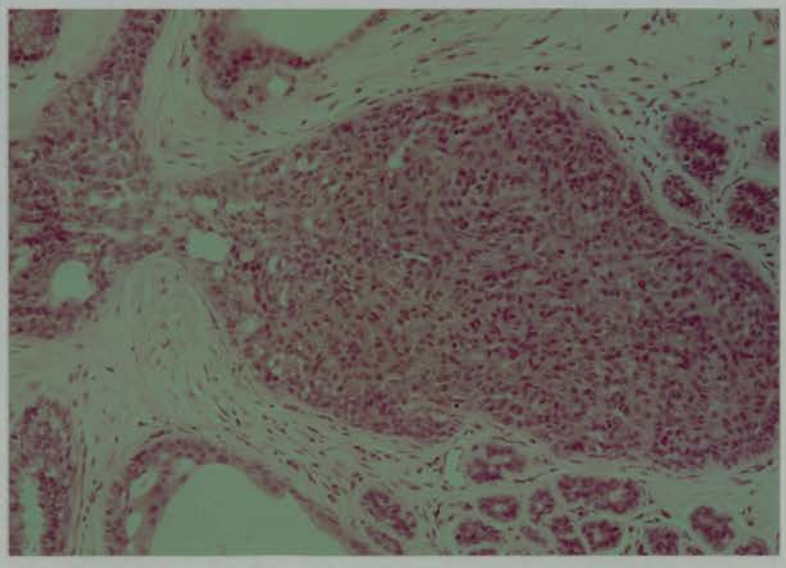

Figure 3.6. Florid hyperplasia of usual type (ductal). The enlarged central unit is filled by a heterogeneous population of cells with small slit-like spaces. Cytological features are benign. x40

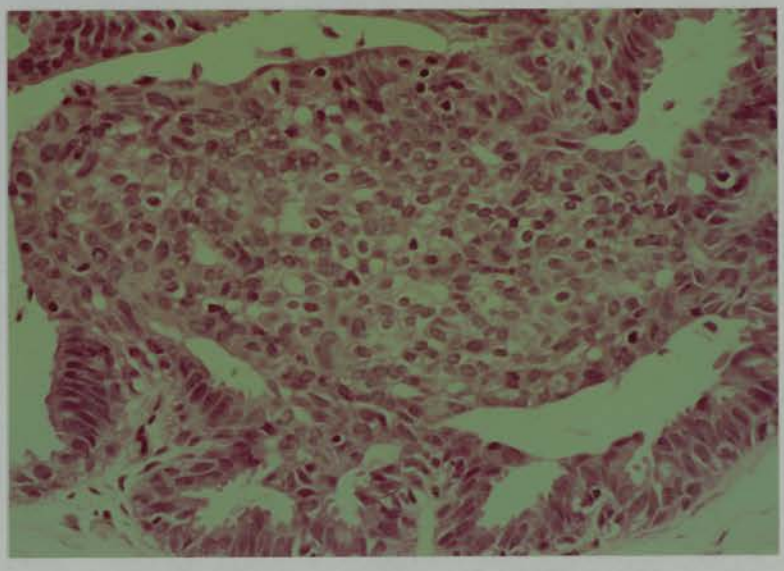

Figure 3.7. Atypical ductal hyperplasia: Cellular monotony with mild cytological atypia and punched-out spaces are atypical. Full criteria for DCIS are not met. x100

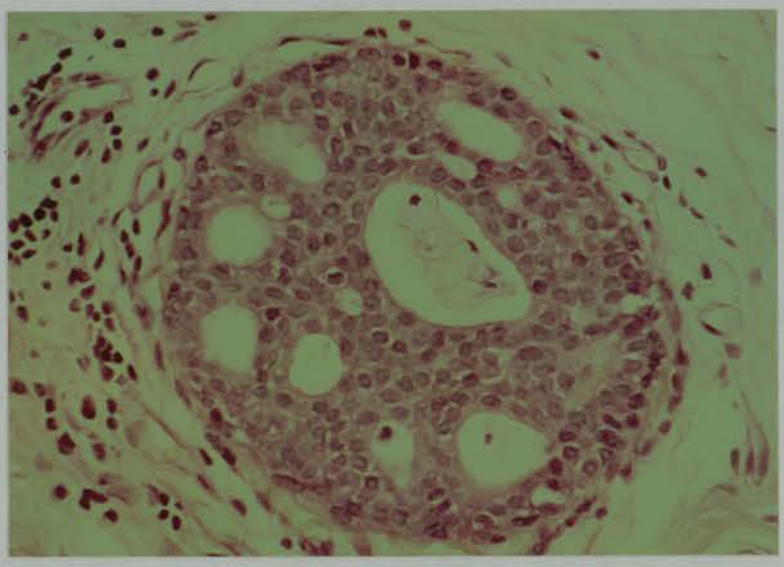

Figure 3.8. Ductal carcinoma in situ: Cribriform type. Contrast with figure 3.13. The monotonous cellular population and structural uniformity identify this as DCIS. x100

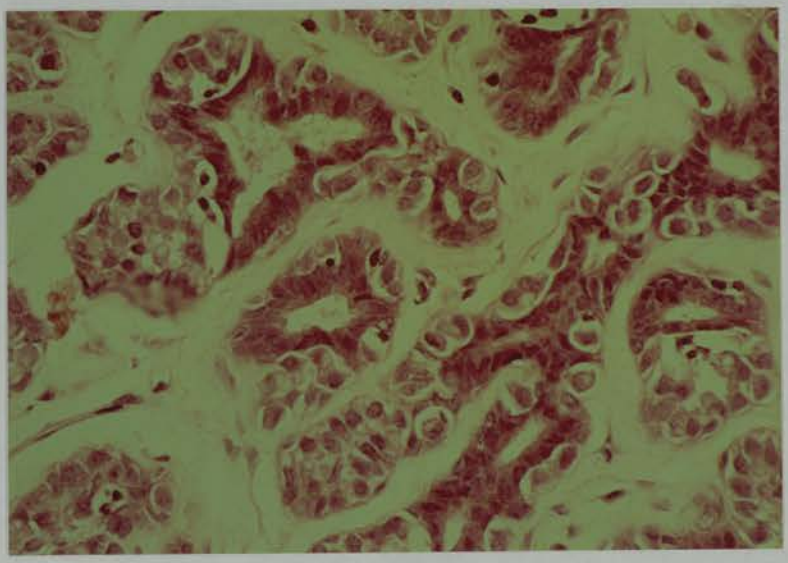

Figure 3.9. Atypical lobular hyperplasia. Normal epithelium infiltrated by small atypical cells with pale cytolasm and intracytoplasmic lumina. Residual normal epithelium identifies this as ALH. x100

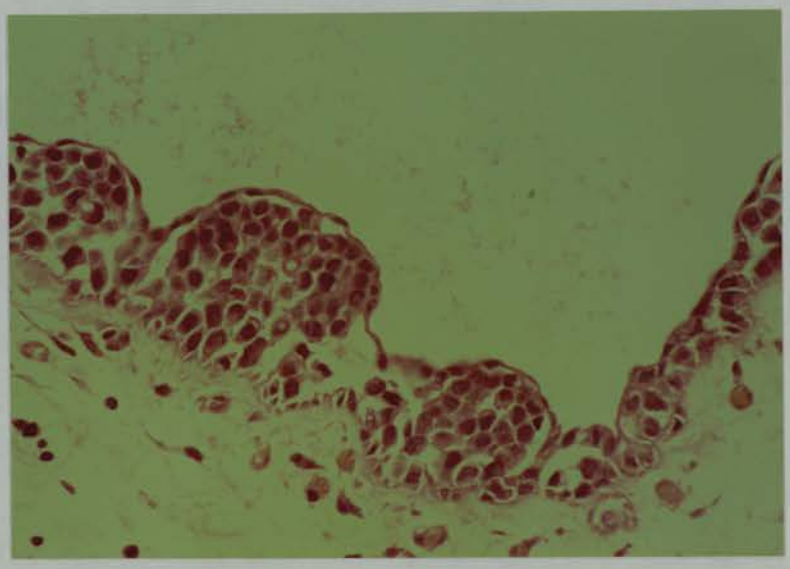

Figure 3.10. Ductal involvement by cells of ALH. Attenuated normal epithelium is stretched over groups of ALH cells in which intracytoplasmic lumina are obvious. x100

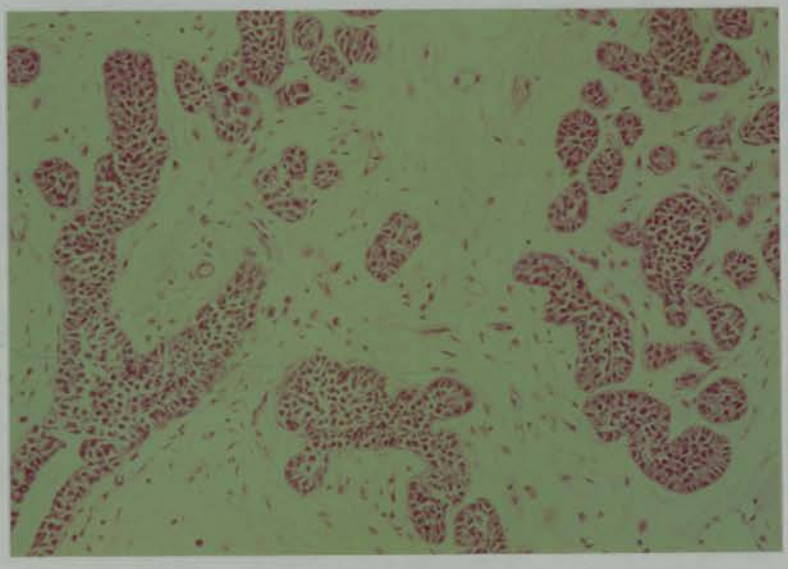

Figure 3.11. Lobular carcinoma <u>in</u> <u>situ</u>. Characteristic atypical cells occupy the entire lobular unit and are present in the terminal duct (lower left), in which there are remnants of normal epithelium. Lobular expansion is minimal. x40

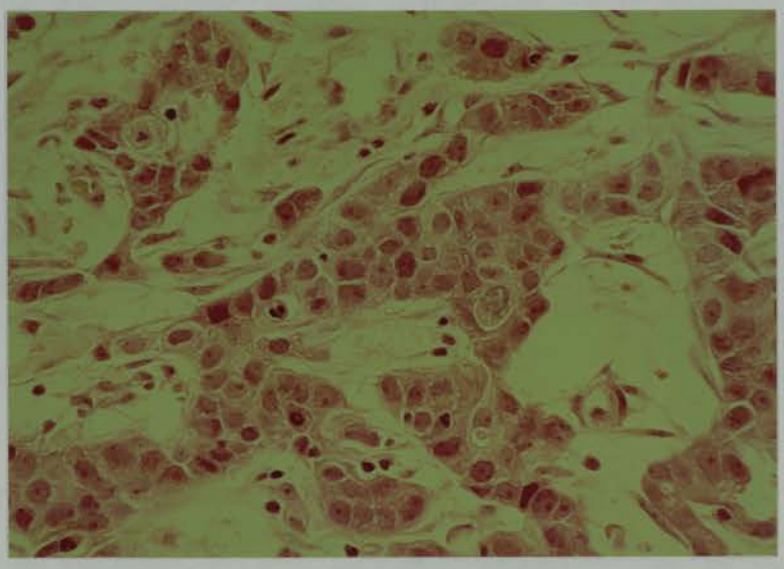

Figure 3.12. Invasive carcinoma: No special type. Irregular nests of pleomorphic cohesive malignant cells are typical. x100

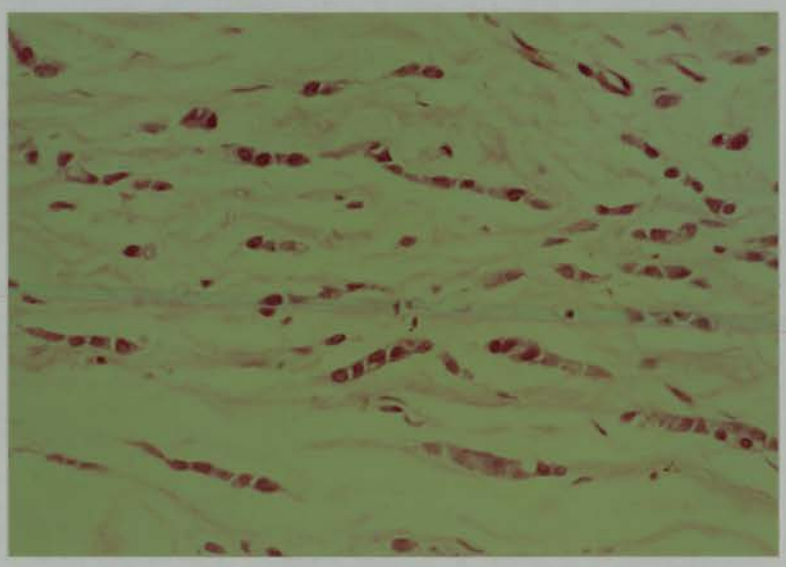

Figure 3.13. Invasive carcinoma: Lobular type. Single files of small malignant cells stream through the tissue. Intracytoplasmic lumina are present in some cells. x100

CHAPTER 4 IMMUNOCYTOCHEMISTRY FOR LIGHT MICROSCOPY: METHODS

4.1 CHL cells and the cell line FHO5T1

FHO5T1 and CHL cells provided positive and negative controls for immunochemistry. They have been described by Spandidos and Wilkie [122]. Briefly, the FH05T1 cell line was derived by transfection of an early passage Chinese hamster lung fibroblast strain (designated CHL) with the plasmid pHO5T1, which contains the mutationally activated human T24 Harvey-*ras* oncogene ligated to viral enhancing sequences.

4.2 Conditions of culture

FH05T1 and CHL cells were maintained in Dulbecco's modification of minimum Eagle's medium, containing 10 per cent newborn calf serum, penicillin, and streptomycin. Cell suspensions were prepared from monolayers by treatment with 0.02 per cent EDTA and 0.1 per cent trypsin in Dulbecco's phosphate buffered saline (PBS) and washing in PBS.

4.3 FHO5T1 experimental tumours

Female CBA mice about 6 weeks old, immune-deprived by thymectomy, whole-body irradiation and treatment with cytosine arabinoside, were obtained from the colony prepared by Dr CM Steel, MRC Human Genetics Unit, Edinburgh. Subcutaneous injection of FHO5T1 cells engenders malignant fibroblastic tumours as described by Wyllie *et al* [156]. Samples of such tumours sliced to 3-5mm were placed immediately in PLPD. Fixation and

subsequent processing were as described for human tissues.

4.4 Preparation of cell cultures for microscopy

4.4.1 Cytospin preparations and smears

Twenty microlitres of suspensions containing five million FHO5T1 or CHL cells per ml of culture medium were used to prepare air-dried smears on plain slides subsequently fixed in acetone for 10 minutes. PLP and PLPD fixation of such preparations detached the cells. Cytospin preparations on plain or gelatin-coated glass slides were fixed in acetone for control purposes. Smears and cytospins were used at once or stored at -70C in sealed containers.

4.4.2 Agar-paraffin cell blocks

The most useful control materials (after the FHO5T1 tumours) were prepared by suspending briefly fixed CHL and FHO5T1 cells in low-melting point agarose (FML Bioproducts) and post-fixing before processing to paraffin. Approximately five million cells were fixed for 15 minutes at 4C, washed in PBS, and resuspended in 0.5ml of 2 per cent agarose in PBS at 40C. After setting, this pellet was post-fixed for up to 24h, washed in PBS, and processed to paraffin. Fixatives included PLP, PLPD, half-strength PLP, buffered 4 per cent formaldehyde and 2 per cent glutaraldehyde. Sections were cut as for tissues. These agar-paraffin cell blocks had the advantage of yielding many control sections fixed and processed like tissues.

4.5 Fixatives for control cells and tissues.

As mentioned briefly above, a variety of fixatives were used in the fixation of control cells and tissues. To those mentioned in the last paragraph Carson's fixative [17] may be added. These various fixatives were used for a variety of purposes and are described in more detail where relevant.

4.6 Monoclonal antibody Y13-259

The hybridoma was a gift from Dr Demetrios Spandidos. This well-characterised pan-ras antibody recognises an epitope encoded by a conserved region of the gene and represented in the proteins encoded by Ha-ras, Ki-ras, and N-ras. Activation of the oncogene is not associated with mutation affecting the amino acids recognised by this antibody. There is no specificity, therefore, for mutated or non-mutated forms of ras protein; both are recognised. Antibody was purified by ammonium sulphate precipitation from serum-free culture supernatant and dialysed exhaustively against PBS.

4.7 Storage of antibody Y13-259

Aliquots of 300ul of concentrated dialyzed culture supernatant were stored at -70C in 1ml Eppendorf tubes. For use, the aliquots were thawed and stored at 4C with sodium azide (0.1 per cent w/v) added to prevent infection. To confirm that sodium azide as a preservative did not interfere with immunostaining the results of staining with the primary antibody at four dilutions (1:20, 1:40, 1:80 and 1:160) were compared with and without 0.1 or 0.01 per cent sodium azide. These concentrations of azide exceeded the concentration

obtained when primary antibody preserved with azide at 0.1 per cent was diluted 1:50, which was the usual working dilution. It was determined that azide preservation had no harmful effects on immunostaining. Nor did preserved primary antibody show any deterioration of staining over at least three months, judged on positive control material. This method proved more satisfactory than storage of multiple small frozen aliquots, which gave inconstant immunostaining.

4.8 ABC immunostaining

4.8.1 ABC immunostaining procedures

Avidin-biotin complex immunostaining was selected for its sensitivity and specificity. The protocol is given in chapter 9. Initial immunostaining runs with cryostat sections fixed in acetone were poorly reproducible on positive controls (cryostat sections of FHO5T1 tumours from mice or smears or cytospin preparations of cultured FHO5T1 cells). Variations in technique were tried to improve sensitivity and consistency but changing buffer preparations, batch and lot of second and third layer reagents (biotinylated goat anti-rat antibody and streptavidin-biotin-peroxidase complex), blocking serum, diaminobenzidine, hydrogen peroxide, xylene and alcohols did not help.

An alternative to ABC immunostaining that might be more sensitive was sought, and immunogold-silver (IGS) staining methods were considered [62] in conjunction with specialised fixatives periodate-lysine-paraformaldehyde (PLP) and its dichromate derivative (PLPD). Published data show that these fixatives preserve many antigens which do not survive conventional formaldehyde fixation

and paraffin embedding, especially if sensitive IGS staining methods are used [63]. As cryostat section morphology was poor, the combination of PLP or PLPD fixation, paraffin embedding and IGS staining offered solutions to several difficulties. In practice, consistent immunostaining was achieved when storage of hybridoma culture supernatant preserved with sodium azide at 4C was adopted. It is presumed that the previous variation in staining related to storage of primary antibody as small frozen aliquots. Avidin-biotin complex immunostaining was retained but the good morphology and immunoreactivity of PLP and PLPD fixed paraffin-embedded tissue were reasons for their use in preference to cryostat sections.

Various dilutions of Y13-259 (1:10, 1:20, 1:30, 1:40, 1:50, 1:60, 1:80, 1:100, 1:120, 1:160, 1:200, 1:400, 1:800, 1:1600, 1:3200) were used on breast and control tissues to establish optimal conditions. It was found that the dilution subsequently employed (1:50, corresponding to 50 µg/ml) gave most consistently reproducible immunostaining of positive control material (FHO5T1 cells and tumours) and breast tissue, with acceptably low background.

It was noted informally in the course of this optimization process that as greater dilutions of Y13-259 were used, immunostaining of DCIS and invasive carcinoma decreased by equivalent amounts with each increase in dilution. This was noticed in several cases but not formally quantified.

4.8.2 ABC immunostaining specificity

Positive and negative controls ensured sensitivity and specificity of immunostaining. The FHO5T1 cell line as cultured cells and as tumour in immune-deprived mice was the cornerstone positive control (figures 4.1, 4.2). Every run included positive control slides, often more than one, to provide checks on inter- and intra-run variability. A variety of negative controls were included. Omission of primary antibody, replacing it with buffer plus blocking serum alone, was a standard control included for every slide examined. This allowed appreciation of endogenous peroxidase activity and avoided confusion with natural or artefactual pigments.

A second control used in some runs was to replace Y13-259 with non-immune rat polyclonal IgG at the same concentration. If such antibody is used without modification, a complex immunostaining pattern is seen in human material (figure 4.3). This is not surprising in view of the complex mixture of antibodies present. A more useful control was obtained by absorbing rat polyclonal immunoglobulin with acetone-treated human liver powder [92]. This removes cross-reacting antibodies and such absorption essentially abolished immunostaining (figure 4.4), which implied that non-specific reactions with the Fc portion of the immunoglobulin molecule were unimportant. Figure 4.5 shows the same carcinoma immunostained with Y13-259.

A third negative control, of a different type, was provided by CHL cells which express p21 <u>ras</u> at levels 30-60 times less than FHO5T1 cells [156]. Immunostaining of these cells with Y13-259 was always negative (figure 4.6). During routine staining runs, the only positive

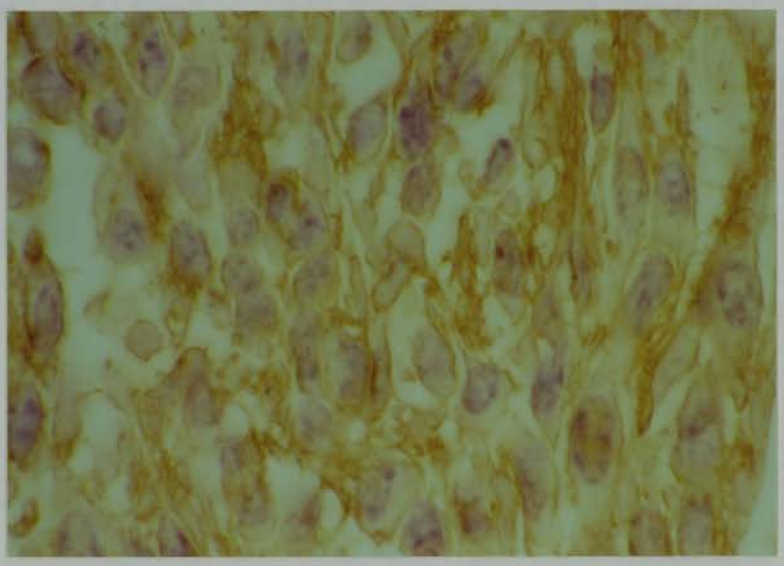

Figure 4.1. PLPD-fixed FHO5T1 cells growing as tumour in immune-deprived mice. Y13-259 50µg/ml, ABC detection. x250

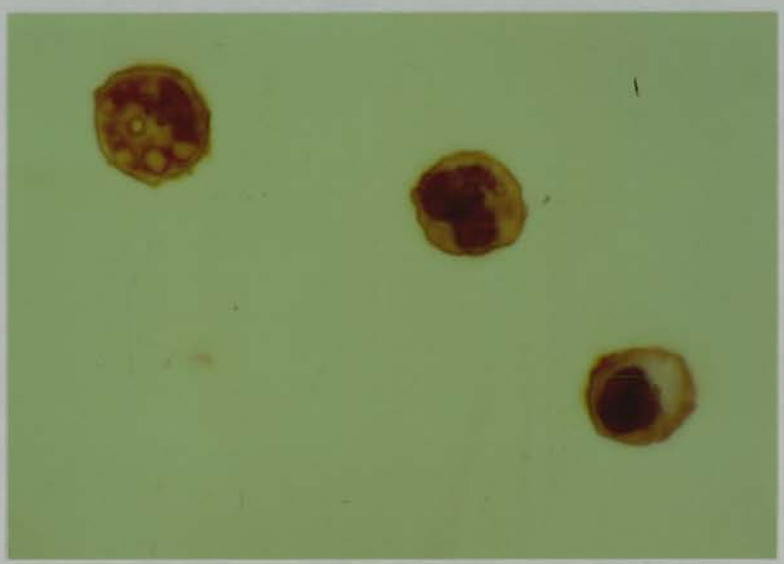

Figure 4.2. PLPD-fixed cultured FHO5T1 cells embedded in agar and paraffin. Y13-259 50µg/ml, ABC detection. x400

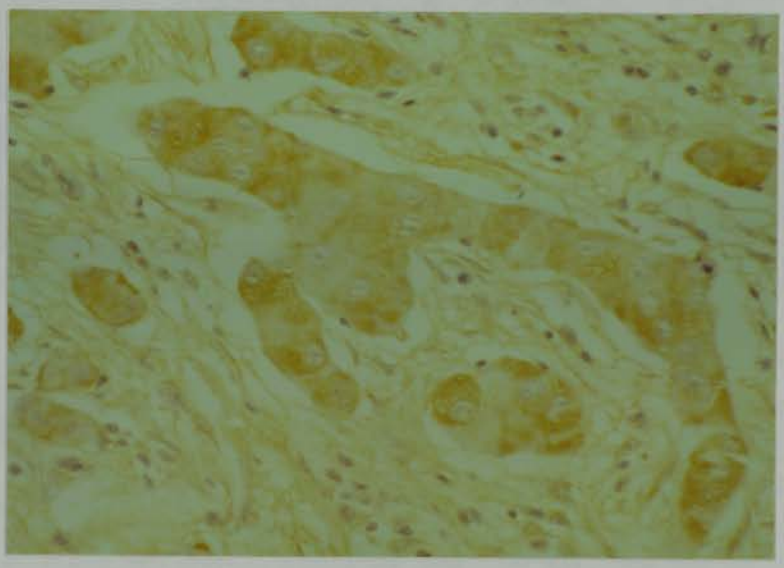

Figure 4.3. PLPD-fixed breast carcinoma. Unabsorbed non-immune rat IgG, 50µg/ml, with ABC detection gave pronounced non-specific immunoreactivity. x250

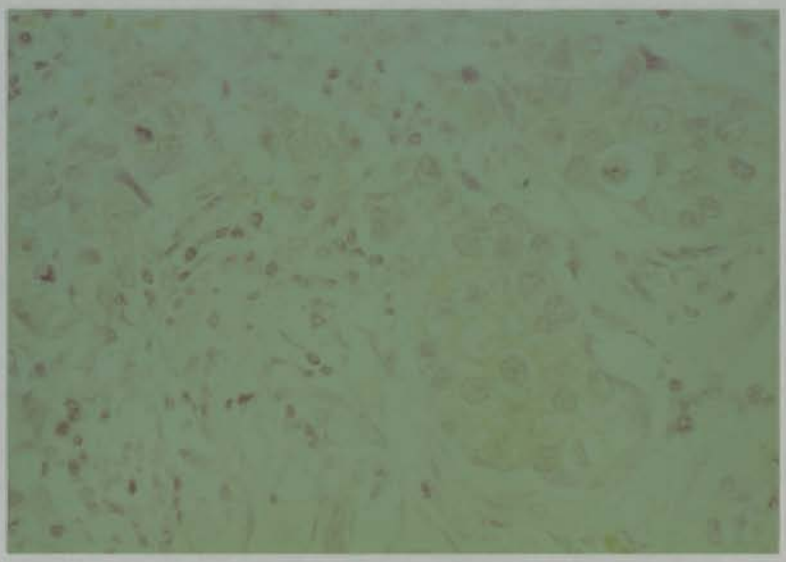

Figure 4.4. The same PLPD-fixed breast carcinoma. Non-specific immunostaining abolished by pre-absorbtion with acetone-treated human liver powder. Absorbed non-immune rat IgG 50µg/ml, ABC detection. x250

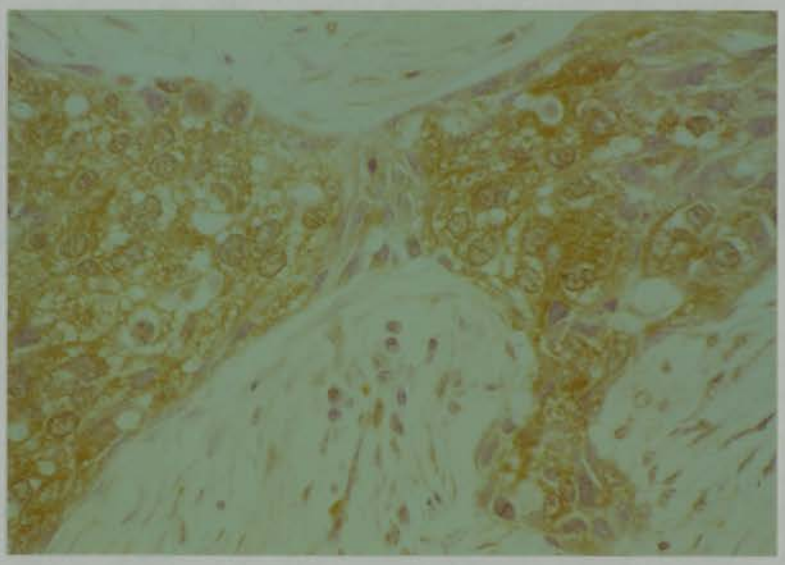

Figure 4.5. The same PLPD-fixed breast carcinoma. Y13-259 50µg/ml, ABC detection. There is strong specific immunostaining. x250

Figure 4.6. PLPD-fixed cultured CHL cells embedded in agar and paraffin. Y13-259 50µg/ml, ABC detection. x400

control always included was a section of PLPD-fixed paraffin-embedded FHO5T1 tumour. Negative controls omitting the primary antibody were processed for every section in every run. Positive control breast sections were not considered necessary in every run. In a run of ten cases there was always positive immunostaining in some or all of the test sections, in particular of elements such as vascular smooth muscle. Experience showed that if FHO5T1 controls showed positive immunostaining, then test sections always did so too.

The relationship between fixation and the level and subcellular distribution of p21 ras was investigated in several ways. Animal FHO5T1 tumours were fixed in PLP or PLPD immediately and after a 10 minute or 1 hour delay, which had no effect on the intensity or distribution of immunostaining. With human tissues, the time between surgery and fixation was always minimised, but in four cases trucut biopsy cores of large malignant tumours were obtained and placed in PLPD within one or two seconds of removal from the breast. These four neoplasms showed typical cytoplasmic rather than membrane staining.

4.9 Measurement of Y13-259 concentration

The concentration of immunoglobulin in purified culture supernatant was measured by Mancini single radial immunodiffusion [68]. Procedural details are given in the chapter 9 but the principle is that antigen put into wells bored in an agar gel containing a known antibody dilution will diffuse from the well until an immunoprecipitin halo forms when antigen-antibody equivalence is reached. Mancini showed that the diameter of the halo is proportional to antigen concentration. Polyclonal goat anti-rat IgG (Sigma) diluted 1:10 and

1:20 was used to precipitate Y13-259 from culture supernatant diluted 1:5-1:80 and immunoprecipitation ring diameters were standardized against dilutions of rat IgG 10 mg/ml (Sigma). At least 48 hours were allowed for equilibration before gels were stained with Kenacid Blue R to enhance rings which were measured to the nearest 0.1mm with a magnifying eyepiece micrometer. Figure 4.7 shows the rings. Figure 4.8 represents one experiment comparing ring diameters for dilutions of Y13-259 culture supernatant (unknown) and of rat IgG, 10mg/ml standard. The lines fitted by least squares are parallel and show the standard concentration was four times that of Y13-259, which was therefore 2.5mg/ml. Identical results were obtained on repeating the test.

To see whether absorption of non-immune rat immunoglobulin with acetone-treated human liver powder materially reduced the concentration of immunoglobulin, Mancini gels were set up using the same dilutions of unabsorbed and absorbed immunoglobulin. The result is depicted in figure 4.9 and no difference in immunoglobulin concentration can be detected.

4.10 Immunogold-silver staining

Immunogold staining has developed since the 1970s and silver enhancement widens its applicability. Many different proteins may be adsorbed onto colloidal gold and methods exist for the preparation of colloidal particles as small as 3nm. In various sizes these are excellent probes for electron microscopy. For light microscopy deposition of metallic silver on gold nuclei by 'physical development' confers signal amplification up to several orders of

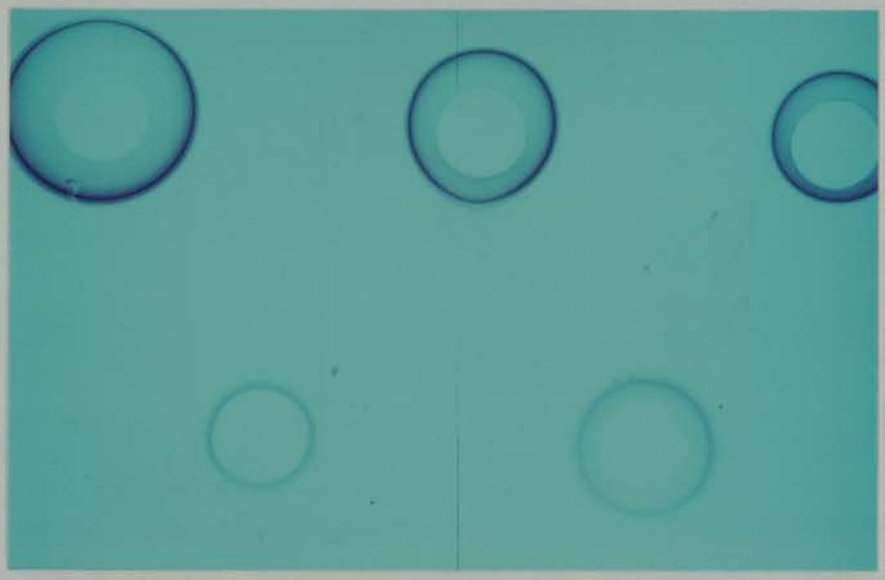

Figure 4.7. Immunoprecipitation rings in Mancini gel intensified with Kenacid Blue R. x3

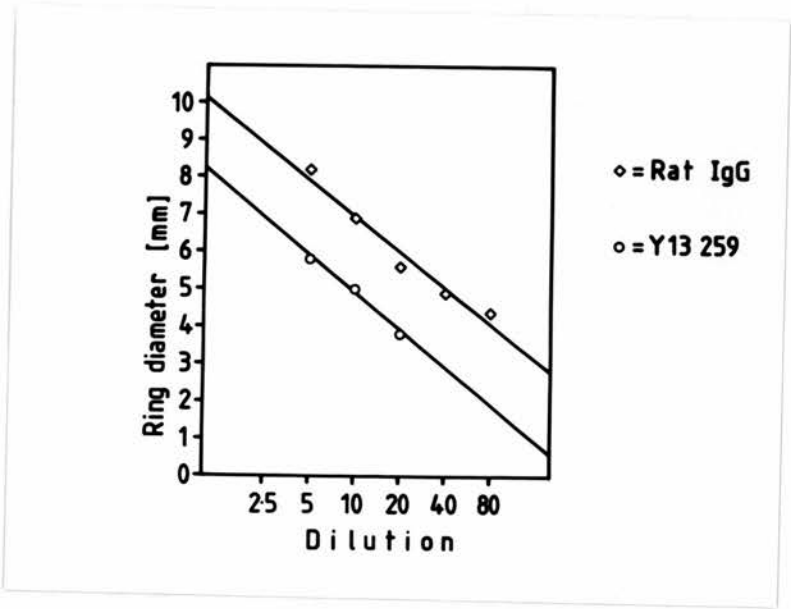

Figure 4.8. Ring diameters in Mancini gels for rat IgG standard (known concentration) and Y13-259 (unknown) for different dilutions. Dilutions of rat IgG four times greater than Y12-259 for same ring diameter imply same ratio of concentrations.

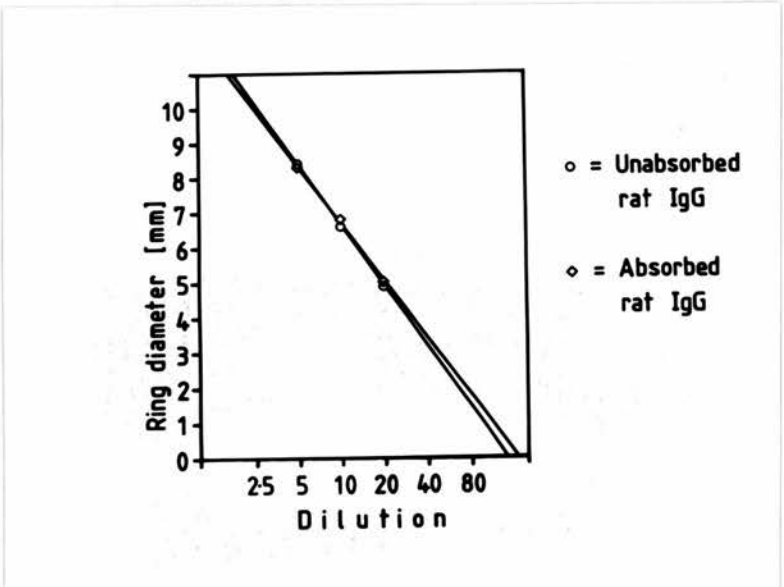

Figure 4.9. Ring diameters in Mancini gels for non-immune rat IgG before and after absorbtion with acetone-treated human liver powder. Absorbtion did not measurably reduce IgG concentration.

magnitude permitting detection of scarce antigens or use of high dilutions of primary antibody in immunochemical procedures. These properties suggested IGS staining when it was proving difficult to get good ABC immunostaining with Y13-259. In practice, although IGS staining worked well (figure 4.10), once the problems with ABC immunostaining had been solved, it offered no routine advantage and was not therefore used for most light microscopic work but has been used for electron microscopy.

Several authors state that maximum sensitivity of IGS staining requires pre-treatment of sections with Lugol's iodine solution for 5 minutes [62,63,124]. The use of Lugol's iodine was investigated and it was shown that exposure of sections to Lugol's iodine before the primary antibody was applied invariably abolished immunostaining whether applied for 5 seconds, 5 minutes or intermediate times. This was true for ABC detection and IGS staining. Iodine was clearly inimical to the epitope recognised by Y13-259 and its use was abandoned.

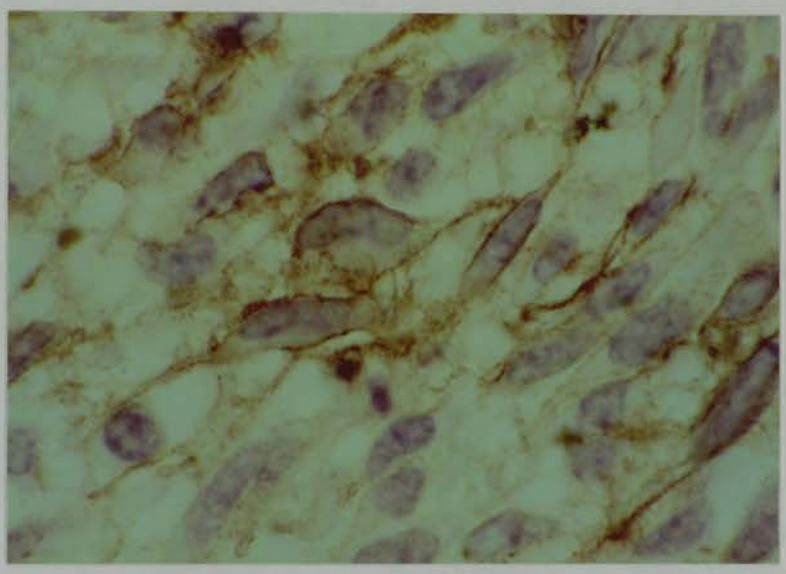

Figure 4.10. PLPD-fixed FHO5T1 cells growing as tumour in immune-deprived mice. Y13-259 50µg/ml, IGS detection. x400

CHAPTER 5 IMMUNOCYTOCHEMISTRY FOR LIGHT MICROSCOPY: RESULTS

5.1 Results: Control tissue

In this chapter qualitative accounts of Y13-259 immunostaining in controls and breast are followed by a description of the development and validation of a semiquantitative scoring system incorporating extent and intensity of immunostaining. Results for different cell populations of normal and abnormal breast are presented in terms of this score, which permitted statistical testing of staining differences between populations. Discussion of results follows in chapter 8.

5.1.1 ABC Immunostaining

Once methodological problems were resolved reliable immunostaining of FHO5T1 cells, whether as smears, cytospins, agar-paraffin blocks, or growing as experimental tumours was attained. Immunostaining was predominantly related to plasma membrane, especially in experimental tumours (figures 4.1, 4.10). Cells harvested from culture showed membrane but also some cytoplasmic staining. Omission of primary antibody or replacement with absorbed non-immune rat immunoglobulin gave no staining.

Scoring of immunostaining was confined to runs in which positive controls showed strong positive staining, and the range of appearances of the test sections were considered to be representative on the basis of previous experience. "Positive" staining was regarded as the presence of an unequivocal signal; very weak signals were not considered acceptable evidence of immunostaining,

although in the scoring process borderline positivity was scored appropriately (+/-). Vascular smooth muscle, being consistently positive in test sections, were useful internal positive controls.

PLPD gave better preservation of Y13-259 immunoreactivity in agar-paraffin blocks than PLP. This was probably a consequence of the lower aldehyde concentration in PLPD rather than any positive effect of the dichromate, because half-strength PLP, which has exactly the same composition as PLPD without dichromate, gives if anything better immunoreactivity than PLPD, but poorer morphology.

5.1.2 Immunogold-silver staining

Immunogold-silver staining gave similar results to ABC detection. Using the first version of Janssen's 'IntenSE' silver enhancement kit (see chapter 9 for details) it was possible with repeated cycles of enhancement to attain very strong signals (figure 4.10) but for routine use the more cumbersome procedure had no advantage, nor was the ratio of signal to background any better.

5.2 Results: Breast Tissue

5.2.1 General description

Most breast tissue showed some immunoreactivity with monoclonal antibody Y13-259. In general, tissues fixed in PLPD showed stronger immunoreactivity than tissues fixed in PLP, but with slightly stronger background staining. Tissues fixed in Carson's fixative (a buffered formaldehyde solution) showed minimal or no immunoreactivity. As some authors have found that Y13-

259 immunoreactivity survives in formaldehyde-fixed paraffin-embedded tissues [95], this was explored by comparing the results of immunostaining of separate portions of three carcinomas each fixed in PLP, PLPD and Carson's fixative and processed together to eliminate variation in post-fixation conditions. Superiority of PLP and PLPD was obvious. Figures 5.1 and 5.2 illustrate immunostaining in PLPD and Carson's fixed tissue. As morphological preservation was perhaps slightly better with PLPD, this fixative was favoured for routine assessment. Among non-neoplastic tissues, some elements consistently showed immunostaining. Most notable were the smooth muscle in small muscular blood vessels, myoepithelial cells, and cells showing apocrine metaplasia. Epithelium of large and small ducts showed heterogeneity of staining within and between cases. In general, hyperplastic epithelium stained more strongly than non-hyperplastic epithelium. Other stromal elements usually showed little staining. In general, most cancers (both invasive and non-invasive) showed strong immunostaining and were generally stronger in their staining than adjacent benign epithelial elements. Atypical proliferations appeared to stain with intermediate intensity. Strong membrane staining was rare in human breast tissue, including carcinomas. Figure 5.3 shows an exception: In this lobular carcinoma *in situ* membrane staining was obvious, although there was also cytoplasmic staining. Cf. figures 4.5 and 5.1.

To investigate these relationships further a method of codifying staining was necessary, which would have a semi-quantitative relationship to p21 *ras* expression if possible. The approach devised is described in the next section.

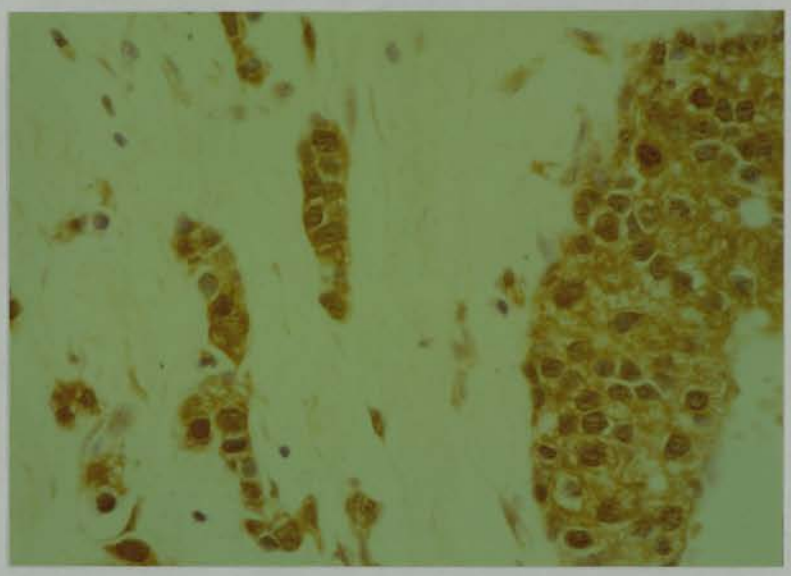

Figure 5.1. PLPD-fixed paraffin-embedded breast carcinoma. Y13-259 50µg/ml, ABC detection. Same case as figure 5.2. x250

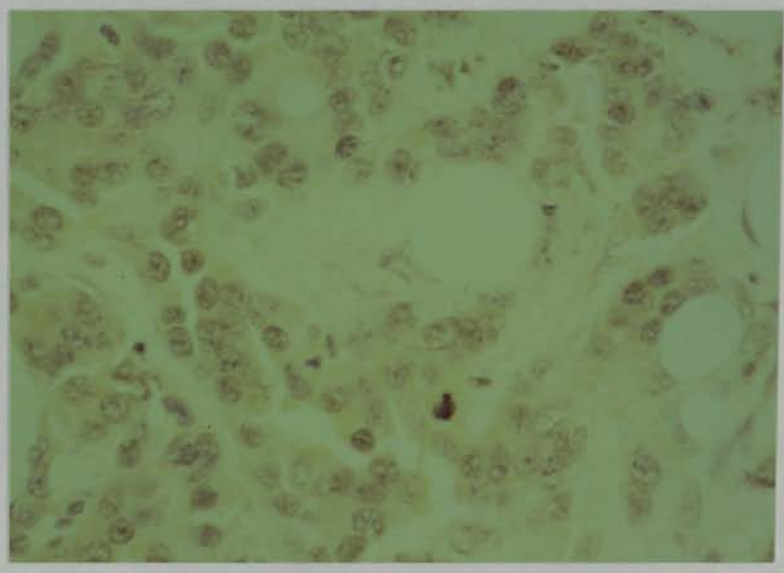

Figure 5.2. Carson's-fixed paraffin-embedded breast carcinoma. Y13-259 50µg/ml, ABC detection. Same case as figure 5.1. x250

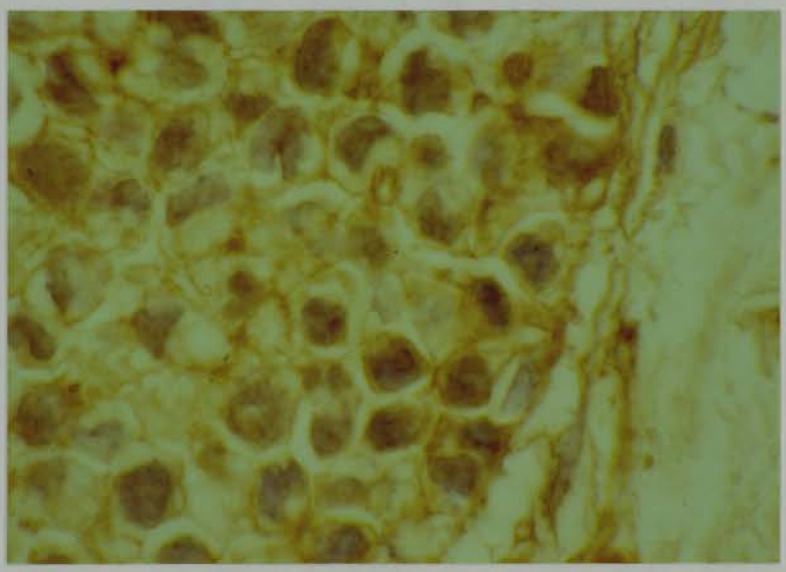

Figure 5.3. PLPD-fixed lobular carcinoma *in situ* showing membrane staining. Y13-259 50µg/ml, ABC detection. x400

5.2.2 Quantification of staining

Immunocytochemistry presents problems for quantitation, chiefly because the relationship between intensity of staining and quantity of antigen is non-linear, rising steeply with increasing antigen at low concentrations of antigen but flattening off and scarcely rising with large increases when the antigen is more abundant [52]. Nonetheless the same source shows that a relationship does exist and given reasonably reproducible positive controls from run to run a scoring system is worthwhile. A four point score for intensity of staining was adopted, as follows. No staining, score 0; weak, equivocal staining (+/-), score 1; definite positivity (+), score 2; strong positivity (++), score 3. The other chief variable is the percentage of cells immunostaining within a given population. As staining heterogeneity was marked, it seemed proper to incorporate this into a scoring system. This was estimated by determining for a particular element whether positivity was present within 0-25 per cent, 25-50 per cent, 50-75 per cent, or 75-100 per cent of cells. These were scored as 1,2,3, or 4 in that order. These two scores, representing extent and intensity, were combined as shown in table 5.1. No staining scored 0. Weak, equivocal staining of less than 50 per cent of cells scored 1, greater than 50 per cent scored 2. The scores for positive or strongly positive staining were added to the extent score as shown in table 5.1. Thus the overall score was from 0 to 7 (no staining, to more than 75 per cent of cells strongly positive).

Elements scored included normal epithelium and stroma, hyperplastic, atypical, and neoplastic epithelium and other elements (table 5.2). In order to determine

		Extent score			
		1	2	3	4
Intensity score	0	0	0	0	0
	1	1	1	2	2
	2	3	4	5	6
	3	4	5	6	7

Table 5.1. Combined scoring system for immunocytochemistry.

	Epithelium	Myoepithelium	Stroma
Normal parenchyma:			
Large ducts	( )	( )	
Small ducts	( )	( )	
TDLU	( )	( )	
Normal stroma:			
Lobular stromal cells			( )
Extralobular stromal cells			( )
Vascular smooth muscle			( )
Nerve			( )
Sclerosing units:			
Sclerosing adenosis	( )	( )	( )
Radial scars	( )	( )	( )
Cyst epithelium:			
Apocrine	( )		
Papillary apocrine	( )		
Flattened epithelium	( )		
Hyperplastic epithelium:			
Ductal	( )		
Ductal, atypical	( )		
Lobular	( )		
Lobular, atypical	( )		
Non-invasive carcinoma			
DCIS	( )		
LCIS	( )		
Invasive carcinoma (Type:	)		
Carcinoma cells	( )		( )
Carcinoma in lymphatics	( )		
Carcinoma in lymph nodes	( )		

Table 5.2. Structural elements for which scores were assigned.

reliability and validity of scoring, forty-two cases were scored twice, on separate occasions and without reference to the previous score on the second occasion. This allowed scores to be compared for 311 separate epithelial and stromal elements. The result of this exercise is presented in figure 5.4. The areas of squares are proportional to the number of paired scores in each cell of the matrix. Complete concordance is represented by squares on the diagonal from lower left to upper right, ie tied pairs. The smallest squares represent single pairs of scores. Overall agreement is good (Spearman rank correlation coefficient 0.75, $p<0.001$). There is no evidence of systematic bias in either direction between the two comparisons (Wilcoxon matched-pairs signed-ranks test).

A few outlying single points in figure 5.4 represent poor reproducibility of scoring. It is not unusual to see variation in the intensity of immunostaining within a single section, particularly near the edge where staining intensity may be stronger, if evaporation concentrates reagents, or weaker, if reagents are not spread uniformly over the section. Considerable care was taken during immunostaining to avoid these effects, but they are difficult always to eliminate, and it is not always easy to be certain which area of staining of a section is truly representative. It is considered that the small number of markedly discrepant points represent different interpretation of the correct area to score on separate occasions.

A second exercise compared scores for 155 elements present in a further 26 cases for which tissue fixed in PLP and PLPD was available. PLP and PLPD fixed tissues were scored separately and independently as before.

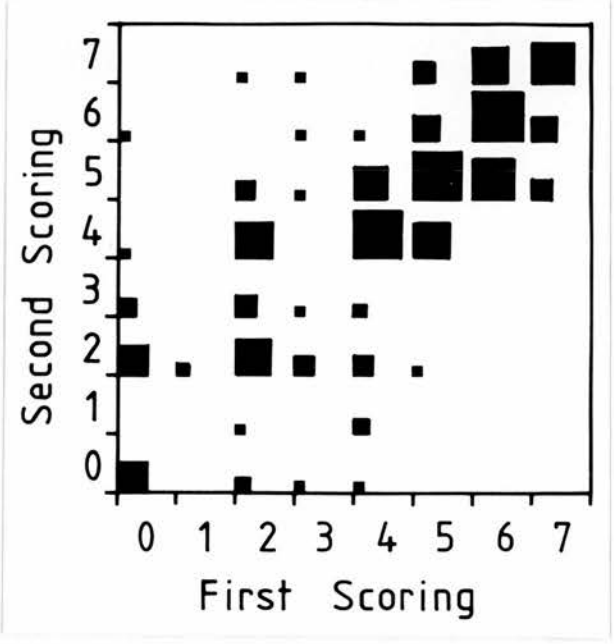

Figure 5.4. Comparison of repeated scoring of immunostaining for 311 paired observations from 42 cases. Area of squares is proportional to number of pairs in that box. Smallest squares represent single pairs.

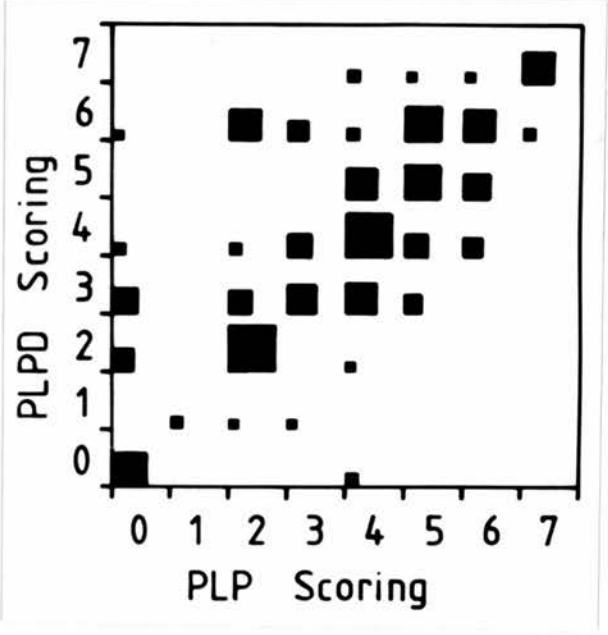

Figure 5.5. Comparison of scoring for 155 paired observations from 26 cases fixed in PLP and PLPD. Construction as figure 5.10.

Results are presented in figure 5.5. Again correlation is good (Spearman rank correlation coefficient 0.67, $p<0.001$). In this case there is a systematic bias, scores for PLPD fixed tissue tending to be higher than those for tissues fixed in PLP (70 ties, 53 with PLPD score greater than PLP score, 32 with PLP score greater than PLPD score; $p=0.02$). This confirms the subjective impression that antigenic preservation is better with PLPD.

These comparisons validated the scoring system and it was adopted for case assessment. This assessment was recorded on the pro-forma in table 5.2 and completed for all cases before data analysis.

It should be noted that the data in figure 5.5, comparing immunostaining of different blocks from the same cases, fixed in PLP and PLPD, allow one to assess the variability of p21 ras immunostaining from block to block, and from staining batch to staining batch. As the variability observed was no greater than that observed on repeated scoring of the same blocks (figure 5.4), it was considered that variability from these sources was not significant.

5.2.3 Results of quantification

It was felt that normal epithelium was the proper standard with which to compare pathological epithelial alterations. The first analysis was to determine whether expression of p21 ras depended upon site in the duct tree, separating large ducts, small ducts and TDLU. These data are presented in figure 5.6 (upper three boxes). Within each box scores are indicated on the x axis while the percentage of cases with that score is

given on the y axis. It will be seen that the patterns are very similar for all three boxes, suggesting no topographic correlation with p21 ras expression. If comparable data for myoepithelial cells are examined, a different but also internally consistent pattern is seen. Larger numbers of cases show stronger staining than for the epithelial cells. To analyse these differences the Kolmorogov-Smirnov two-sample test was selected. This non-parametric test requires no assumptions about data distribution. To perform the test cumulative frequency tables are compiled for the two samples and the maximum unsigned difference between the two cumulative frequencies is determined. This constitutes the test statistic, D. The null hypothesis is that there is no difference between the two samples and the test assesses the probability of a D value as great as that observed. Tabulated values for various sample sizes are available [118].

The Kolmogorov-Smirnov test suggests a graphical representation of the data already presented in figure 5.6, which makes similarities and differences more apparent. This is to plot the cumulative proportion of cases associated with each score rather than the proportion for that score only. Clearly, for any pair of curves, the one on the left represents a set of observations with generally lower scores than the one on the right. Figure 5.7 presents the data for epithelial and myoepithelial cells of large ducts (the data in the two left-hand boxes in figure 5.6). The vertical line indicates D, the greatest difference in cumulative frequency, and for the numbers here, this difference is highly significant ($p<0.001$), confirming the visual impression that myoepithelial cells stain more intensely. In figure 5.8 the data for small ducts and TDLU have been

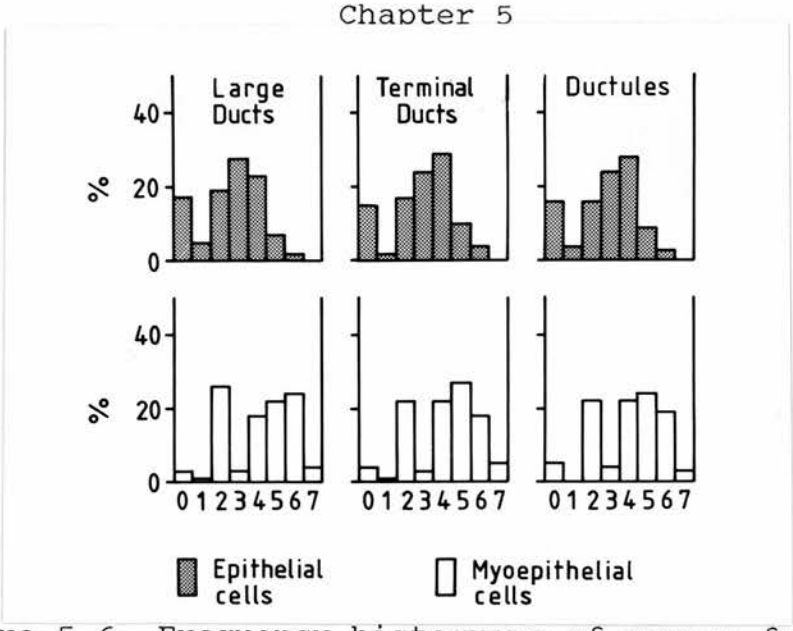

Figure 5.6. Frequency histograms of scores for Y13-259 ABC immunostaining. Normal epithelial and myoepithelial cells in large ducts (148 cases), extra-lobular terminal ducts (144 cases), and ductules within TDLU (153 cases).

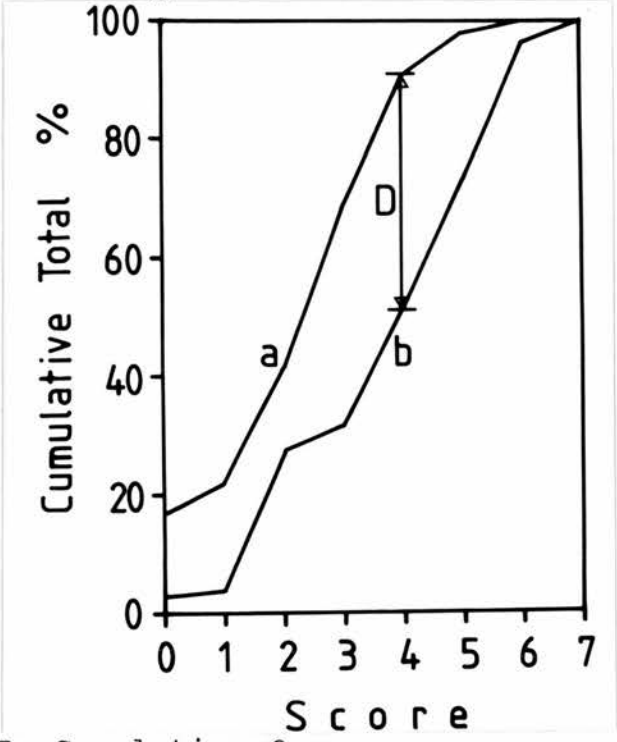

Figure 5.7. Cumulative frequency curves of scores for Y13-259 ABC immunostaining. Normal epithelial and myoepithelial cells of large ducts. D represents the greatest difference between the two curves and constitutes the Kolmogorov-Smirnov test statistic.

added, but rather than give all points, the areas within which the lines for epithelial and myoepithelial cells lie are indicated. It will be seen that the curves for epithelial cells lie within narrow limits as do those for myoepithelial cells. Testing shows no differences between epithelial cells or myoepithelial cells at different loci in the duct tree but highly significant differences between p21 ras expression of epithelial and myoepithelial cells at all levels.

In practical terms it was obvious that it did not matter which ducts were chosen to represent normal epithelium. Lobular ductules were in fact chosen since TDLU are considered to be the units from which precursors of carcinoma arise.

5.3 Expression of p21 ras in ductal hyperplasias and carcinomas

5.3.1 Differences between groups

Scores for p21 ras expression in normal epithelium (156 cases), terminal duct hyperplasia without atypia (72), atypical ductal hyperplasia (33), ductal carcinoma in situ (63) and invasive carcinomas of all types (86) are shown in figure 5.9. The number of cases in each group is given by the bracketed figures above. A trend towards higher scores is seen with increasing deviation from normality, and the large majority of carcinomas show strongly positive staining. This trend is more obvious in figure 5.10, in which cumulative frequency curves are plotted. Five curves yield ten comparisons between pairs of curves and if these are tested for statistical significance, the results in table 5.3 are obtained.

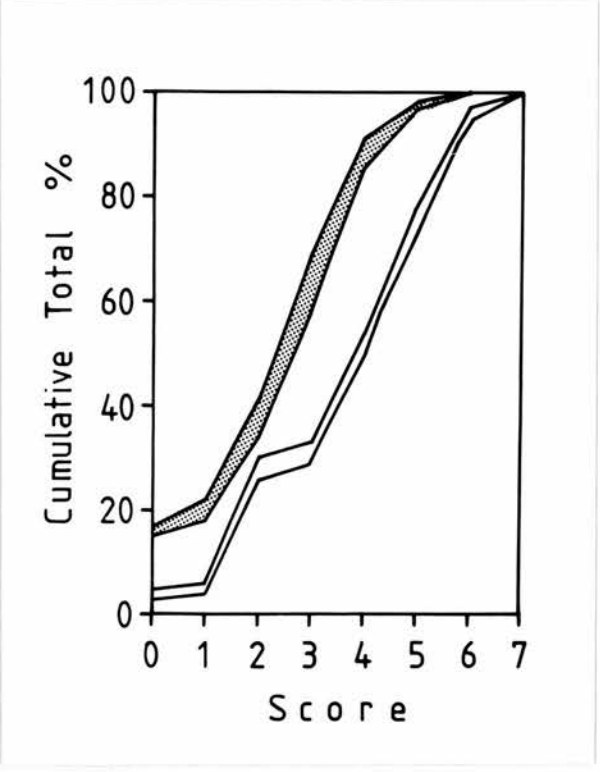

Figure 5.8. Cumulative frequency curves of scores for Y13-259 ABC immunostaining. Same data as figure 5.6. Curves for epithelial cells lie within narrow shaded area irrespective of position in the duct tree. Myoepithelial cell curves all lie in the unshaded narrow zone to the right of the shaded zone.

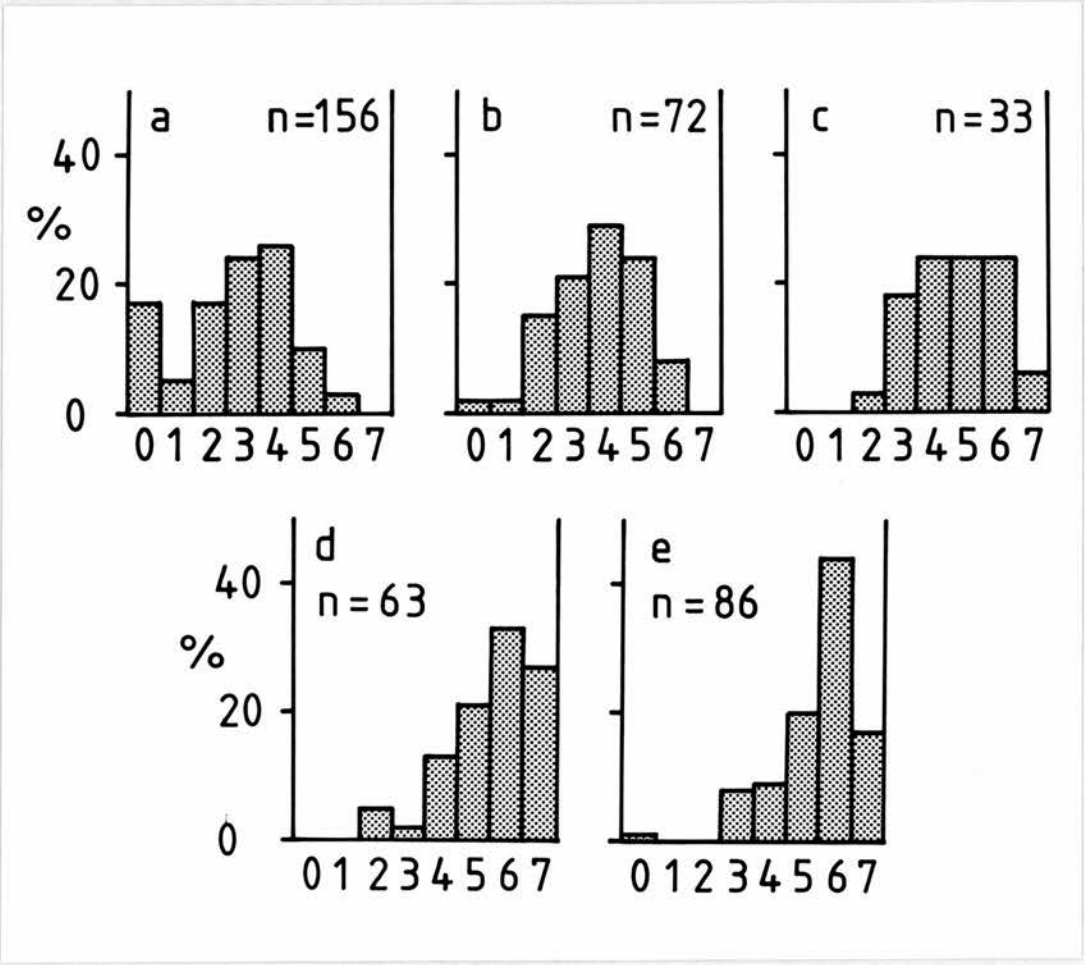

Figure 5.9. Frequency histograms of scores for Y13-259 ABC immunostaining. a, Normal epithelium of TDLU. b, ductal hyperplasia without atypia. c, atypical ductal hyperplasia. d, ductal carcinoma <u>in situ</u>. e, invasive carcinoma (all types).

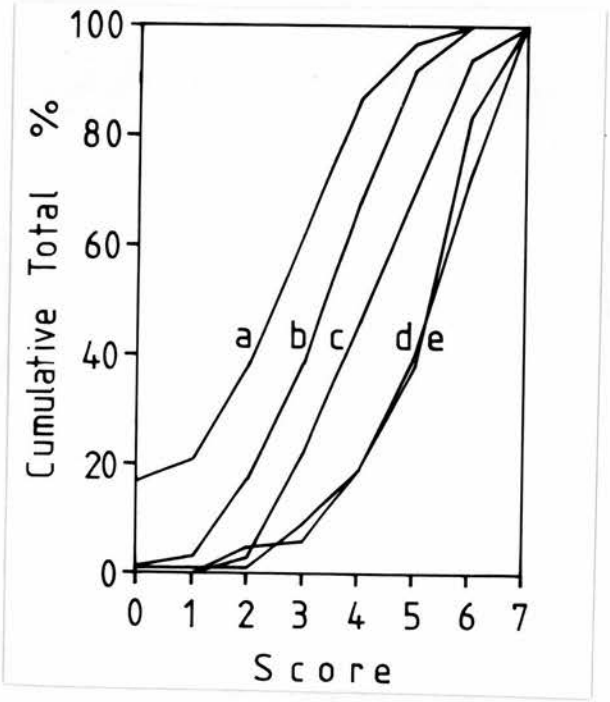

Figure 5.10. Cumulative frequency curves of scores for Y13-259 ABC immunostaining. a, normal epithelium of TDLU. b, ductal hyperplasia without atypia. c, atypical ductal hyperplasia. d, ductal carcinoma in situ. e, invasive carcinoma.

	a	b	c	d
b	p<0.05			
c	p<0.001	p>0.05		
d	p<0.001	p<0.001	p<0.05	
e	p<0.001	p<0.001	p<0.05	p>0.05

Table 5.3. Statistical significance of difference between curves a-e in figure 5.15, assessed by Kolmogorov-Smirnov test. The groups referred to are a= normal epithelium. b= hyperplastic epithelium without atypia. c= atypical ductal hyperplasia. d= ductal carcinoma in situ. e= invasive carcinoma.

Differences between these curves are statistically significant with the exception of d and e, representing non-invasive and invasive carcinoma, these curves being practically coincident; and b and c, representing hyperplasia without and with atypia. While these curves are not coincident, the numbers of cases are smaller (72 and 33 respectively) and if epithelial hyperplasias of usual type (72 cases) are compared with combined atypical hyperplasias of ductal and lobular types (43 cases), stronger immunostaining of atypical hyperplasias is demonstrated ($p<0.05$). Greater expression of p21 ras with greater deviation from normality is firmly established.

Rather than combining scores for extent and intensity of immunostaining as has been done so far, it is possible to present the data separately for the same epithelial populations for which data has been presented in figures 5.8-5.10. This is done in table 5.4 and figure 5.11. In table 5.4 the raw data is presented while figure 5.11 graphs the percentage of cases on the z axis for each combination of intensity and extent of immunostaining on the x and y axes respectively.

A thing of note is that carcinoma cells dying by apoptosis or coagulative necrosis often show reduced expression of p21 ras. These phenomena are illustrated in figures 5.12 and 5.13.

To see whether there is a difference in p21 ras expression between normal lobules from women with cancer, and normal lobules from women without cancer, cumulative scores for epithelial and myoepithelial cells have been plotted in figure 5.14 for 83 and 72 women in these two groups respectively. There is no difference.

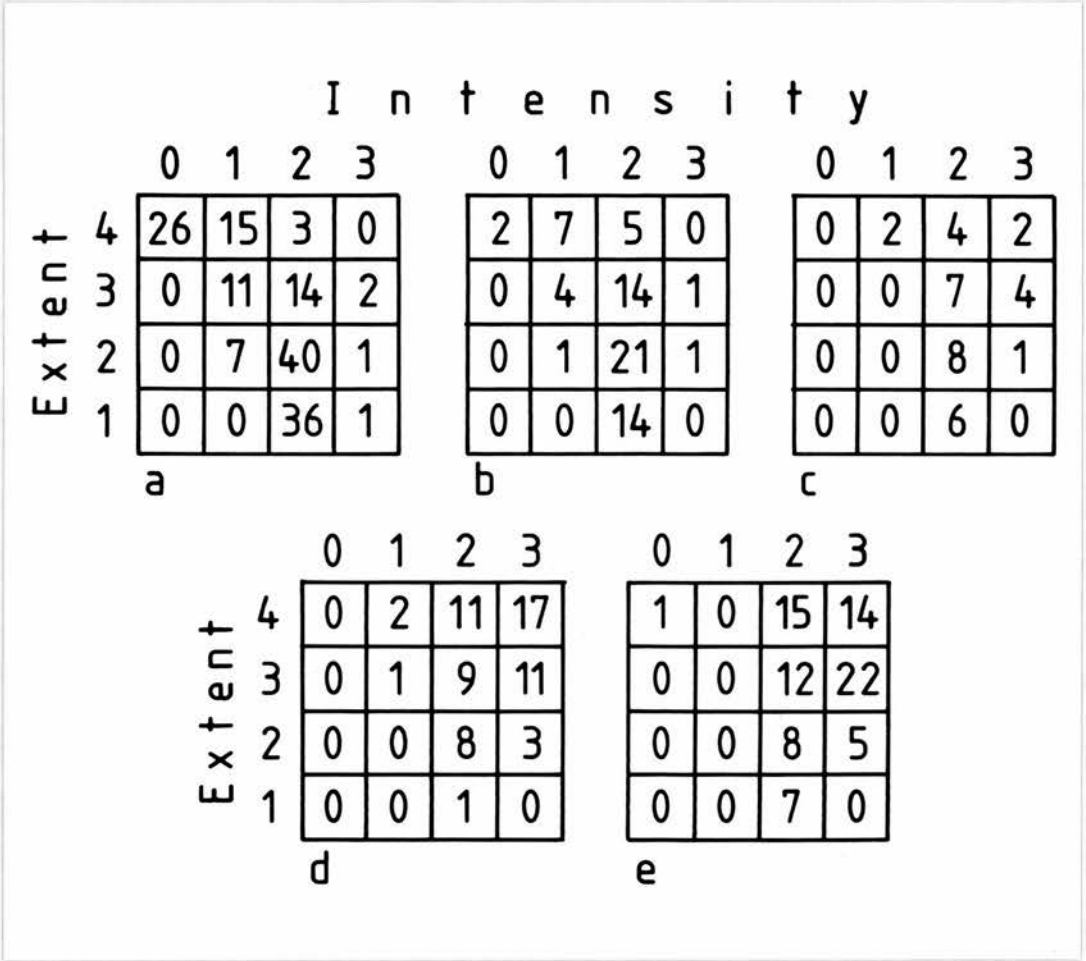

Table 5.4. Distribution of cases by individual scores for intensity and strength of Y13-259 immunostaining. a, normal epithelium of TDLU. b, ductal hyperplasia without atypia. c, atypical ductal hyperplasia. d, ductal carcinoma <u>in situ</u>. e, invasive carcinoma.

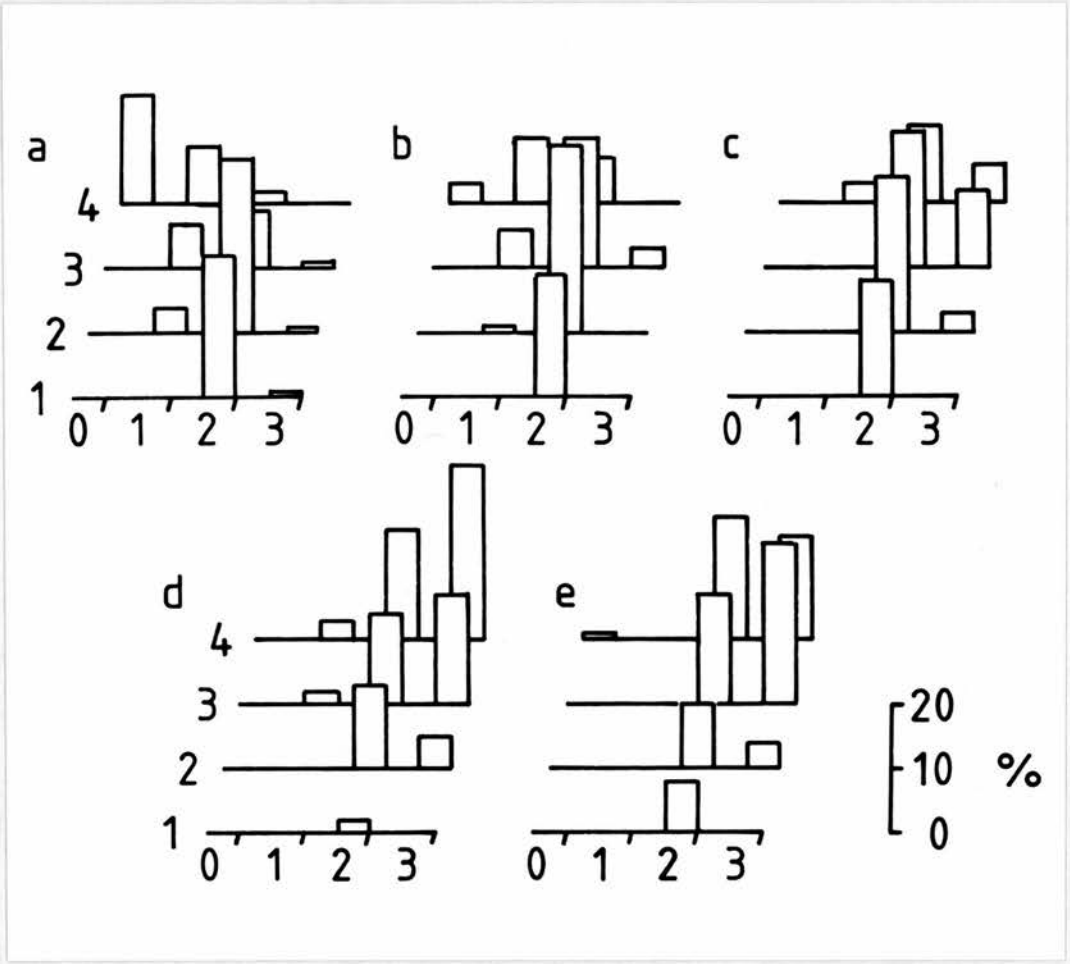

Figure 5.11. Graphical representation of the data presented in table 5.4. Intensity and extent of immunostaining are indicated on the x and y axes while the percentage of cases associated with each score combination is indicated on the z axis.

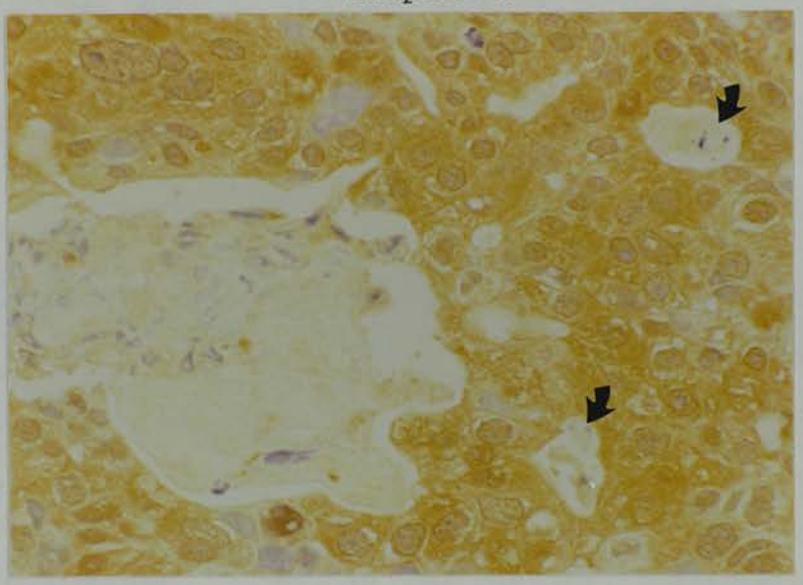

Figures 5.12. Invasive breast carcinoma. Viable carcinoma cells express p21 ras strongly. In the area of necrosis on the left, immunostaining is lost. Scattered apoptotic cells (arrows) are similarly negative. Y13-259, 50 µg/ml, ABC detection. x250

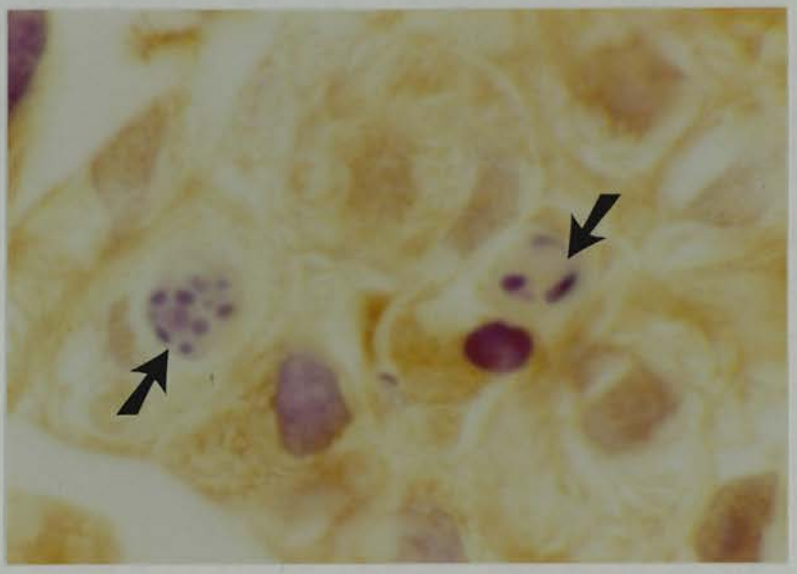

Figure 5.13. Invasive breast carcinoma. Again, viable carcinoma cells express p21 ras strongly. Apoptotic cells (arrows) do not. Y13-259, 50 µg/ml, ABC detection. x400

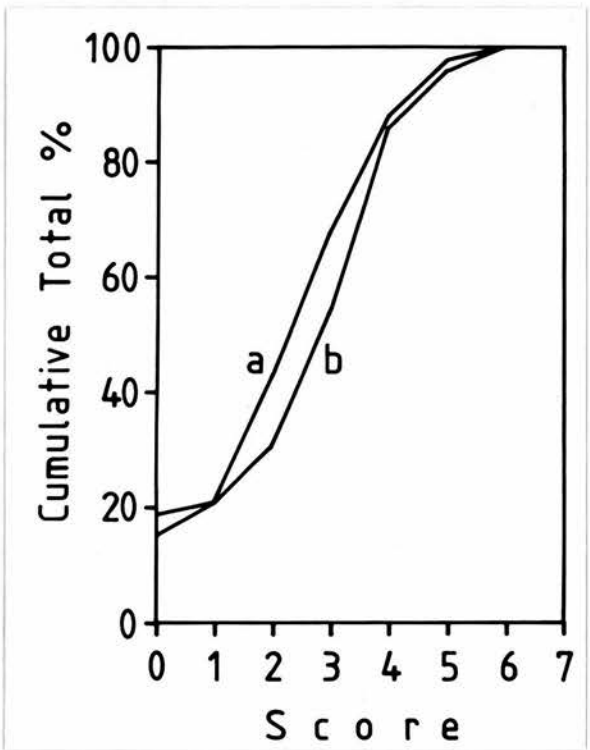

Figure 5.14. Cumulative frequency curves of scores for Y13-259 ABC immunostaining. a, epithelium of normal TDLU from 83 women with cancer. b, epithelium of normal TDLU from 72 women with benign breast disease or no abnormality.

5.3.2 Vascular and lymph node invasion.

Carcinoma cells in peritumoural lymphatics or venules are a bad prognostic sign [25], and for this reason p21 ras expression has been related to the presence or absence of this feature. There are two ways to do this. Expression of p21 ras by carcinoma cells within vessels can be compared with expression by cells of the same carcinoma outside vessels, in other words those in intimate contact with stromal cells. Alternatively expression by carcinomas without vascular invasion may be compared with expression by carcinomes with it. This section presents both comparisons. Lymph node status at primary surgery has also been considered.

An initial attempt to assess blood and lymph vascular invasion separately was rejected as impractical. It is not often possible to be certain whether small vessels are lymphatics or venules. Great care to find endothelial cells was taken to avoid confusing vessels with other tissue spaces and only definite examples of vascular invasion were scored.There were twenty cases in which PLPD-fixed blocks showed carcinoma in vessels as well as embedded in stroma. The cumulative scores for these cases are shown in figure 5.15. The p21 ras score for carcinoma cells in vessels is less than that of the cancers which have given rise to them ($p<0.05$). If these cases, plus a further nine cases which showed vascular invasion in diagnostic blocks fixed in Carson's fluid but not in the PLPD-fixed blocks, are compared with fifty-six cases which showed no vascular invasion in either PLPD-fixed or diagnostic blocks, the curves of figure 5.16 are obtained. There is no difference between these two curves, and no difference, therefore, in p21 ras

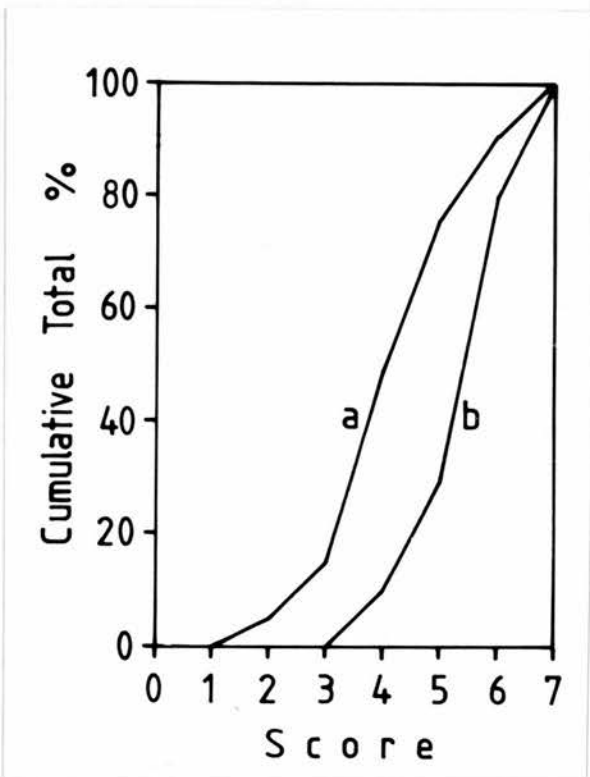

Figure 5.15

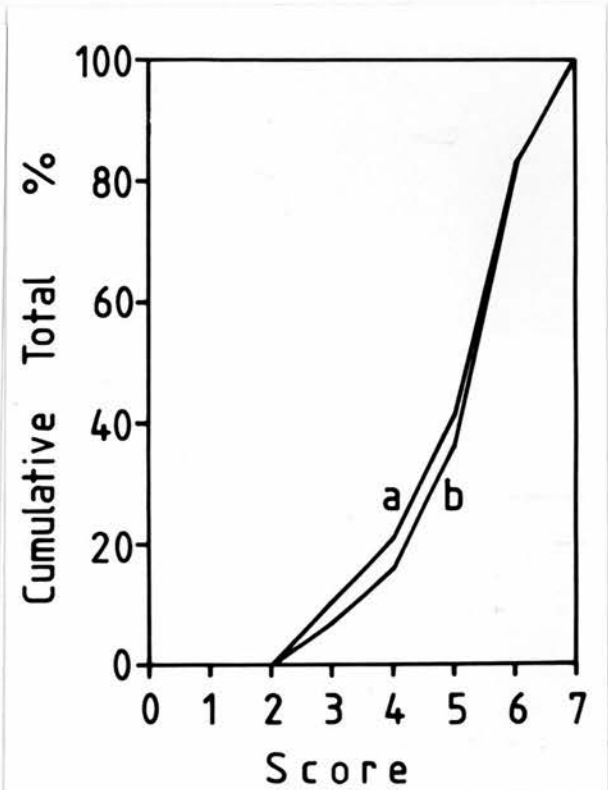

Figure 5.16

Figure 5.15. Cumulative frequency curves of scores for Y13-259 ABC immunostaining. Data for 20 carcinomas with malignant cells in vessels in blocks scored. a, data for carcinoma cells in vessels. b, data for carcinoma cells surrounded by stroma (same 20 cases).

Figure 5.16. Cumulative frequency curves of scores for Y13-259 ABC immunostaining. a, 29 carcinomas with vascular invasion. b, 56 carcinomas without vascular invasion in any block.

expression by carcinomas with or without vascular invasion.

Figure 5.17 shows comparable curves for 66 carcinomas with accurate information about lymph node involvement at the time of primary surgery. 39 were node-negative, 27 had one or more involved nodes. There is no difference between these groups. In figure 5.18 the curve for node-positive cases is split between cases with one or two positive nodes only (14), and cases with three or more positive nodes (13). Again there is no difference between the curves.

5.3.3 Size of primary carcinoma

Size of primary breast carcinoma is also related to prognosis [58], and its relationship to p21 ras expression was examined. Accurate sizes (greatest diameter of the carcinoma in millimetres) were available for 57 cases, and are shown graphically against p21 ras score in figure 5.19. There is no correlation. Small cancers are as likely to express p21 ras strongly as large ones. Cumulative curves show no difference between carcinomas smaller or larger than 24mm (this size chosen as dividing the 57 carcinomas into approximately equal groups of 29 and 28 cases).

5.3.4 Oestrogen receptor status

Oestrogen receptor status is another variable related to prognosis [138], and it has been suggested that a relationship exists between expression of p21 ras and of oestrogen receptor protein [21]. The oestrogen receptor data have been provided by courtesy of Dr RA Hawkins of the Department of Clinical Surgery, Universiy of

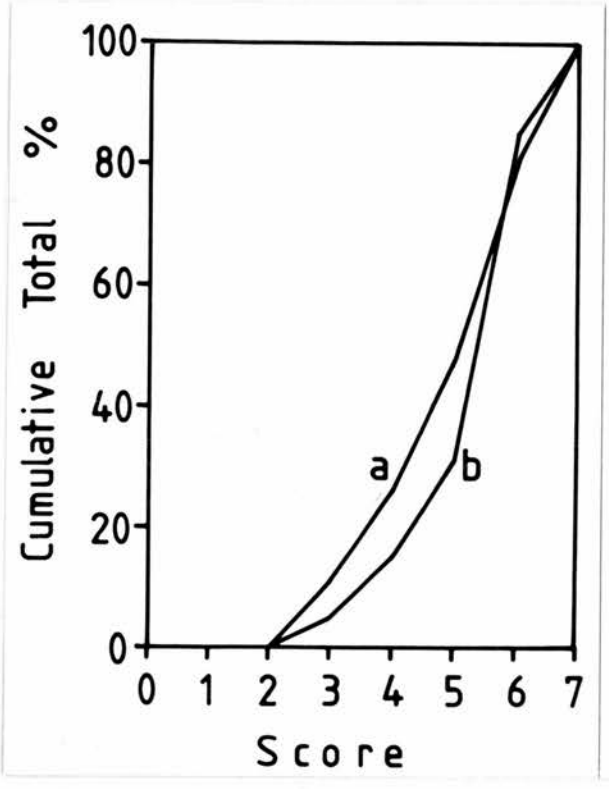

Figure 5.17

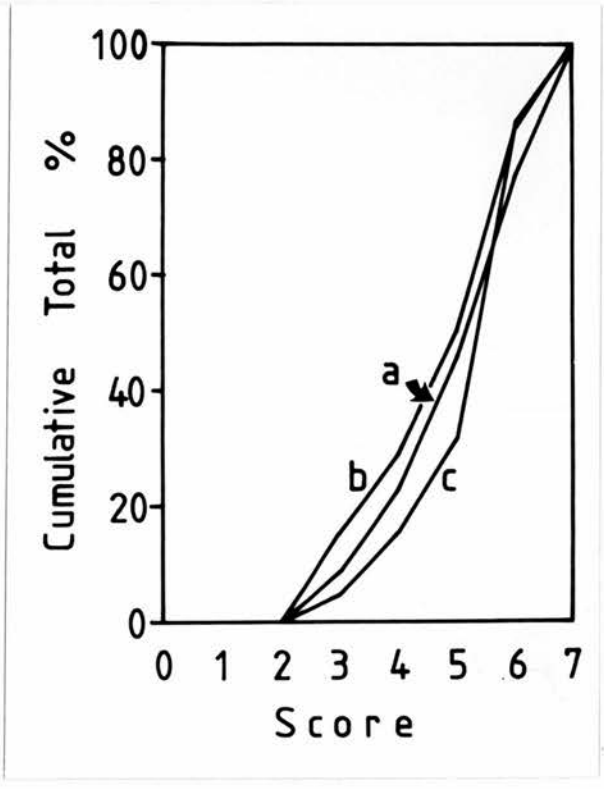

Figure 5.18

Figure 5.17. Cumulative frequency curves of scores for Y13-259 ABC immunostaining. a, Node-negative carcinomas. b, Node-positive carcinomas.

Figure 5.18. Cumulative frequency curves of scores for Y13-259 ABC immuno- staining. a, Node negative carcinomas. b, carcinomas with one or two positive nodes. c, carcinomas with three or more positive nodes.

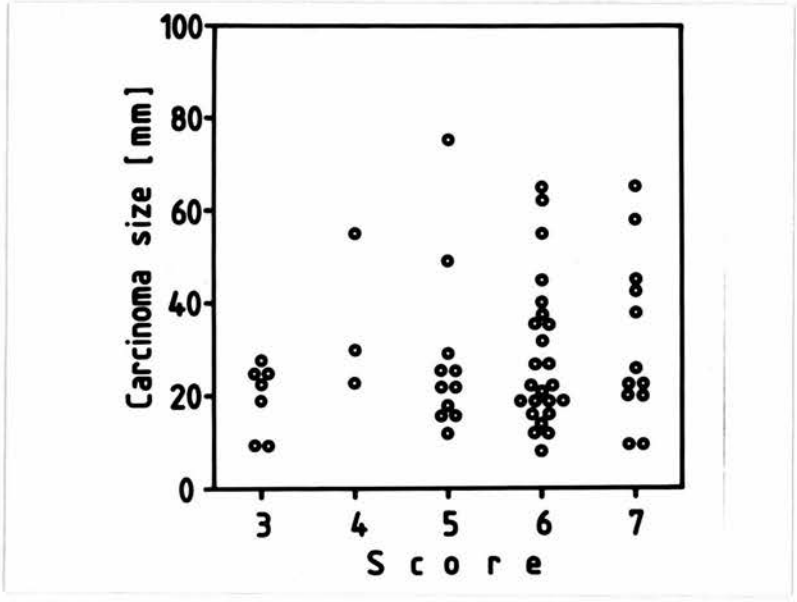

Figure 5.19. Greatest diameter of primary carcinoma plotted against scores for Y13-259 ABC immunostaining.

Edinburgh. The assay uses a standard dextran-coated charcoal method [60]. Data for 85 cases are presented in figure 5.20. Taking 20 fmol/mg as the cut-off between negative and positive oestrogen-receptor expression, and separating low p21 ras scores (3,4) from high scores (5,6,7), there is a relative deficit of oestrogen receptor negative carcinomas with low p21 ras scores. The corresponding 2x2 contingency table (table 5.5) gives $chi^2 = 5.93$, $p<0.025$.

5.4 Expression of p21 ras in lobular hyperplasias and carcinomas

Fewer cases are available for study in these groups. If the scores are plotted as before, a trend towards stronger expression of p21 ras is again seen with greater devation of morphology from normality, and this is well seen in the cumulative score plot, figure 5.21. But these differences do not attain statistical significance.

5.5 Expression of p21 ras in carcinomas of special type

The distribution of p21 ras scores between carcinomas of different special types which occurred in the series is documented in table 5.6. There was no difference between carcinomas of no special type and those which did belong to special categories.

5.6 Expression of p21 ras in myoepithelium

As shown in figures 5.6, 5.7 and 5.8, p21 ras immunostaining is associated with significantly higher scores in the outer, myoepithelial layer of normal two-layered breast epithelium at all levels from large ducts to TDLU. These cells do not often show the fully

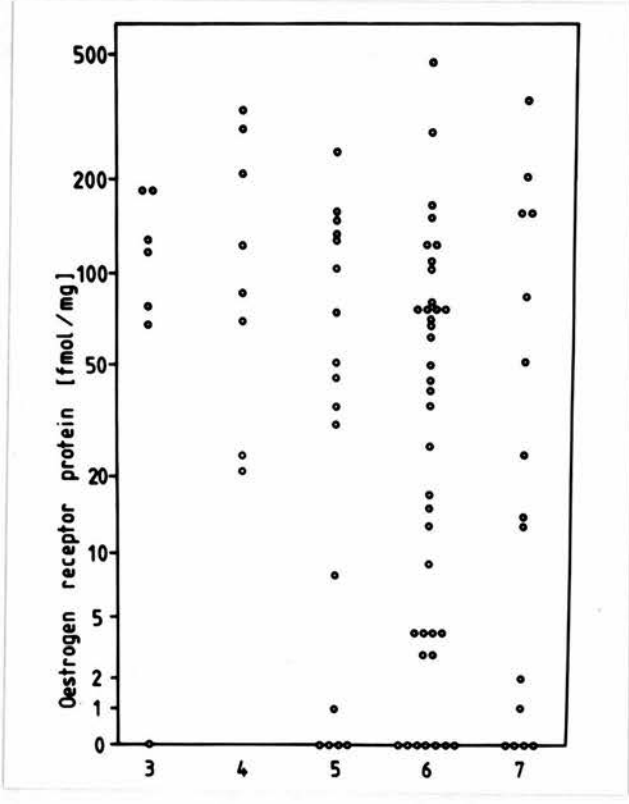

Figure 5.20. Oestrogen receptor protein (fmol per mg of protein) plotted against Y13-259 ABC immuno-staining. OR protein is plotted on a logarithmic scale, as $\log_{10}([OR]+3)$.

	p21 score less than 5	p21 score 5 or greater
[OR]>20fmol/mg	14	39
[OR]<20fmol/mg	1	31

Table 5.5. Contingency table relating expression of p21 ras and oestrogen receptor in carcinomas. χ^2 = 5.93, p<0.025 (using Yates' correction for continuity).

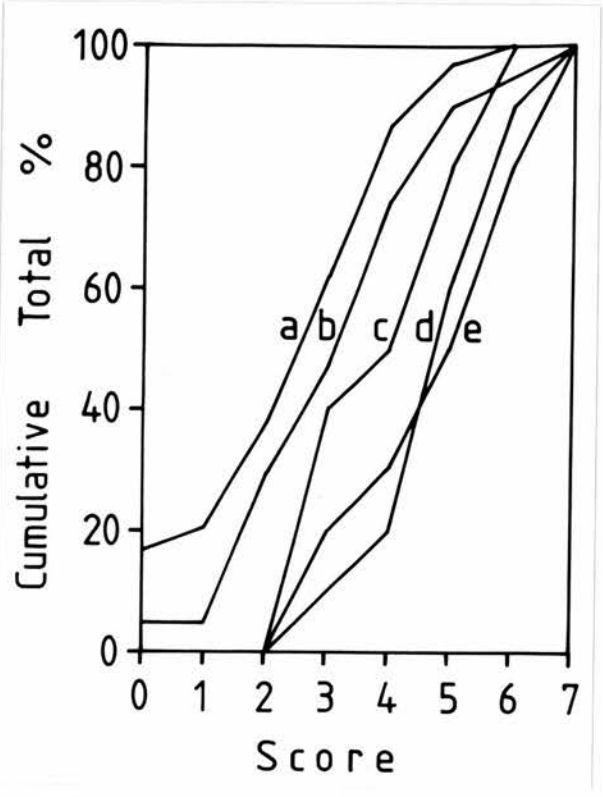

Figure 5.21. Cumulative frequency curves of scores for Y13-259 ABC immuno- staining. a, normal epithelium of TDLU. b, altered lobules without atypia. c, atypical lobular hyperplasia. d, lobular carcinoma in situ. e, invasive lobular carcinoma.

Type	p21 *ras* score							
	0	1	2	3	4	5	6	7
Ductal (NST)	1	-	-	4	6	12	30	13
Lobular	-	-	-	2	1	2	3	2
Medullary	-	-	-	-	-	-	2	-
Mucoid-	-	-	-	1	-	1	-	-
Cribriform	-	-	-	-	-	1	2	-
Tubular	-	-	-	-	-	1	-	-

Table 5.6. Expression of p21 *ras* in carcinomas by histological type.

differentiated, elongated form of differentiated myoepithelial cells but for convenience will be referred to as myoepithelium nonetheless. Figure 5.22 illustrates an example of strongly positive staining of elongated myoepithelium.

5.7 Expression of p21 ras in stromal elements

5.7.1 Stroma of benign tissues

In normal breast, fibroblasts in TDLU and in extralobular stroma express little p21 ras. Most striking is strong positivity in smooth muscle of small blood vessels, illustrated in figure 5.23. Endothelial cells may show faint positivity, and neural elements also show some positivity, but not as strongly as vascular smooth muscle.
Positivity of stromal cells is sometimes more conspicuous in sclerosing parenchyma, such as sclerosing adenosis and radial scars. In one case, the cells of an active granulation tissue formed at the site of a previous biopsy procedure were strongly positive.

5.7.2 Stroma of carcinomas

In general, most stromal cells of carcinomas showed positive p21 ras staining which was not so intense as the staining of carcinoma cells themselves. This relationship is illustrated in figure 5.24. The difference between carcinoma cells and supporting stromal cells is significant ($p<0.001$) As with epithelial cells, staining was as much cytoplasmic as membrane-associated.

Figure 5.22. PLPD-fixed breast tissue, Y13-259 50 µg/ml, ABC detection. Strong immunoreactivity in myoepithelial cells. x400

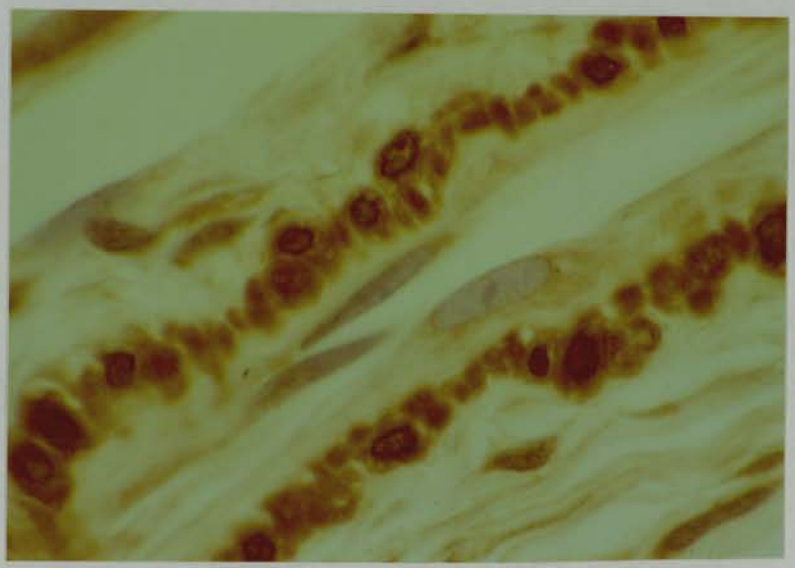

Figure 5.23. PLPD-fixed breast tissue, Y13-259 50 µg/ml, ABC detection. Strong immunoreactivity in vascular smooth muscle. x400

5.8 Expression of p21 ras in cyst epithelium

A striking difference existed in the expression of p21 ras between different types of cyst. In general, apocrine cyst epithelium expressed p21 ras strongly. In some cases this expression was clearly related to the basal aspect of cells, while in other cases it was present in the apical portion of the cell (figures 5.25 and 5.26). In contrast, cysts with a flattened epithelium were devoid of p21 ras expression. Apocrine and flattened epithelium cysts were present in 29 and 78 cases respectively (figure 5.27).

5.9 Expression of p21 ras in normal parenchyma with age

Proliferative activity in normal breast parenchyma decreases with increasing age [120]. The relationship of p21 ras expression to age was examined,and it emerged that p21 ras expression was a function of age, being more strongly expressed in younger women. Taking age 45 as a cut-off, figure 5.28 shows cumulative expression curves for younger and older women, which differ markedly; ($p<0.01$). There is, however, considerable scatter, and much overlap at all ages.

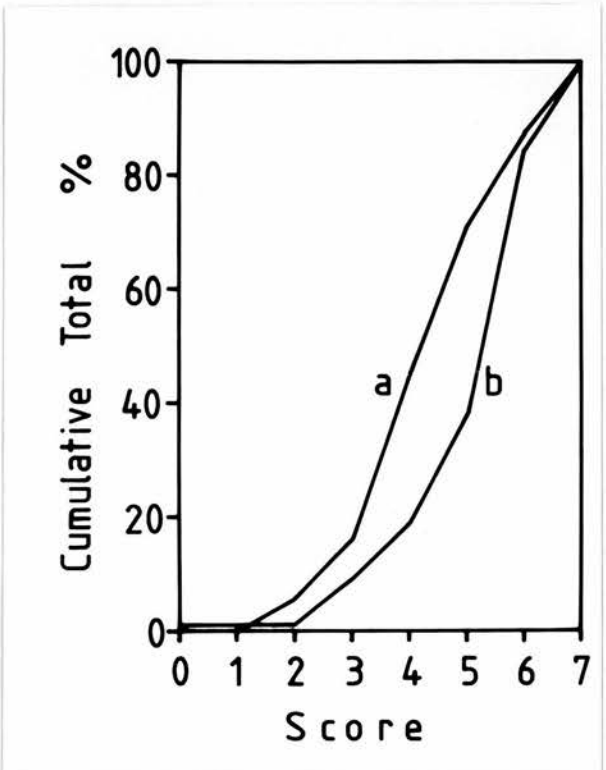

Figure 5.24. Cumulative frequency curves of scores for Y13-259 ABC immunostaining. a, stromal cells of carcinomas. b, carcinoma cells. $p<0.001$.

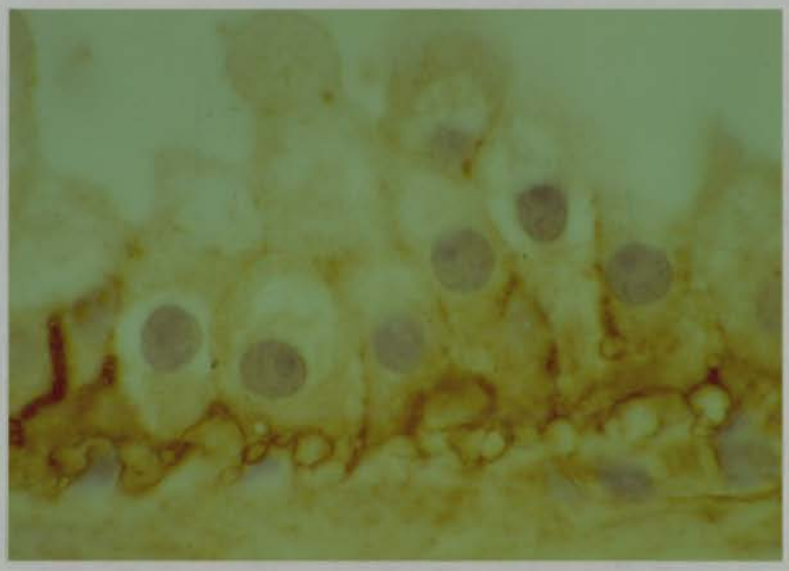

Figure 5.25. PLPD-fixed breast tissue, Y13-259 50 µg/ml, ABC detection. Basal immunoreactivity in apocrine cells. x400

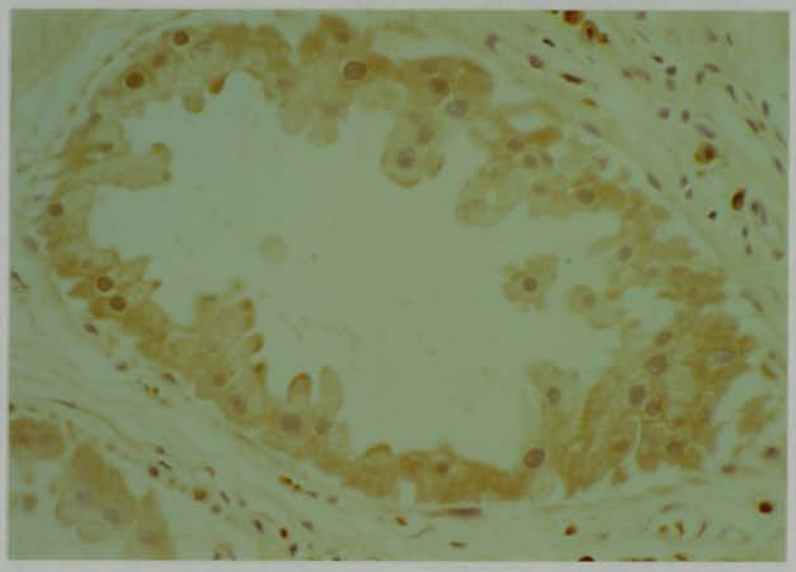

Figure 5.26. PLPD-fixed breast tissue, Y13-259 50 µg/ml, ABC detection. Apical immunoreactivity in apocrine cells. x100

Figure 5.27. PLPD-fixed breast tissue, Y13-259 50 µg/ml, ABC detection. There is no immunoreactivity in flattened epithelial cells. x100

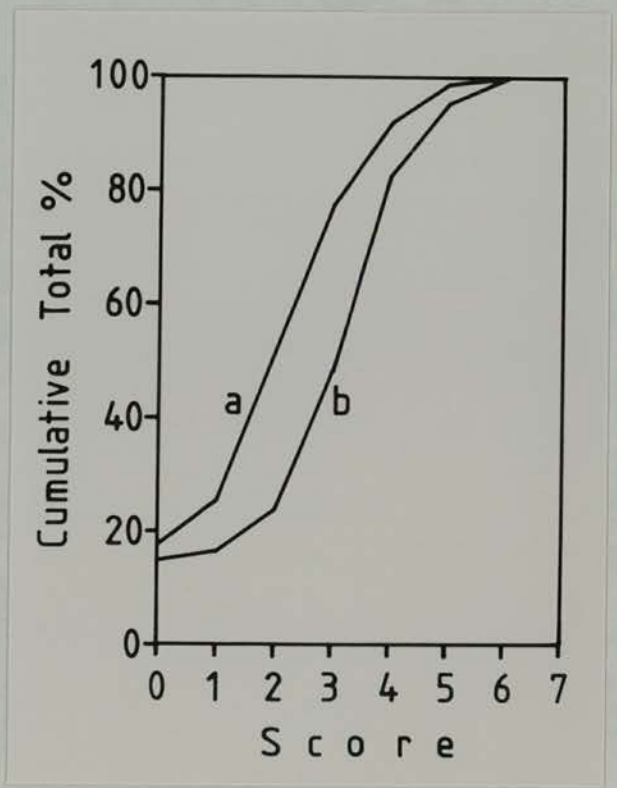

Figure 5.28. Cumulative frequency curves of scores for Y13-259 ABC immuno- staining. Data for unselected patients. a, 79 women younger than 45. b, 77 women 45 or older.

CHAPTER 6 IMMUNOCYTOCHEMISTRY FOR ELECTRON MICROSCOPY: METHODS

The location of p21 ras within cells was of interest principally because of the contrast between cytoplasmic immunostaining of human breast tissue including carcinomas, and membrane immunostaining in FHO5T1 cells. Membrane localisation in cultured cells expressing p21 ras is well established [147,154], and most discussions of p21 ras physiology take its membrane location for granted. But all morphological and biochemical studies which consider p21 ras location within cells are concerned with cultured cell lines, often lines engineered artificially to express large amounts of p21 ras, and there are no published ultrastructural studies dealing specifically with cells of human tissues, whether normal or neoplastic. Intracellular location of p21 ras might be more important than its total quantity, hence the present studies.

6.1 Pre-embedding ABC staining

A detailed protocol for pre-embedding ABC immunohistochemistry for electron microscopy is given in 9.7. In brief fixed tissue was cryoprotected by infiltration with sucrose and glycerol in buffer, and frozen sections cut at 50μm thickness. This freeze/thaw cycle makes cells permeable to proteins, and detergent is not considered necessary for reagent penetration. The thick sections were processed free-floating in culture plate wells, using overnight incubations with primary and secondary antibody and avidin-biotin complex and prolonged washes before DAB development. The oxidized DAB polymeric pigment is not of itself electron-dense but becomes so after osmication. Sections were then embedded

in Araldite on edge, and thick (1um) sections viewed to select areas for ultramicrotomy. The results of this technique were disappointing. Free-floating sections exposed to primary antibody appeared strongly stained after development with DAB, while negative controls were unstained. This signal was faint but visible to a depth of 5-6μm in toluidine-blue stained thick sections of Araldite blocks, but when thin sections were viewed by electron microscopy, it was impossible to distinguish between test sections and negative controls. Further osmication of thin sections did not remedy this lack of signal and this procedure was not pursued. In a modification of the procedure frozen sections of similarly fixed and cryopotected tissues were mounted on gelatin or poly-L-lysine coated slides and immunostained with a standard ABC method (9.3) and processed for electron microscopy by an Araldite-capsule technique [105].

6.2 Pre-embedding immunogold and immunogold-silver labelling

A detailed protocol for pre-embedding immunogold immunohistochemistry for electron microscopy is given in 9.9. This method was applied to control cells growing on cover slips and to cryoprotected frozen sections of carcinomas on poly-L-lysine coated slides. A two-stage indirect immunochemical method was used, the second antibody (goat anti-rat) being adsorbed onto 5nm colloidal gold particles (Janssen). In the case of control cells growing on cover slips, a brief exposure to Triton X-100 in buffer preceded fixation in order to permeablize the cells. In the case of frozen sections of cryoprotected tissues this step was omitted. Both control cells and tissues were processed for electron

microscopy by the Araldite-capsule method. Parallel test preparations and negative controls were prepared for light microscopy with several cycles of silver enhancement using Janssen's 'IntenSE' kit.

PLPD-fixed paraffin-embedded sections of control tissues immunostained by a three-stage avidin-biotin-gold complex method followed by several cycles of silver enhancement developed a very strong light microscopic signal (figure 4.9). If such sections were reprocessed for electron microscopy by the Araldite capsule method, conspicuous labelling was obtained, large silver grains being obvious at low powers. These particles were about 100nm in diameter. Not surprisingly, morphological preservation was poor.

6.3 Post-embedding immunogold labelling

The detailed protocol for post-embedding immunogold labelling is given in 9.10. This was an indirect immunogold method using the same goat anti-rat antibody adsorbed onto 5nm gold particles. Thin sections were carried on gold grids. Two embedding media were used: Araldite and the hydrophilic Lowikryl K4M resin. Araldite sections were etched with sodium ethoxide to expose antigenic sites. This was omitted for Lowikryl-embedded cells. These methods were used on tumours and on control FHO5T1 and CHL cells but without success. No signal was obtained even with FH05T1 cells. That immunostaining ought to be possible with Lowikryl K4M was demonstrated by positive light-microscopic ABC immunostaining of 1μm sections of FHO5T1 cells embedded in that medium.

CHAPTER 7 IMMUNOCYTOCHEMISTRY FOR ELECTRON MICROSCOPY: RESULTS

7.1 Control tissue

The strongest signal was obtained by gold-silver immunostaining of paraffin sections of PLPD-fixed FHO5T1 tumour reprocessed for electron microscopy. The signal was predominantly located on the plasma membrane (figure 7.1) but was also present on membranes lining vesicular spaces in the cytoplasm (figure 7.2). Poor ultrastructural morphology made it impossible to identify these structures with confidence. FHO5T1 cells growing on cover slips and exposed to a two-stage indirect immunogold procedure demonstrated satisfactory penetration by the 5nm gold probe as judged by electron microscopy (figure 7.3) and by light microscopy of identically-treated cover slips which were prepared for light microscopy by several cycles of silver enhancement. Results of this process are illustrated in figures 7.4 and 7.5 for FHO5T1 cells. The purpose of this experiment was to examine the distribution of the p21 ras signal in FHO5T1 cells and their parent CHL cells, and incidentally to look at three other cell lines: A transformed rat fibroblast line, 208F, which does not express abundant p21 ras, and two cell lines derived therefrom, known as RFHO5T1 and RFHO6N1. Both incorporate Homer vector with sequences to ensure expression of mutated and normal p21 ras respectively. They are fully described in [122]. This experiment was successful in that preparations for light microscopy showed good penetration of the probe into the cells, which is always a cause for concern with colloidal gold probes even as small as 5nm, and, equally important, little background signal in negative controls. But the preparations for electron microscopy were

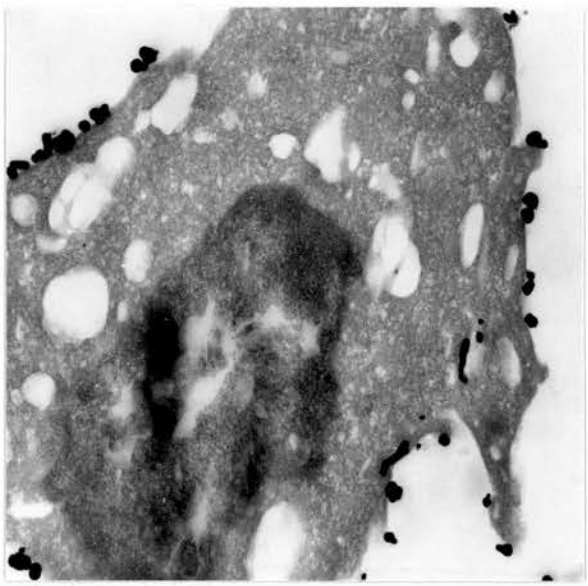

Figure 7.1. PLPD fixed paraffin-embedded FHO5T1 tumour. Y13-259 50µg/ml, IGS detection, reprocessed for electron microscopy. Large silver grains (c. 100nm) are predominantly associated with the plasma membrane. x10,000.

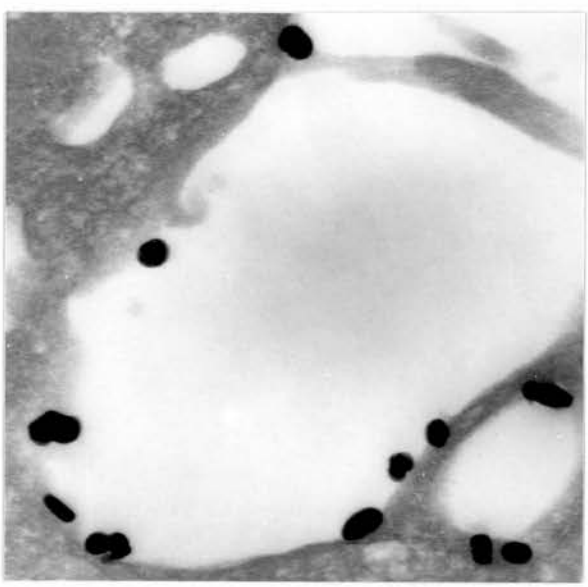

Figure 7.2. PLPD fixed paraffin embedded FHO5T1 tumour. Y13-259 50µg/ml, IGS detection, reprocessed for electron microscopy. Silver grains associated with membrane-bound cytoplasmic vesicles. x30,000.

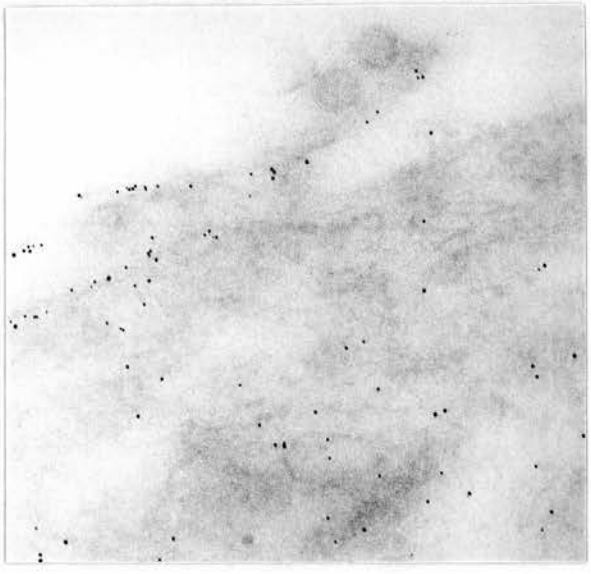

Figure 7.3. Indirect immunogold labelling of FHO5T1 cells growing on cover slips. The signal is more subtle than in figures 7.1 and 7.2. The signal is membrane-associated and cytoplasmic. x35,000.

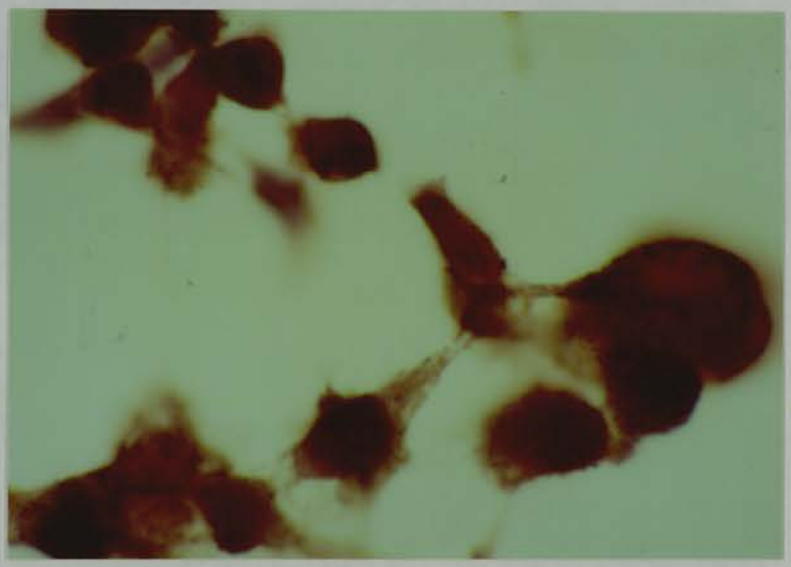

Figure 7.4. Indirect immunogold labelling of FHO5T1 cells growing on cover slips, followed by silver enhancement. Y13-259 50µg/ml, IGS. x400

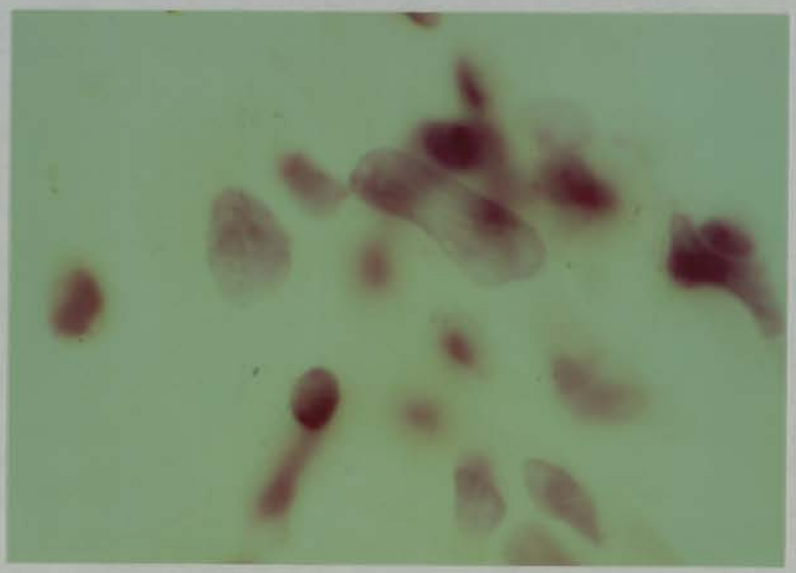

Figure 7.5. Negative control prepared as 7.4 but primary antibody omitted. x400

unsuccessful, except for the FHO5T1 and CHL cells, because the technically exacting Araldite capsule method failed to harvest cells for ultrastructural inspection. It was felt that the potential of this method had been demonstrated.

The p21 ras-expressing cell lines mentioned above showed both membrane and cytoplasmic staining. This is difficult to photograph as the flattened shape of cells adherent to cover slips tends to make membrane-staining less obvious as it is viewed en face, rather than edge-on which emphasizesmembrane-staining, as seen in figures 5.1 and 5.2. It was to resolve this difficulty that electron microscopy was attempted.

7.2 Breast tissue

The results of pre-embedding ABC immunostaining of free-floating frozen sections and indirect post-embedding immunogold labelling of thin sections were disappointing, in that no definite signal was obtained. An attempt to obtain ultrastructural information on the distribution of p21 ras in breast carcinoma was made on trucut samples from carcinomas taken immediately after excision, in the operating theatre. This avoided any delay before tissue reached fixative, and the trucut tissue cores were thin enough for fixative to penetrate rapidly. After fixation and cryoprotection with glycerol and sucrose in buffer, cryostat sections were picked up on poly-L-lysine coated slides and immunostained by ABC and indirect immunogold methods, osmicated and reprocessed for electron microscopy by the Araldite-capsule method. Some immunogold-labelled sections were silver enhanced for light microscopy. Although some labelling was detected in sections of osmicated ABC-labelled tissue (figures

7.6, 7.7), localization was indistinct and did not resolve the location of p21 ras in breast carcinomas. This particular group of immunogold preparations for electron microscopy gave no signal.

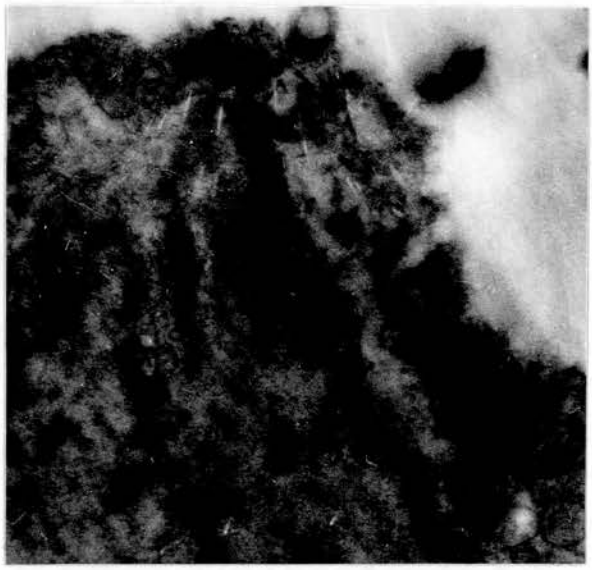

Figure 7.6. PLPD-fixed breast carcinoma. Cryoprotected frozen section, Y13-259 50 µg/ml, ABC detection, osmicated, reprocessed for electron microscopy. Indistinct membrane and possible cytoplasmic staining are present. x18,000.

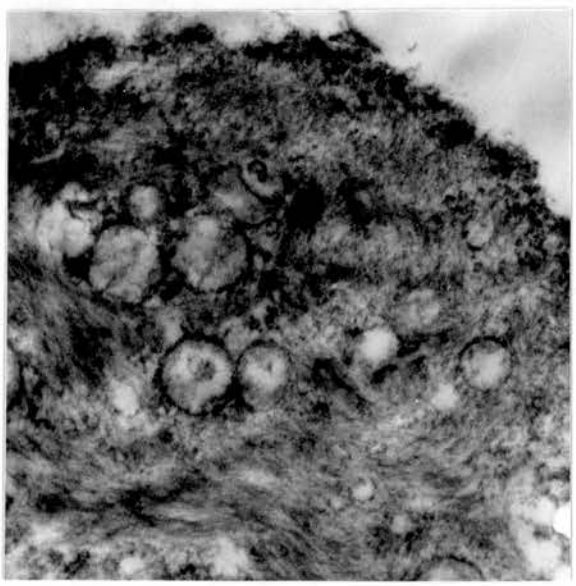

Figure 7.7. Negative control prepared as 7.6 but primary antibody omitted. x18,000.

CHAPTER 8 DISCUSSION

8.1 Ras expression and epithelial breast pathology

Three immunocytochemical studies [15,41,45] found little difference in p21 ras expression between benign and malignant breast tissue, and one study of ras mRNA came to the same conclusion [152], but evidence opposing this view is strong [21,27,64,95,119]. The present studies show consistently greater expression of p21 ras in carcinomas than normal breast epithelium and relate p21 ras expression to morphological abnormalities associated with increased risk of carcinoma, that is hyperplasias especially of atypical ductal and lobular type. This has only been systematically attempted by one study, on a smaller scale, by Ohuchi et al [95], whose immunohistochemical study based on 53 cancer and 46 benign control cases is the largest study of p21 ras immunohistochemistry in breast excluding the studies described in this thesis, which are based on 99 cancer and 72 control cases. They found a gradient of increased expression from normal epithelium through hyperplastic and atypical epithelium to carcinoma in situ. On the basis of their results, Ohuchi et al [95] suggested that ras gene activation by increased expression might be an early feature of carcinogenesis. Our results are in keeping with this view. Ohuchi et al also noted greater p21 ras expression in TDLU than extralobular ducts, a finding which the present studies did not confirm; p21 ras expression was not a function of location within the ductal tree.

Although there was a relationship between greater p21 ras expression and epithelial lesions associated with greater risk of carcinoma, there were striking differences in

expression between other tissue elements, not easily related to carcinoma risk, notably expression of p21 ras in myoepithelial cells and in vascular smooth muscle. Strong expression in apocrine epithelium was constant while expression was absent from flattened cyst epithelium. There are biochemical differences between the fluids in these two types of cyst [32], and the present histochemical studies further justify the separation of apocrine and flattened cysts into populations with distinct biological properties. The possibility that one type evolves into the other is not excluded.

It has been suggested [21,41,81] that increased p21 ras expression in breast carcinomas is associated with more aggressive behaviour. Clair et al [21] found that patients with tumours shown to express more p21 ras were less likely to remain disease-free at 4 years than patients with tumours expressing smaller quantities of p21 ras. They also found positive correlations of p21 ras with node status and carcinoma size and between positive oestrogen receptor status and higher p21 ras levels, but their numbers were small. Fromowitz et al [41,81] have suggested on the basis of histochemical studies with RAP-5 that p21 ras expression is related to histological correlates of aggressiveness (invasion, vascular invasion) and to the number of positive nodes. These issues were examined in the present studies and the results differ from the findings of the workers cited. Specifically, no relationship was found with carcinoma maximum diameter; presence or absence of lymph nodes involved by carcinoma; presence or absence of vascular invasion; and the relationship with oestrogen receptor status found in the present studies is the inverse of that described by Clair et al [21] and DeBortoli et al

[27]. The identical range of p21 ras expression in the minority of special-type carcinomas and the majority of no special type is further evidence against a correlation between p21 ras expression and prognosis in breast carcinoma.

Our immunohistochemical finding, that p21 ras immunostaining in intraduct carcinoma and invasive carcinoma are broadly comparable, is in support of the finding of Ohuchi et al [95] who used antibody Y13-259, but contradicts the finding of Fromowitz et al, who used RAP-5 and claimed that p21 ras expression was consistently greater in invasive than intraduct carcinoma. In the same paper, it was stated that expression of p21 ras in carcinoma cells within vascular spaces was greater than contiguous carcinoma outside vessels, ie cells with a supporting stroma. The present studies documented the opposite.

The differences described here from the published findings of others may reflect several factors. Many groups have used the antibody RAP-5 in their studies because the epitope it recognises survives well in formaldehyde-fixed, paraffin-embedded tissues. Published studies cast doubt on the specificity of this antibody for the p21 ras protein [45,103]. It was impossible with RAP-5 to distinguish on immunoblots between lysates of FHO5T1 and CHL cells, which express p21 ras in high and low quantities respectively, wheras Y13-259 made this distinction easily. RAP-5 also failed to differentiate between acetone-fixed cytospin preparations of FHO5T1 and CHL cells, a test which Y13-259 passed [103]. The conclusion that RAP-5 immunoreactivity has little to do with p21 ras expression is hard to escape. Other differences may reflect small numbers of cases in some

studies, and differences in technique. Walker and Wilkinson [146] used Y13-259 on acetone-fixed cryostat sections of breast tissue, with an alkaline phosphatase/anti-alkaline phosphatase technique. They found decreased expression of p21 ras in half of the carcinomas they examined, by comparison with normal breast tissue. It is difficult to reconcile this to our findings.

8.2 Significance of ras expression in breast

This must remain speculative until the physiological and biochemical roles of ras are clarified. Expression of p21 ras in hyperplastic lesions exceeds that in the surrounding normal TDLU. This suggests a link between p21 ras expression and proliferation, but this is not certain in that more cells in a population may follow decreased cell loss rather than increased production. It was notable in some carcinomas that cells undergoing apoptosis showed no p21 ras expression, and in areas of confluent necrosis, such as in comedonecrotic ductal carcinoma in situ, cells in the transitional zone between viable carcinoma and necrotic debris often showed no p21 ras immunoreactivity. Thus a relationship may exist between lack of p21 ras expression and cell death.

The increased p21 ras expression in carcinomas over normal breast tissue makes a role for p21 ras in the evolution of neoplasia possible but whether p21 ras is directly concerned with the transformed phenotype of breast cancer cells remains undetermined. One carcinoma patient showed p21 ras expression in normal parenchymal epithelium but cells of the carcinoma in the same block were negative for immunoreactive p21 ras. This example

proves that quantitative overexpression of p21 ras is not essential for malignancy in the breast.

Identical curves representing p21 ras scores of intraduct and invasive carcinoma do not imply identical quantitative expression. Immunocytochemistry is not quantitative and intensity of pigment developed by immunoperoxidase methods is not a linear function of antigen concentration. Intensity rises steeply with small increases at low antigen concentrations, but hardly at all with large increases at higher concentrations [52]. Expression in DCIS strong enough to give a near-maximal signal could mask major differences between DCIS and invasive carcinoma. On the other hand, runs using greater dilutions of Y13-259 than 50μg/ml suggested that the immunostaining in DCIS and invasive carcinoma diminished pari passu and may therefore have been quantitatively comparable. This would require more formal studies to resolve.

Although increased expression of non-mutated p21 ras alone does not transform normal cells, overexpression in abnormal cells such as NIH3T3 does transform them [100]. Increased expression of p21 ras in breast parenchyma associated with increased carcinoma risk, ie atypical hyperplasias and in situ carcinomas, could permit an abnormality affecting another oncogene, or loss of an anti-oncogene, to cause neoplastic transformation which might not develop in the absence of p21 ras overexpression.

If greater p21 ras expression in breast epithelium predisposes to breast cancer, then p21 ras expression in morphologically normal TDLU of cancer patients might be greater than in TDLU of women without cancer. But breast

cancer evolves over years to decades, and the parenchyma which originally gave rise to a carcinoma may have changed by the time that carcinoma is detected. Data from the present study show no difference in p21 ras expression in normal TDLU between women with cancer and women with benign breast disease, but there is significantly higher expression in younger women. Whether p21 ras expression in normal TDLU bears any relationship to cancer risk remains unclear.

To regard oncogenes as concerned exclusively with cellular proliferation is to oversimplify their complex physiology. Injection of p21 ras stimulates DNA synthesis and cell division in quiescent fibroblastic cells [35], and antibodies to p21 block this effect. But injection of p21 N-ras induces neuronal differentiation in the phaeochromocytoma cell line PC 12 [55] and nerve-growth-factor induced neuronal differentiation is blocked by microinjected anti-p21 antibodies.

That p21 ras may influence cell proliferation in the breast is suggested by the age-related decrease in p21 ras expression in normal TDLU, which parallels the age-related decrease in thymidine labelling index previously demonstrated [47]. But this is circumstantial, and direct evidence dissociates p21 ras expression and proliferation in some differentiated cellular populations in the breast. Unfortunately, good thymidine uptake data are lacking for hyperplastic and atypical lesions in the breast. Autoradiography shows that myoepithelial cells of breast do not divide [69], yet myoepithelial cells with or without the characteristic elongated habit enfolding parenchymal structures show strong p21 ras expression. A link with myoid differentiation continues with p21 ras positivity in vascular smooth muscle and in

the stroma of sclerosing lesions which show ultrastructural evidence of myofibroblastic differentiation [8]. Granulation tissue is a proliferative tissue but myofibroblastic differentiation is present ultrastructurally [109] and p21 ras expression can be conspicuous.

Another notable finding is that p21 ras expression in carcinoma cells within lymphatic vascular channels is less than in the parent carcinoma cells which are in intimate contact with stromal cells. The stromal cells of invasive carcinomas may show immunoreactivity for p21 ras, and this may reflect interaction with malignant cells in that stromal cells outwith the carcinomas usually show little positivity. It seems possible that expression of p21 ras in carcinoma cells is modulated by the local environment and in the absence of paracrine growth factors, such as fibroblast growth factor, its expression could be downregulated.

8.3 Comparison with ras expression in other systems

It is interesting to compare our breast findings with other systems in which ras expression has been studied in well established morphological progressions from normal through benign changes to malignancy. The adenoma-carcinoma sequence in large bowel represents spontaneously occurring human disease while the papilloma-carcinoma sequence in carcinogen-exposed mouse skin is an archetype of experimental carcinogenesis.

Several groups have studied ras expression in adenomas and carcinomas of colon and rectum. In keeping with increased expression early in the evolution of carcinoma, Spandidos and Kerr [121] showed increased Ha-ras and Ki-

ras mRNA in colo-rectal adenomas as well as carcinomas. The increase in adenomas was sometimes greater than in carcinomas in the same patients. Gallick et al (1985) [44] examined p21 ras in Y13-259 immunoblots and showed greatest levels in early carcinomas. Thor et al [137] considered that p21 ras expression was greatest in advanced carcinomas but used antibody RAP-5, so their conclusions cannot be accepted for reasons discussed in 8.1. Williams et al [153] used Y13-259 for immunocytochemical studies which showed greatest p21 ras expression in adenomas while carcinomas showed little increase in expression compared with normal mucosa. In their immunocytochemical studies Kerr et al [71] used Y13-259 and another Furth antibody, YA6-172. They showed increased expression in adenomas and carcinomas, but less differential expression between normal and neoplastic tissues.

Forrester et al [40] examined 66 colonic neoplasms by mismatch cleavage analysis and found K-ras codon 12 mutations in 26 (39 per cent), while NIH3T3 transfection assay was positive in only 20 per cent. Levels of p21 Ki-ras expression in neoplasms were not related to the presence or absence of codon-12 mutations. Mutations were not detected in normal colonic mucosa. This study did not compare mutation rates between adenomas and carcinomas. Bos et al [11] used hybridization analyses to show ras mutations in 11 of 27 colo-rectal carcinomas, ten affecting codon 12 of Ki-ras, one codon 12 of N-ras. In five tumours containing residual adenoma tissue, the same mutation was present in both adenoma and carcinoma. A subsequent study [144] showed ras mutations in 9 per cent of adenomas smaller than 1cm but in 58 per cent of larger adenomas.

The case for ras mutation playing an important part in colorectal carcinogenesis is strong. Accurate incidence data for ras mutation in adenomas which have not made the transition to carcinoma will clarify the importance of ras mutations in the adenoma-carcinoma transition. Quantitative overexpression of p21 ras may still be important. Balmain and his colleagues have studied the tumours initiated by treating mouse skin with dimethylbenzanthracene and promoted with 12-0-tetradecanoyl-phorbol-13-acetate. They have shown a quantitative increase in Ha-ras message in papillomas and carcinomas induced in this system, and carcinogen-specific Ha-ras mutations in both [4,101].

Comprehensive ras mutation data for breast carcinomas are not available. Spandidos (1987) showed Ha-ras-1 mutations in two of 24 carcinomas using oligonucleotide hybridization analysis [70]. This relatively low incidence does not exclude more frequent mutation at other ras loci and more data are needed before ras mutation can be dismissed as unimportant in the breast. There are no published data for pre-malignant breast lesions. The two systems discussed above illustrate how important such data may be for understanding of the role of ras mutation in mammary carcinogenesis.
Recently a new slant on ras activation was demonstrated by Cohen and Levinson [23]. They showed that the T24/EJ Ha-ras oncogene owes its strong oncogenic activity not only to the well-known codon-12 point mutation [16,102,129,133] but also to a guanine for adenine substitution of nucleotide 2,719 in the fourth intron. This substitution increased gene expression tenfold. Experimental insertion of a sequence including nucleotide 2,719 into the third intron of human growth hormone gene had the same strong upregulation effect irrespective of

the promoter, suggesting a widely applicable but currently unknown mechanism. Such large quantitative alterations in ras expression could well be biologically significant. In case the substitution at nucleotide 2,719 was a polymorphism Cohen and Levinson sought but did not find it in 44 samples of human genomic DNA. They did, however, find that other substitutions in the same region could affect ras expression. Such studies suggest a possible mechanism altering the expression of different ras alleles, with relevance to their potential for oncogenic activation.

8.4 Cellular location of p21 ras

Little attention has been paid in the literature to the cellular location of p21 ras. It is generally accepted that p21 ras is a cell-membrane protein, but this cell-membrane relationship is only seen clearly in cell lines, often artificially engineered. In many immunocytochemical studies of p21 ras expression in genuine tissues, the detected immunoreactivity is predominantly cytoplasmic, not membrane-related, but this location has attracted little attention. It may have been assumed that cytoplasmic staining reflects antigenic diffusion from the original site in the cell, ie the cell membrane.

But p21 ras is not a labile protein. In cultured cells it has a long half life, and it is securely attached to the inner face of the plasma membrane. When Grand et al [54] wished to detach p21 ras from the cell membrane of cells engineered to express abundant p21 N-ras, they had to use powerful membrane-disrupting detergents like Triton-X100 to extract it. These are not the properties of a labile protein liable to diffuse rapidly from its normal site in the presence of fixing agents. And in the

case of FHO5T1 cells and their derived tumours, we know that the fixatives PLP and PLPD give a strong membrane signal with little cytoplasmic staining. It seems that the distribution of p21 ras in normal human tissues and in carcinoma cells is different from the distribution in engineered cell lines, which as model systems may poorly reflect the physiology of human p21 ras expression. The recent discovery of the GTPase activating cytoplasmic protein, GAP [14,139], which may be an upstream regulator of p21 ras but could be the long-sought downstream target of p21 ras [114], emphasizes the importance of this localization question. If the target of p21 ras is a cytoplasmic protein, p21 ras might not need to be confined to the cytoplasmic membrane to exert physiological or patho-physiological effects. If the physiology and pathophysiology of p21 ras are to be elucidated in tissues, attention must be paid to the localization of p21 ras in such cellular populations, and not just in cell lines.

8.5 Future studies

It would be desirable to study other oncogenes and to relate their expression and that of growth-factor and growth-factor receptors to precursor lesions of breast cancer. The c-erbB2 gene and its rodent homologue, c-neu, are particularly interesting. A point mutation in the transmembrane domain activates c-neu [7]. Muller et al [91] recently showed that a strain (TG.NF) of transgenic mice bearing activated c-neu fused with mouse mammary tumour virus (MMTV) promoter invariably develop metastasizing mammary gland adenocarcinomas. In these mice the entire mammary epithelium overexpresses p185 neu and undergoes malignant transformation. In a second strain (TG.NK) p185 neu expression and neoplastic

transformation are less frequent, but p185 neu is overexpressed in all carcinomas which do develop. These results contrast with transgenic mice carrying MMTV/ras and MMTV/myc [127] fusion genes in which mammary carcinomas are less common and develop stochastically. Even when ras and myc genes are co-expressed, and act synergistically [115], further events appear necessary for malignant transformation, while overexpression of activated neu alone is sufficient for oncogenesis. The effects of neu were tissue specific. Epithelial hyperplasia occurred in parotid gland and epididymis, but neoplasms did not occur in these sites of neu overexpression. These findings and the relationships between erbB2 expression and human breast cancer [73,116] suggest that c-neu/erbB2 will be an important target for investigators. The present data suggest that increased ras expression may be important in breast carcinogenesis. Is such expression essential, or do other genes, such as erbB2, mediate similar effects? Questions concerning breast carcinogenesis which will require answers before a unified picture can emerge include possible relationships between ras and erbB2 expression, and whether erbB2 is capable of one-step malignant transformation in the human breast.

The present studies confront the problem of quantifying immunohistochemical staining. The scoring system used is probably as complex as essentially non-quantitative peroxidase-based immunochemical methods justify. Although IGS staining did not offer greater sensitivity for detection of this particular antigen, it might be the basis for quantifiable detection. Supra-optimal dilutions of primary antibody, a second-stage colloidal gold reagent labelled with protein G or protein A (which combine with single antibody molecules), followed by

high-gain enhancement with silver to render each colloidal gold nucleus visible to light microscopy, might permit quantifiable grain counting. Rigorous controls would be necessary but the information yielded might justify the effort involved.

The distribution of p21 ras in cells has been little investigated and its exploration would of great interest. Immunoelectron microscopy is exacting and the present studies only began to explore this area. Video enhanced contrast microscopy permits visualization within living cells of colloidal gold probes as small as 5nm [28,29,113] and would be a potent tool for investigating dynamics of p21 ras expression in cultured cells.

The importance of ras mutation to carcinogenesis in the breast remains an area in which more information is needed, particularly in relation to pre-malignant lesions.

Chapter 9

9 PROTOCOLS FOR EXPERIMENTAL PROCEDURES

9.1 Carson's fixative

This fixative was devised to give adequate fixation for electron microscopy as well as being suitable for routine histological use [17]. It is a minimally modified Millonig's phosphate buffered formaldehyde solution, the buffer system being dibasic sodium phosphate and sodium hydroxide. The pH is neutral and osmolality excluding formaldehyde is 290.

Composition per litre:

Technical grade 37-40% Formaldehyde	100.0ml
Monobasic sodium phosphate	18.6g
Sodium hydroxide	4.2g
Tap water	900.0ml

Carson found neither 'commercially pure' 37-40 per cent formaldehyde (which like most 37-40 per cent formaldehyde solutions contains 10-15 per cent methanol for preservation), nor formaldehyde prepared from paraformaldehyde, nor deionized water, gave better morphology.

9.2 Periodate-lysine-paraformaldehyde (PLP) and its dichromate derivative (PLPD)

PLP was described by McLean and Nakane [89]. As it does not keep, it is better to prepare small quantities.

To make up 100ml of PLP.

0.05M phosphate buffer	100.0ml
8% 'paraformaldehyde' solution	25.0ml

Anhydrous sodium metaperiodate	0.22g
Lysine monohydrochloride	1.37g

The 0.05M phosphate buffer has this composition:

Dibasic sodium phosphate, dihydrate	15.6g
Monobasic sodium phosphate, dihydrate	2.0g
Deionized water	2.0L

8 per cent 'paraformaldehyde' solution is prepared by suspending 40g of paraformaldehyde in 500ml of deionized water at 70C and adding 500mg of sodium hydroxide (five pellets). The polyoxymethylene paraformaldehyde polymer is dissociated by this process yielding a methanol-free formaldehyde solution.

To prepare periodate-lysine-paraformaldehyde-dichromate (PLPD), PLP is diluted with an equal volume of 5 per cent potassium dichromate in water. This fixative was introduced by Holgate et al [63].

9.3 ABC Immunostaining for light microscopy

Cut four micron sections from paraffin blocks	
Dry at 50C overnight	
Dewax in xylene	10 minutes
Rehydrate through graded alcohols to tap water	
Transfer to TRIS buffered 0.9 per cent saline (TBS)	
Dry round sections and transfer to humid chamber	
Apply 10 per cent normal goat serum in TBS (NGS/TBS)	5 minutes
Drain excess NGS/TBS and dry round sections	
Apply Y13-259 1:50 in NGS/TBS	60 minutes
Wash in TBS in Steiner vessel on rocker	2x5 minutes
Apply NGS/TBS	5 minutes

Drain excess NGS/TBS and dry round sections	
Transfer to humid chamber	
Apply biotinylated goat-anti-rat IgG 1:50 in NGS/TBS	30 minutes
Wash in TBS in Steiner vessel on rocker	2x5 minutes
Dry round sections and transfer to humid chamber. Apply avidin-biotin complex (Amersham) 1:200 in TBS or Dako ABC reagent	15 minutes
Wash in TBS in Steiner vessel on rocker	3x5 minutes
Develop with diaminobenzidine-hydrogen peroxide in TRIS-imidazole buffer	1-2 minutes
Wash in running tap water	10 minutes
Dehydrate, clear, mount	

9.4 TRIS-buffered saline

Stock solution of TRIS, (Tris(hydroxymethyl)aminomethane), MW 121.14. Dissolve 30.3g in 500ml of DDW. Add 1 Molar HCl until pH = 7.6. Approximately 200ml will be needed. Dilute to 2L. Molar HCl contains 85ml of concentrated acid per litre. To make up TRIS-buffered saline (TBS), dilute tenfold with 0.9 per cent NaCl in DDW.

9.5 TRIS-imidazole buffer and peroxidase development

0.1 Molar HCl	38.0ml
0.2 Molar TRIS	24.0ml
DDW	38.0ml
Imidazole (MW 68.1)	68.1mg

Final pH should be 7.6. If a detergent such as Triton X-100 is incorporated at low concentration (0.05 per cent) in the buffer, it is easier to wet sections evenly which gives more uniform development. 1mg/ml of

diaminobenzidine (DAB) in TRIS-imidazole buffer is activated with 5µl/ml of 100 volume hydrogen peroxide immediately before use.

9.6 Immunogold-silver staining for light micoscopy

9.6.1 Indirect (2-stage) immunogold-silver staining

Cut four micron sections from paraffin blocks	
Dry at 50C overnight	
Dewax in xylene	10 minutes
Rehydrate through graded alcohols to tap water	
Transfer to TRIS buffered 0.9 per cent saline (TBS)	
Dry round sections and transfer to humid chamber	
Apply 10 per cent normal goat serum in TBS (NGS/TBS)	5 minutes
Drain excess NGS/TBS and dry round sections	
Transfer to humid chamber	
Apply Y13-259 1:50 in NGS/TBS	60 minutes
Wash in TBS in Steiner vessel on rocker	2x5 minutes
Apply NGS/TBS	5 minutes
Drain excess NGS/TBS and dry round sections	
Transfer to humid chamber	
Apply LM grade goat anti-rat IgG-colloidal-gold (Janssen) 1:50 in NGS/TBS	30 minutes
Wash in TBS in Steiner vessel on rocker	3x5 minutes
Wash in deionized distilled water (DDW) in Steiner dish on rocker	6x2 minutes
Enhance (control under staining microscope)	
Counterstain, Dehydrate, Clear, Mount	

Enhance sections with Janssen's 'IntenSE' or 'IntenSE II' kit as per manufacturer's instructions. The pH of the 'IntenSE' reagent is low (3.2) and a stronger signal results if sections are post-fixed in 2 per cent

glutaraldehyde in PBS (not TBS) before enhancement. Wash in running tap water for ten minutes after post-fixation then proceed with washes in DDW. IntenSE II reagent has neutral pH.

9.6.2 Immunogold-silver staining with streptavidin-biotin-gold complex

Cut four micron sections from paraffin blocks
Dry at 50C overnight
Dewax in xylene 10 minutes
Rehydrate through graded alcohols to tap water
Transfer to TRIS buffered 0.9 per cent saline (TBS)
Dry round sections and transfer to humid chamber
Apply 10 per cent normal goat serum
in TBS (NGS/TBS) 5 minutes
Drain excess NGS/TBS and dry round sections
Transfer to humid chamber
Apply Y13-259 1:50 in NGS/TBS 60 minutes
Wash in TBS in Steiner vessel on rocker 2x5 minutes
Apply NGS/TBS 5 minutes
Drain excess NGS/TBS and dry round sections
Transfer to humid chamber
Apply biotinylated goat-anti-rat IgG 1:50
in NGS/TBS 30 minutes
Wash in TBS in Steiner vessel on rocker 2x5 minutes
Dry round sections and transfer to humid chamber
Apply streptavidin-biotin-gold complex (Janssens)
1:50 in TBS 30 minutes
Wash in TBS in Steiner vessel on rocker 3x5 minutes
Wash in deionized distilled water (DDW)
in Steiner dish on rocker 6x2 minutes
Enhance (control under staining microscope)
Counterstain, Dehydrate, Clear, Mount

9.7 Pre-embedding ABC immunostaining for electron microscopy

Fix thin tissue blocks overnight in PLP or PLPD at 4C	
Wash in Sorensens phosphate buffer, pH 7.4 (SPB)	4x2 hours
Cryoprotect by immersion in the following series:	
5 per cent glycerol, 10 per cent sucrose in SPB	30 minutes
10 per cent glycerol, 15 per cent sucrose in SPB	60 minutes
10 per cent glycerol, 20 per cent sucrose in SPB	Overnight
Freeze onto cryostat chuck with OCT	
Cut thick frozen sections (50-100um)	

All subsequent manipulations are on free-floating sections in culture-plate wells. Reagents are conveniently added and removed with a cut-down pipette tip fitted to a 5ml syringe. Needles catch sections and are better avoided.

Wash in SPB or TBS	2x5 minutes
Suspend NGS/TBS	60 minutes
Replace with Y13-259 1:50 in NGS/TBS; keep at 4C	Overnight
Wash in TBS	4x2 hours
Suspend NGS/TBS	60 minutes
Replace with biotinylated goat-anti-rat IgG 1:50 in NGS/TBS; keep at 4C	Overnight
Wash in TBS	4x2 hours
Suspend in ABC as for light microscopy	Overnight
Wash in TBS	4x2 hours
Suspend in DAB-TRIS-imidazole buffer without H_2O_2	10 minutes

Replace with DAB-TRIS-imidazole buffer	
with H_2O_2	10 minutes
Wash in TBS	10 minutes
Osmicate in one per cent OsO_4	2 hours
Process for electron microscopy	

9.8 Sorensen's phosphate buffer pH 7.4

Potassium dihydrogen phosphate, anhydrous	3.6g
Disodium hydrogen phosphate dihydrate	19.0g
DDW	2.0L

9.9 Pre-embedding immunogold labelling for electron microscopy

This technique was applied to cultured cells grown on coverslips, not to tissue sections. Make up fixative containing 2 per cent paraformaldehyde, 0.1 per cent glutataldehyde, 0.1 per cent Triton X-100 in Sorensen's phosphate buffer (SPB); also 0.1 per cent Triton X-100 in SPB, and SPB alone.

Pretreat cells on coverslips with	
Triton X-100/SPB	20 seconds
Transfer to fixative	10 minutes
Wash in SPB	3x5 minutes
Apply NGS/TBS	5 minutes
Drain and apply Y13-259 1:50 in NGS/TBS	1 hour
Wash in TBS	2x5 minutes
Apply NGS/TBS	5 minutes
Drain and apply EM-grade goat-anti-rat IgG	
5nm colloidal gold probe 1:5 in NGS/TBS	1 hour
Wash in TBS	3x5 minutes
Wash in SPB	
Postfix in one per cent OsO_4	

in cacodylate buffer	10 minutes
Process for electron microscopy	

9.10 Post-embedding immunogold labelling for electron microscopy

Fix tissue in PLP or PLPD, wash in buffer, embed in Araldite, or Lowikryl or other hydrophilic resin.	
Collect sections of gold interference colour onto gold grids	
Etch with fresh saturated NaOH in ethanol	6-8 seconds
Rinse in two changes of sterile DDW	
Check sections have survived sodium ethoxide etching	
Apply normal goat serum (NGS) 1:30 in phosphate buffered saline (PBS) containing 1 per cent bovine serum albumin and 0.01M glycine (PBSAG)	10 minutes
Transfer to Y13-259 1:50 in PBSAG	Overnight
Wash in PBS	6x5 minutes
Apply PBSAG	10 minutes
Transfer to EM-grade goat-anti-rat IgG 5nm colloidal gold probe 1:10 in PBSAG	60 minutes
Wash in PBS	6x5 minutes
Wash in sterile DDW	6x2 minutes
Transfer to saturated uranyl acetate	10 minutes
Rinse in sterile DDW	

These manipulations are conveniently performed in drops on a slab of dental wax. The etching stage is omitted for material embedded in hydrophilic resins. Solutions should be filtered through an 0.2um Millipore filter before use. The washes are necessary for low background.

9.11 Mancini gels

Gels were poured from 2 per cent low-melting-temperature agarose in PBS containing 0.1 per cent sodium azide, mixed with an equal volume of goat anti-rat IgG (Sigma) diluted in PBS-azide. Undiluted antibody was certified by Sigma to precipitate 0.92mg of rat IgG per ml and gels were prepared at final dilutions 1:10, 1:20, 1:40, 1:100. Best results were given at 1:20. 3ml gels were poured on plain glass slides 40x75mm on a levelling table. Ten 5ul wells were cast with a specially made former. Test samples were placed in the wells and the gels kept at 4C for 48 hours. Ring diameters were read with a graduated magnifying eyepiece.

Gels were stained for one hour with the following solution:

Coomassie Brilliant Blue or Kenacid Blue R		1.0g
Methanol		225.0ml
Glacial acetic acid		50.0ml
Deionized distilled water	to	500.0ml

And destained until appropriately differentiated in:

Methanol		225.0ml
Glacial acetic acid		35.0ml
Deionized distilled water	to	500.0ml

Gels could be air-dried without measurable change in ring diameter, and covered with a large cover-slip to make a permanent preparation.

CHAPTER 5 REFERENCES

001. Alpers CE, Wellings SR. The prevalence of carcinoma in situ in normal and cancer-associated breasts. Hum Pathol 16, 796-807, 1985.

002. Ashikari R, Hajdu SI, Robbins GF. Intraductal carcinoma of the breast (1960-1969). Cancer 28, 1182-1187, 1971.

003. Azzopardi JG. Problems in breast pathology. London, W B Saunders Company, 1979.

004. Balmain A, Ramsden M, Bowden GT, Smith J. Activation of the mouse cellular Harvey-ras gene in chemically induced benign skin papillomas. Nature 307, 658-660, 1984.

005. Bar-Sagi D, Feramisco JR. Microinjection of the ras oncogene protein into PC12 cells induces morphological differentiation. Cell 42, 841-848, 985.

006. Barbacid M. Ras genes. Annu Rev Biochem 56, 779-827, 1987.

007. Bargmann CI, Hung M-C, Weinberg RA. Multiple independent activations of the c-neu oncogene by a point mutation altering the trans-membrane domain of p185. Cell 45, 649-657, 1986.

008. Battersby S, Anderson TJ. Myofibroblast activity of radial scars. J Pathol 147, 33-40, 1985.

009. Biunno I, Pozzi MR, Pierotti MA, Pilotti S, Cattoretti G, Della Porta G. Structure and expression of

oncogenes in surgical specimens of human breast carcinomas. Br J Cancer 57, 464-468, 1988.

010. Black MM, Chabon AB. In situ carcinoma of the breast. Pathol Annu 4, 185-210, 1969.

011. Bos JL, Fearon ER, Hamilton SR, et al. Prevalence of ras gene mutations in human colorectal cancers. Nature 327, 293-297, 1987.

012. Brown PW, Silverman J, Owens E, Tabar DC, Terz JJ, Lawrence WJ. Intraductal 'non-infiltrating' carcinoma of the breast. Arch Surg 111, 1063-1067, 1976.

013. Buehring GC, Jensen HM. Lack of toxicity of methylene blue chloride to supravitally stained human mammary tissues. Cancer Res 43, 6039-6044, 1983.

014. Cales C, Hancock JF, Marshall CJ, Hall A. The cytoplasmic protein GAP is implicated as the target for regulation by the ras gene product. Nature 332, 548-551, 1988.

015. Candlish W, Kerr IB, Simpson HW. Immunocytochemical detection and significance of p21 ras family oncogene product in benign and malignant breast disease. J Pathol 150, 163-167, 1986.

016. Capon DJ, Chen EY, Levinson AD, Seeburg PH, Goeddel DV. Complete nucleotide sequence of the T24 human bladder carcinoma oncogene and its normal homologue. Nature 302, 33-37, 1983.

017. Carson FL, Martin JH, Lynn JA. Formalin fixation for electron microscopy: A reevaluation. Am J Clin Pathol 59, 365-373, 1973.

018. Chang EH, Furth ME, Scolnick EM, Lowy DR. Tumorigenic transformation of mammalian cells induced by a normal human gene homologous to the oncogene of Harvey murine sarcoma virus. Nature 297, 479-483, 1982.

019. Chesa PG, Rettig WJ, Melamed MR, Old LJ, Niman HL. Expression of p21 ras in normal and malignant human tissues: Lack of association with proliferation and malignancy. Proc Natl Acad Sci USA 84, 3234-3238, 1987.

020. Clagett OT, Plimton NC, Root GT. Lesions of the breast. The relationship of benign disease to carcinoma. Surgery 15, 413-419, 1944.

021. Clair T, Miller WR, Cho-Chung YS. Prognostic significance of the expression of a ras protein with a molecular weight of 21,000 by human breast cancer. Cancer Res 47, 5290-5293, 1987.

022. Clark R, Wong G, Arnheim N, Nitecki D, McCormick F. Antibodies specific for amino acid 12 of the ras oncogene product inhibit GTP binding. Proc Natl Acad Sci USA 82, 5280-5284, 1985.

023. Cohen JB, Levinson AD. A point mutation in the last intron responsible for increased expression and transforming activity of the c-Ha-ras oncogene. Nature 334, 119-124, 1988.

024. Coussens L, Yang-Feng TL, Liao Y-C et al. Tyrosine kinase receptor with extensive homology to EGF receptor

shares chromosomal location with neu oncogene. Science 230, 1132-1139, 1985.

025. Davis BW, Gelber R, Goldhirsch A et al. Prognostic significance of peritumoral vessel invasion in clinical trials of adjuvant therapy for breast cancer with axillary node metastasis. Human Pathology, 16, 1212-1218, 1985.

026. Dawson EK. Carcinoma in the mammary lobule and its origin. Edinburgh Medical Journal 40, 57-82, 1933.

027. De Bortoli ME, Abou-Issa H, Haley BE, Cho-Chung YS. Amplified expression of p21 ras protein in hormone-dependent mammary carcinomas of humans and rodents. Biochem Biophys Res Commun 127, 699-706, 1985.

028. De Brabander M, Geuens G, Nuydens RM, Moeremans M, De Mey, J. Probing microtubule-dependent intracellular motility with nanometre particle video ultramicroscopy (nanovid ultramicroscopy). Cytobios 43, 273-283, 1985.

029. De Brabander M, Nuydens R, Geuens G, Moeremans M, De Mey J. The use of submicroscopic gold particles combined with video contrast enhancement as a simple molecular probe for the living cell. Cell Motil Cytoskel 6, 105-113, 1986.

030. DeFeo D, Gonda MA, Young HA et al. Analysis of two divergent rat genomic clones homologous to the transforming gene of Harvey murine sarcoma virus. Proc Natl Acad Sci USA, 78, 3328-3332, 1981.

031. Der CJ, Krontiris TG, Cooper GM. Transforming genes of human bladder and lung carcinoma cell lines are

homologous to the ras genes of Harvey and Kirsten sarcoma virus. Proc Natl Acad Sci USA 79, 3637-3640, 1982.

032. Dixon JM, Scott WN, Miller WR. Natural history of cystic disease: The importance of cyst type. Br J Surg 72, 190-192, 1985.

033. Dupont WD, Page DL. Risk factors for breast cancer in women with proliferative breast disease. N Engl J Med 312, 146-151, 1985.

034. Feramisco JR, Clark R, Wong G, Arnheim N, Milley R, McCormick F. Transient reversion of ras oncogene induced cell transformation by antibodies specific for amino acid 12 of ras protein. Nature 314, 639-642, 1985.

035. Feramisco JR, Gross M, Kamata T, Rosenberg M, Sweet RW. Microinjection of the oncogene form of the human H-ras (T24) protein results in rapid proliferation of quiescent cells. Cell 38, 109-117, 1984.

036. Fisher ER, Brown R. Intraductal signet-ring cell carcinoma: A hitherto undescribed form of intraductal carcinoma of the breast. Cancer 55, 2533-2537, 1985.

037. Foote FW, Stewart FW. A histologic classification of carcinoma in the breast. Surgery 19, 74-99, 1946.

038. Foote FW, Stewart FW. Comparative studies of cancerous versus noncancerous breasts. Ann Surg 121, 197-223, 1945.

039. Foote FW, Stewart FW. Lobular carcinoma in situ. Am J Pathol 17, 491-495, 1941.

040. Forrester K, Almoguera C, Han K, Grizzle WE, Perucho M. Detection of high incidence of K-ras oncogenes during human colon tumorigenesis. Nature 327, 298-303, 1987.

041. Fromowitz FB, Viola MV, Chao S et al. Ras p21 expression in the progression of breast cancer. Hum Pathol 18, 1268-1275, 1987.

042. Furth ME, Aldrich TH, Cordon-Cardo C. Expression of ras proto-oncogene proteins in normal human tissues. Oncogene 1, 47-58, 1987.

043. Furth ME, Davis LJ, Fleurdelys B, Scolnick EM. Monoclonal antibodies to the p21 products of the transforming gene of Harvey murine sarcoma virus and of the cellular ras gene family. J Virol 43, 294-304, 1982.

044. Gallick GE, Kurzrock R, Kloetzer WS, Arlinghaus RB, Gutterman JU. Expression of p21 ras in fresh primary and metastatic human colorectal tumours. Proc Natl Acad Sci USA 82, 1795-1799, 1985.

045. Ghosh AK, Moore M, Harris M. Immunohistochemical detection of ras oncogene p21 product in benign and malignant mammary tissue in man. J Clin Pathol 39, 428-434, 1986.

046. Gibbs JB, Sigal IS, Poe M, Scolnick EM. Intrinsic GTPase activity distinguishes normal and oncogenic ras p21 molecules. Proc Natl Acad Sci USA 81, 5704-5708, 1984.

047. Going JJ, Anderson TJ, Battersby S, Macintyre CCA. Proliferative and secretory activity in human breast

during natural and artificial menstrual cycles. Am J Pathol 130, 193-204, 1988.

048. Going JJ, Anderson TJ, Wyllie AH. Expression of p21 ras in normal and pathological breast tissue. J Pathol 155, 357A, 1988.

049. Going JJ, Anderson TJ, Wyllie AH. Expression of p21 ras in normal, atypical and neoplastic breast tissue. XVII International Congress, International Academy of Pathology, Dublin, september 1988; abstract 1.

050. Going JJ, Anderson TJ, Wyllie AH. Expression of p21 ras in normal, atypical and neoplastic breast tissue. Poster, international ras workshop, Athens, november 1988.

051. Going JJ, Williams ARW, Wyllie AH, Anderson TJ, Piris J. Optimal preservation of p21 ras immunoreactivity and morphology in paraffin-embedded tissue. J Pathol 155, 185-190, 1988.

052. Goudie RB. Immunohistology in diagnostic histopathology. Chapter 13 in: Recent advances in histopathology, Volume 13. (Anthony PP, MacSween RNM, eds.) Edinburgh, Churchill Livingstone, 233-254, 1987.

053. Goyette M, Petropoulos CJ, Shank PR, Fausto N. Expression of a cellular oncogene during liver regeneration. Science 219, 510-512, 1983.

054. Grand JA, Smith KJ, Gallimore PH. Purification and characterisation of the protein encoded by the activated human N-ras gene and its membrane localisation. Oncogene 1, 305-314, 1987.

055. Guerrero I, Wong H, Pellicer A, Burstein DE. Activated N-ras gene induces neuronal differentiation of PC12 rat phaeochromocytoma cells. J Cell Physiol 129, 71-76, 1986.

056. Gusterson BA, Gullick WJ, Venter DJ et al. Immunohistochemical localisation of c-erbB2 in human breast carcinomas. Mol Cell Probes 1, 383-391, 1987.

057. Haagensen CD, Lane N, Lattes R, Bodian C. Lobular neoplasia (so called lobular carcinoma in situ) of the breast. Cancer 42, 737-769, 1978.

058. Haagensen CD. Diseases of the breast. 2nd edition. Philadelphia, W B Saunders Company, 1971.

059. Hagag N, Halegoua S, Viola M. Inhibition of growth-factor induced differentiation of PC12 cells by microinjection of antibody to ras p21. Nature 319, 680-682, 1986.

060. Hawkins RA, Black R, Steele RJC, Dixon JMJ, Forrest APM. Oestrogen receptor concentration in primary breast cancer and axillary node metastases. Breast Cancer Res Treat 1, 245-251, 1981.

061. Hochwalt AE, Solomon JJ, Garte SJ. Mechanism of H-ras oncogene activation in mouse squamous carcinoma induced by an alkylating agent. Cancer Res 48, 556-558, 1988.

062. Holgate CS, Jackson P, Cowen PN, Bird CC. Immunogold-silver staining: New method of immunostaining with enhanced sensitivity. J Histochem Cytochem 31, 928-944, 1983.

063. Holgate CS, Jackson P, Pollard K, Lunny D, Bird CC. Effect [of] fixation on T and B lymphocyte surface membrane antigen demonstration in paraffin processed tissue. J Pathol 149, 293-300, 1986.

064. Horan Hand P, Thor A, Wunderlich D, Muraro R, Caruso A, Schlom J. Monoclonal antibodies of predefined specificity detect activated ras gene expression in human mammary and colon carcinomas. Proc Natl Acad Sci USA 81, 5227-5231, 1984.

065. Hyland JK, Rogers CM, Scolnick EM, Stein RB, Ellis R, Baserga R. Microinjected ras family oncogenes stimulate DNA synthesis in quiescent mammalian cells. Virology 141, 333-336, 1985.

066. Itoh H, Kozasa T, Nagata S et al. Molecular cloning and sequence determination of cDNAs for alpha subunits of the guanine nucleotide binding proteins Gs, Gi and Go from rat brain. Proc Natl Acad Sci USA 83, 3776-3780, 1986.

067. Jensen HM, Rice JR, Wellings SR. Preneoplastic lesions in the human breast. Science 191, 295-297, 1976.

068. Johnstone A, Thorpe R. Immunochemistry in Practice. 2nd edition. Oxford, Blackwell Scientific Publications, 125-127, 1986.

069. Joshi K, Smith JA, Perushinge N, Monoghan P. Cell proliferation in the human mammary epithelium: Differential contribution by epithelial and myoepithelial cells. Am J Pathol 124, 199-206, 1986.

070. Kaziro Y. The role of guanosine 5'-triphosphate in polypeptide chain elongation. Biochim Biophys Acta 505, 95-127, 1978.

071. Kerr IB, Lee FD, Quintanilla M, Balmain A. Immunocytochemical detection of p21 ras family oncogene product in normal mucosa and in premalignant and malignant tumours ofthe colorectum. Br J Cancer 52, 695-700, 1985.

072. Kiaer W. Relationship of fibroadenomatosis ('chronic mastitis') to cancer of the breast. Copenhagen, Munksgaard, 1954.

073. King CR, Kraus MH, Aaronson SA. Amplification of a novel v-erbB related gene in a human mammary carcinoma. Science 229, 974-976, 1985.

074. Kraus MH, Yuasa Y, Aaronson SA. A position 12 activated H-ras oncogene in all HS578T mammary carcinoma cells but not normal mammary cells of the same patient. Proc Natl Acad Sci USA 81, 5384-5388, 984.

075. Krontiris TG, DiMartino NA, Colb M, Parkinson DR. Unique allelic restriction fragments of the human Ha-ras locus in leucocyte and tumour DNAs of cancer patients. Nature 313, 369-374, 1985.

076. Lacal JC, Anderson PS, Aaronson SA. Deletion mutants of Harvey ras p21 protein reveal the absolute requirement of at least two distant regions for GTP-binding and transforming activities. EMBO J 5, 679-687, 1986.

077. Lacal JC, Srivastava SK, Anderson PS, Aaronson SA. Ras p21 proteins with high or low GTPase activity can efficiently transform NIH 3T3 cells. Cell 44, 609-617, 1986.

078. Land H, Parada LF, Weinberg RA. Tumorigenic conversion of primary embryo fibroblasts requires at least two cooperating oncogenes. Nature 304, 596-602, 1983.

079. Lidereau R, Escot C, Theillet C et al. High frequency of rare alleles of the human c-Ha-ras1 protooncogene in breast cancer patients. J Natl Cancer Inst 77, 697-701, 1986.

080. Lochrie MA, Hurley JB, Simon MI. Sequence of the alpha subunit of photoreceptor G protein: homologies between transducin, ras, and elongation factors. Science 228, 96-99, 1985.

081. Lundy T, Grimson R, Mishricki Y et al. Elevated ras oncogene expression correlates with lymph node metastasis in breast cancer patients. J Clin Oncol 14, 1321-1325, 1986.

082. Mackay J, Elder PA, Porteous DJ et al. Partial deletion of chromosome 11 in breast cancer correlates with size of primary tumour and oestrogen receptor level. Br J Cancer (in press).

083. Manne V, Bekesi E, Kung H-F. Ha-ras proteins exhibit GTPase activity: Point mutations that activate Ha-ras gene products result in decreased GTPase activity. Proc Natl Acad Sci USA 82, 376-380, 1985.

084. McDivett RW, Stewart FW, Berg JW. Tumours of the breast. Atlas of tumour pathology. Second series part 2. Washington DC, Armed Forces Institute of Pathology, 1968.

085. McGee J O'D. The c-H-ras1 gene and its expression in human breast cancer: Its role in growth factor signal transduction. Lecture, 157th meeting Pathological Society of Great Britain and Ireland, Newcastle upon Tyne, July 1988.

086. McGrath JP, Capon DJ, Goeddel DV, Levinson AD. Comparative biochemical properties of normal and activated human ras p21 protein. Nature 310, 644-649, 1984.

087. McGurrin JF, Doria MI Jr, Dawson PJ, Karrison T, Stein HO, Franklin WA. Assessment of tumour cell kinetics by immunohistochemistry in carcinoma of breast. Cancer 59, 1744-1750, 1987.

088. McKay IA, Marshall CJ, Cales C, Hall A. Transformation and stimulation of DNA synthesis in NIH 3T3 cells are a titratable function of normal p21 N-ras expression. EMBO J 5, 2617-2621, 1986.

089. McLean IW, Nakane PK. Periodate-lysine-paraformaldehyde fixative: A new fixative for immunoelectron microscopy. J Histochem Cytochem 22, 1077-1083, 1974.

090. Mulcahy LS, Smith MR, Stacey DW. Requirement for ras proto-oncogene function during serum-stimulated growth of NIH 3T3 cells. Nature 313, 241-243, 1985.

091. Muller WJ, Sinn E, Pattengale PK, Wallace R, Leder P. Single-step induction of mammary adenocarcinoma in transgeneic mice bearing the activated c-neu gene. Cell 54, 105-115, 1988.

092. Nairn RC. Fluorescent protein tracing. 4th edition. Edinburgh, Churchill Livingstone, 371-372, 1976.

093. Nielsen M, Thomsen JL, Primdahl S, Dyreborg U, Andersen JA. Breast cancer and atypia among young and middle aged women: A study of 110 medicolegal autopsies. Br J Cancer 56, 814-819, 1987.

094. Noda M, Ko M, Ogura A et al. Sarcoma viruses carrying ras oncogenes induce differentiation-associated properties in a neuronal cell line. Nature 318, 73-75, 1985.

095. Ohuchi N, Thor A, Page DL, Horan Hand P, Halter S, Schlom J. Expression of the 21,000 molecular weight ras protein in a spectrum of benign and malignant human mammary tissues. Cancer Res 46, 2511-2519, 1986.

096. Page DL, Anderson TJ. Diagnostic histopathology of the breast. Edinburgh, Churchill Livingstone, 1987.

097. Page DL, Dupont WD, Rogers LW, Rados MS. Atypical hyperplastic lesions of the breast. A long term follow up study. Cancer 55, 2698-2708, 1985.

098. Page DL, Dupont WD, Rogers LW, Landenberger M. Intraductal carcinoma of the breast: Follow-up after biopsy only. Cancer 49, 751-758, 1982.

099. Parada LF, Tabin CJ, Shih C, Weinberg RA. Human EJ bladder carcinoma oncogene is homologue of Harvey sarcoma virus ras gene. Nature 297, 474-478, 1982.

100. Pulciani S, Santos E, Long LK, Sorrentino V, Barbacid M. Ras gene amplification and malignant transformation. Mol Cell Biol 5, 2836-2841, 1985.

101. Quintanilla M, Brown K, Ramsden M, Balmain A. Carcinogen-specific mutation and amplification of Ha-ras during mouse skin carcinogenesis. Nature 322, 78-80, 1986.

102. Reddy EP, Reynolds RK, Santos E, Barbacid M. A point mutation is responsible for the acquisition of transforming properties by the T24 human bladder carcinoma oncogene. Nature 300, 149-152, 1982.

103. Robinson A, Williams ARW, Piris J, Spandidos DA, Wyllie AH. Evaluation of a monoclonal antibody to ras peptide, RAP-5, claimed to bind preferentially to cells of infiltrating carcinomas. Br J Cancer 54, 877-883, 1986.

104. Rosen PP, Lieberman PH, Braun DW Jr, Kosloff C, Adair F. Lobular carcinoma in situ of the breast: Detailed analysis of 99 patients with average follow-up of 24 years. Am J Surg Pathol 2, 225-251, 1978.

105. Ruiter DJ, Mauw BJ, Beyer-Boon ME. Ultrastructure of normal epithelial cells in Papanicolaou stained cervical smears. Acta Cytol 23, 507-515, 1979.

106. Santos E, Tronick SR, Aaronson SA, Pulciani S, Barbacid M. T24 bladder carcinoma oncogene is an

activated form of the normal human homologue of BALB- and Harvey-MSV transforming genes. Nature 298, 343-347, 1982.

107. Schechter AL, Stern DF, Vaidyanathan L et al. The neu oncogene: An erbB related gene encoding a 185,000-Mr tumour antigen. Nature 312, 513-516, 1984.

108. Scolnick EM, Papageorge AG, Shih TY. Guanine nucleotide-binding activity as an assay for src protein of rat-derived murine sarcoma viruses. Proc Natl Acad Sci USA 76, 5355-5359, 1979.

109. Seemayer TA, Schurch W, Lagace R. Myofibroblasts in human pathology. Human Pathology 12, 491-492, 1981.

110. Semba K, Kamata N, Toyoshima K, Yamamoto T. A v-erbB-related protooncogene, c-erbB2, is distinct from the c-erbB1/epidermal growth factor receptor gene and is amplified in a human salivary gland adenocarcinoma. Proc Natl Acad Sci USA 82, 6497-6501, 1985.

111. Shih TY, Papageorge AG, Stokes PE, Weeks MO, Scolnick EM. Guanine nucleotide binding and autophosphorylating activities associated with the p21 src protein of Harvey murine sarcoma virus. Nature 287, 686-691, 1980.

112. Shimizu K, Goldfarb M, Perucho M, Wigler M. Isolation and preliminary characterisation of the transforming gene of a human neuroblastoma cell line. Proc Natl Acad Sci USA 80, 383-387, 1983.

113. Shotton D. The current renaissance in light microscopy. I. Dynamic studies of living cells by video

enhanced contrast microscopy. Proc R Microscopic Soc 22, 37-44, 1987.

114. Sigal IS. The ras oncogene: A structure and some function. Nature 332, 485-486, 1988.

115. Sinn E, Muller W, Pattengale P, Tepler I, Wallace R, Leder P. Coexpression of MMTV/v-Ha-ras and MMTV/c-myc genes in transgenic mice: Synergistic actions of oncogenes in vivo. Cell 49, 465-475, 1987.

116. Slamon DJ, Clark GM, Wong SG, Levin WJ, Ullrich A. Human breast cancer: Correlation of relapse and survival with amplification of the HER-2/neu oncogene. Science 235, 177-182, 1987.

117. Slamon DJ, de Kernion JB, Verma IM, Cline MJ. Expression of cellular oncogenes in human malignancies. Science 224, 256-262, 1984.

118. Sokal RR, Rohlf FJ. Biometry: The principles and practice of statistics in biological research. 2nd edition. San Francisco, W H Freeman, 440-445, 1981.

119. Spandidos DA, Agnantis NJ. Human malignant tumours of the breast, as compared to their respective normal tissue, have elevated expression of the Harvey ras oncogene. Anticancer Res 4, 269-272, 1984.

120. Spandidos DA, Dimitrov T. High expression levels of ras p21 protein in normal mouse heart tissues. Biosci Rep 5, 1035-1039, 1985.

121. Spandidos DA, Kerr IB. Elevated expression of the human ras oncogene family in premalignant and malignant

tumours of the colorectum. Br J Cancer 49, 681-688, 1984.

122. Spandidos DA, Wilkie NM. Malignant transformation of early passage rodent cells by a single mutated human oncogene. Nature 310, 469-475, 1984.

123. Spandidos DA. Oncogene activation in malignant transformation. A study of H-ras in human breast cancer. Anticancer Res 7, 991-996, 1987.

124. Springall DH, Hacker GW, Grimelius L, Polak JM. The potential of the immunogold-silver staining method for paraffin sections. Histochemistry 81, 603-608, 1984.

125. Stacey DW, Kung H-F. Transformation of NIH 3T3 cells by microinjection of Ha-ras p21 protein. Nature 310, 508-511, 1984.

126. Steinhoff NG, Black WC. Florid cystic disease preceding mammary cancer. Annals Surg 171, 501-508, 1970.

127. Stewart TA, Pattengale PK, Leder P. Spontaneous mammary adenocarcinomas in transgenic mice that carry and express MTV/myc fusion genes. Cell 38, 627-637, 1984.

128. Sweet RW, Yokoyama S, Kamata T, Feramisco JR, Rosenberg M, Gross M. The product of ras is a GTPase and the T24 oncogenic mutant is deficient in this activity. Nature 311, 273-275, 1984.

129. Tabin CJ, Bradley SM, Bargmann CI et al. Mechanism of activation of a human oncogene. Nature 300, 143-149, 1982.

130. Tamanoi F, Walsh M, Kataoka T, Wigler M. A product of yeast RAS2 gene is a guanine nucleotide binding protein. Proc Natl Acad Sci USA 81, 6924-6928, 1984.

131. Tanaka T, Ida M, Shimoda H, Waki C, Slamon DJ, Cline MJ. Organ specific expression of ras oncoproteins during growth and development of the rat. Mol Cell Biochem 70, 97-104, 1986.

132. Tanaka T, Slamon DJ, Battifora H, Cline MJ. Expression of p21 ras oncoproteins in human cancers. Cancer Res 46, 1465-1470, 1986.

133. Taparowsky E, Shimizu K, Goldfarb M, Wigler M. Structure and activation of the human N-ras gene. Cell 34, 581-586, 1983.

134. Taparowsky E, Suard Y, Fasano O, Shimizu K, Goldfarb M, Wigler M. Activation of the T24 bladder carcinoma transforming gene is linked to a single amino acid change. Nature 300, 762-765, 1982.

135. Temeles GL, Gibbs JB, D'Alonzo JS, Sigal IS, Scolnick EM. Yeast and mammalian ras proteins have conserved biochemical properties. Nature 313, 700-703, 1985.

136. Theillet C, Lidereau R, Escot C et al. Loss of a c-Ha-ras1 allele and aggressive human primary breast carcinomas. Cancer Res 46, 4776-4781, 1986.

137. Thor A, Horan Hand P, Wunderlich D, Caruso A, Muraro R, Schlom J. Monoclonal antibodies define differential ras expression in malignant and benign colonic diseases. Nature 311, 562-565, 1984.

138. Thorpe SM, Rose C, Rasmussen BB, Mouridsen HT, Bayer T, Kielding N. Prognostic value of steroid hormone receptors: Multivariate analysis of systemically untreated patients with node negative primary breast cancer. Cancer Res 47, 6126-6133, 1987.

139. Trahey M, McCormick F. A cytoplasmic protein stimulates normal N-ras p21 GTPase, but does not affect oncogenic mutants. Science 238, 542-545, 1987.

140. Ullrich A, Coussens L, Hayflick JS et al. Human epidermal growth factor receptor cDNA sequence and aberrant expression of the amplified gene in A431 epidermoid carcinoma cells. Nature 309, 418-425, 1984.

141. Van de Vijver MJ, Mooi WJ, Wisman P, Peterse JL, Nusse R. Immunohistochemical detection of the neu protein in tissue sections of human breast tumours with amplified neu DNA. Oncogene 2, 175-178, 1988.

142. van de Vijver MJ, Peterse JL, Mooi WJ et al. Neu-protein expression in breast cancer: Association with comedo-type ductal carcinoma in situ and limited prognostic value in stage II breast cancer. N Engl J Med 319, 1239-1245, 1988.

143. Venter DJ, Tuzi NL, Kumar S, Gullick WJ. Overexpression of the c-erbB2 oncoprotein in human breast carcinomas: immunohistological assessment correlates with gene amplification. Lancet ii, 69-72, 1987.

144. Vogelstein B, Fearon ER, Hamilton SR et al. Genetic alterations during colorectal tumour development. N Engl J Med 319, 525-532, 1988.

145. Wakelam MJO, Davies SA, Houslay MD, McKay I, Marshall CJ, Hall A. Normal p21 N-ras couples bombesin and other growth factor receptors to inositol phosphate production. Nature 323, 173-176, 1986.

146. Walker RA, Wilkinson N. p21 ras protein expression in benign and malignant human breast. J Pathol 156, 147-153, 1988.

147. Ward JM, Pardue RL, Junker JL, Takahashi K, Shih TY, Weislow OS. Immunocytochemical localization of ras Ha p21 in normal and neoplastic cells in fixed tissue sections from Harvey sarcoma virus-infected mice. Carcinogenesis 7, 645-651, 1986.

148. Warren S. The relation of 'chronic mastitis' to carcinoma of the breast. Surg Gynaecol Obstet 71, 257-273, 1940.

149. Webber BL, Heise H, Neifeld JP, Costa J. Risk of subsequent contralateral breast carcinoma in a population of patients with in situ breast carcinoma. Cancer 47, 2928-2932, 1981.

150. Wellings SR, Jensen HM, Marcum RG. An atlas of subgross pathology of the human breast with special reference to possible precancerous lesions. J Natl Cancer Inst 55, 231-273, 1975.

151. Wellings SR, Jensen HM. On the origin and progression of ductal carcinoma in the human breast. J Natl Cancer Inst 50, 1111-1118, 1973.

152. Whittaker JL, Walker RA, Varley JM. Differential expression of cellular oncogenes in benign and malignant human breast tissue. Int J Cancer 38, 651-655, 1986.

153. Williams ARW, Piris J, Spandidos DA, Wyllie AH. Immunohistochemical detection of the ras oncogene p21 product in an experimental tumour and in human colorectal neoplasms. Br J Cancer 52, 687-693, 1985.

154. Willingham MC, Pastan I, Shih TY, Scolnick EM. Localisation of the src gene product of the Harvey strain of the MSV to plasma membrane of transformed cells by electron microscopic immunocytochemistry. Cell 19, 1005-1014, 1980.

155. Willumsen BM, Papageorge AG, Kung H-F et al. Mutational analysis of a ras catalytic domain. Mol Cell Biol 6, 2646-2654, 1986.

156. Wyllie AH, Rose KA, Morris RG, Steel CM, Foster E, Spandidos DA. Rodent fibroblast tumours expressing human myc and ras genes: Growth, metastasis and endogenous oncogene expression. Br J Cancer 56, 251-259, 1987.

157. Zhou D, Battifora H, Yokota J, Yamamoto T, Cline MJ. Association of multiple copies of the c-erbB2 oncogene with spread of breast cancer. Cancer Res 47, 6123-6125, 1987.

CHAPTER 11 DATA APPENDIX

This chapter lists patient data in three tables. The first (11.1) lists patient biopsy accession numbers (UB numbers), birth date, biopsy date, side and operative procedure. Dates are given in standard computer format (year, month and day being presented in that order as a six digit number) to facilitate data processing. Also given are numbers (prefixed by A or B) which identify cases rather than the more cumbersome UB numbers. In this table the last column lists lesions not specifically included under their own column heading in table 11.2 (see below).

Table 11.2 uses A or B number as sole patient identifier. It lists final scores allocated to p21 ras immunostaining for all elements scored. This table represents therefore a compendium of structural elements present in each case. In some cases other diagnoses are mentioned where relevant in the last column. Each column is headed by a capital or lower case Roman letter. These are the key to the element represented in that column, and what they mean is given in table 11.3.

Table 11.1

A No	UB No	DOBx	DOB	S	Op	Other
A 1	8616435	860812	380713	R	WG	
A 4	8616935	860819	330426	L	LZ	Fibroadenoma
A 5	8617163	860821	410307	L	BX	
A 7	8617443	860826	540209	R	WE	
A 12	8618127	860904	331212	L	MX	
A 15	8619025	860918	470227	R	RE	
A 16	8619805	860930	400716	L	BX	
A 28	8621655	861024	620527	L	BX	
A 31	8621834	861028	380206	L	RE	
A 32	8621833	861028	380108	R	BX	
A 33	8622058	861030	390213	L	WE	
A 34	8622059	861030	310719	L	MX	
A 35	8622408	861104	380603	L	WE	
A 36	8622961	861111	440305	R	MX	
A 37	8623288	861113	410304	R	MX	
A 38	8623289	861113	480602	L	WE	
A 39	8623290	861113	311112	R	WE	Fibroadenoma
A 40	8623292	861114	560119	L	BX	
A 41	8623473	861117	170819	L	LZ	
A 42	8623545	861118	311122	R	NS	
A 43	8623544	861118	400428	R	WG	
A 44	8623819	861120	450202	R	WE	
A 72	8703744	870223	220830	R	LZ	
A 73	8703950	870224	510309	L	WE	
A 74	8704823	870305	510914	R	WE	
A 76	8704825	870303	321006	L	MX	
A 77	8705040	870309	380225	L	BX	
A 78	8705079	870310	301219	R	LZ	Fibroadenoma
A 79	8705443	870313	640807	L	BX	Fibroadenoma
A 80	8705444	870313	640202	R	BX	
A 81	8705693	870316	570526	R	BX	
A 82	8706737	870330	290305	L	LZ	

Table 11.1 (continuation)

A No	UB No	DOBx	DOB	S	Op	Other
A 83	8706735	870330	350619	R	LZ	
A 85	8706981	870402	390419	R	BX	
A 86	8701765	870406	370629	R	MX	
A 87	8707324	870408	481226	L	LZ	
A 88	8707855	870414	500705	R	MX	
A 89	8707954	870416	450617	L	WE	
A 90	8707951	870416	311107	L	WE	
A 91	8707953	870416	680122	R	BX	
A 92	8708552	870423	450109	R	MX	
A 93	8708740	870427	440312	L	BX	Papilloma
A 94	8709026	870430	440809	L	MX	
A 95	8709248	870501	690125	L	BX	Fibroadenoma
A 96	8709488	870505	450528	L	MX	
A 98	8709030	870505	371124	-	LZ	
A 99	8709731	870511	440103	R	LZ	
A100	8709730	870511	201024	R	LZ	
A102	8609924	870512	321201	R	MX	
A103	8710051	870512	450101	R	WE	
A104	8710049	870512	360114	R	WG	
A106	8710188	870515	250501	R	MX	
A112	8710733	870521	431210	R	MX	
A114	8711008	870526	650522	R	BX	Fibroadenoma
A116	8711715	870604	230315	L	WE	
A117	8712170	870609	410516	L	MX	
A118	8712406	870612	220526	R	MX	
A119	8712640	870616	231204	R	WE	
A120	8712812	870618	451206	L	WE	
A121	8712813	870618	190912	R	WG	
A122	8713149	870623	440209	L	MX	Fibroadenoma
A123	8713150	870623	280420	L	WE	
A124	8713148	870623	440106	R	LZ	
A125	8713650	870630	380629	R	LZ	

Table 11.1 (continuation)

A No	UB No	DOBx	DOB	S	Op	Other
A126	8716164	870804	420924	R	LZ	Papilloma
A127	8716165	870804	370530	R	LZ	
A128	8716664	870811	300506	L	LZ	
A129	8716665	870811	200320	R	WE	
A130	8716666	870811	440815	R	LZ	
A131	8716838	870815	530510	L	BX	
A132	8717169	870818	251231	L	WE	Papilloma
A133	8717783	870825	151031	L	NL	
A134	8717782	870825	470224	R	NL	
A135	8718029	870827	520720	L	WE	
A136	8718030	870827	370123	R	BX	
A137	8718320	870901	180707	L	WE	
A138	8718321	870901	500219	R	LZ	
A139	8718322	870901	440810	L	LZ	
A140	8718576	870903	570616	L	WE	
A141	8718578	870903	441222	R	WE	
A142	8718579	870902	380802	R	WE	
A143	8718827	870907	461222	L	WE	
A144	8719591	870915	480706	R	WE	
A147	8720097	870924	310612	L	MX	
A148	8720207	870925	620305	L	BX	
A149	8720325	870928	570703	R	BX	
A150	8720462	870929	090219	L	BX	Papilloma
A151	8720625	871001	441223	R	MX	Phyllodes
A152	8720996	871006	300506	L	MX	
A153	8720924	871006	370418	L	LZ	
A154	8720925	871006	440727	L	LZ	
A155	8721210	871008	260329	L	WE	
A156	8721552	871012	600604	L	BX	
A157	8721471	871013	240731	L	LZ	
A158	8721520	871013	391002	R	LZ	
A159	8722058	871020	410620	-	LZ	

Table 11.1 (continuation)

A No	UB No	DOBx	DOB	S	Op	Other
A160	8722059	871020	420111	-	LZ	
A161	8722149	871020	300305	R	WE	
A162	8722151	871020	591115	L	BX	
A163	8722473	871023	640202	R	BX	
A164	8722620	871026	440206	R	BX	
A165	8722622	871027	470101	L	TC	
A166	8722726	871027	210620	L	WG	
A167	8722658	871027	380306	L	LZ	
A168	8722659	871027	444082	L	LZ	
A169	8722727	871027	300308	R	WE	
A170	8722950	871029	520204	L	WE	
A172	8722951	871029	430204	R	WE	
A173	8723323	871103	631004	R	RE	
A174	8723212	871103	330528	R	LZ	
A176	8723603	871105	320423	L	MX	
A177	8723514	871105	390827	R	WE	
A178	8723870	871109	530307	L	BX	Lactational
A179	8723871	871110	301123	L	MX	
A180	8724479	871117	430818	R	MX	
A181	8724488	871117	201112	R	TC	
A182	8724819	871119	460212	L	WE	
A183	8724902	871120	570914	L	BX	
A184	8724903	871120	550102	L	BX	Fibroadenoma
A186	8725068	871124	520101	R	WE	
A187	8725046	871124	351124	R	LZ	
A188	8725069	871124	360423	-	LZ	
A189	8725125	871124	280924	R	BX	
A192	8726387	871208	550615	L	WE	
A193	8726249	871208	320203	-	LZ	Papilloma
A194	8726255	871208	200605	L	LZ	
A195	8726554	871210	081006	L	MX	
A196	8726596	871215	530105	-	--	

Table 11.1 (continuation)

A No	UB No	DOBx	DOB	S	Op	Other
A197	8726918	871215	520727	L	MX	
A198	8727153	871218	430526	R	WE	
A199	8727035	871218	130913	R	MX	
A200	8727422	871222	570601	L	BX	
A202	8800233	880106	150423	R	MX	
A203	8800290	880107	440616	R	WE	
A204	8800603	880112	460424	R	WE	
A205	8801070	880109	480325	L	BX	
A206	8801026	880119	331122	R	LZ	
A207	8801321	880121	440129	L	WE	
A208	8801486	880126	521222	R	BX	
A209	8801559	880126	201107	R	WG	
A210	8801560	420216	420216	R	WG	
A211	8801556	880126	421016	R	BX	
A212	8801557	880126	551108	L	WE	
A213	8802211	880204	191228	R	WE	
A214	8802212	880219	400629	L	BX	Phyllodes
A215	8802213	880204	400824	L	BX	Phyllodes
A216	8802591	880211	560127	R	WE	
A217	8802942	880216	590815	R	BX	Papilloma
A218	8803102	880218	300617	L	WE	
A219	8803103	880218	311122	L	WE	
A220	8804191	880304	680304	L	BX	Fibroadenoma
A221	8805019	880324	420407	R	MX	
B 1	8612685	860619	300925	L	--	
B 2	8610486	860522	370225	L	--	
B 3	8612060	861206	330323	R	--	
B 4	8613452	860701	381119	L	--	
B 5	8610277	860520	380419	R	--	
B 6	8610030	860515	400529	L	--	
B 7	8615436	860729	570608	R	--	Fibroadenoma
B 8	8613135	860626	200618	L	--	

Table 11.1 (continuation)

A No	UB No	DOBx	DOB	S	Op	Other
B 9	8612556	860619	320603	L	--	
B 11	8611010	860529	110318	L	--	
B 12	8611538	860606	171231	R	--	
B 13	8610029	860515	390604	L	--	
B 14	8612107	860612	160320	R	--	
B 15	8518938	850919	420111	-	--	
B 16	8613132	860626	531018	L	--	Fibroadenoma
B 17	8611011	860529	291016	L	--	
B 18	8525261	860513	550920	L	--	Lactational
B 19	8605967	860318	470929	R	--	
B 20	8523790	851125	460824	R	--	
B 21	8524727	851206	520816	L	--	
B 22	8702210	860218	240525	R	--	Fibroadenoma
B 23	8603615	860218	500304	L	--	
B 24	8601644	000000	000000	L	--	
B 25	8612106	860612	480628	L	--	
B 26	8611537	850605	350315	R	--	
B 27	8716838	850813	530510	R	--	Papilloma
B 28	8605968	860318	380512	-	--	

Table 11.1. Patient data.

Table 11.2

	A	B	C	D	E	F	G	H	I	J	K	L	M	N	O	P	Q	R	S	T	U	V	W	X	Y
A001	3	4	3	3	2	3	4	4	-	-	-	-	-	-	-	-	-	-	-	-	-	-	-	-	-
A004	3	4	-	-	2	-	-	-	-	-	-	-	-	-	-	-	-	-	-	-	-	-	-	-	-
A005	2	4	3	3	2	3	3	2	-	-	-	-	-	3	-	-	-	-	-	-	-	-	-	-	-
A007	4	5	3	3	2	-	-	-	-	-	-	-	-	-	-	6	-	5	-	1	7	4	-	-	-
A012	5	4	3	3	2	-	-	-	-	-	-	6	-	5	5	-	-	-	-	4	3	-	-	-	-
A015	6	7	2	2	2	-	-	-	-	-	-	-	-	-	-	-	6	-	7	2	-	-	-	-	-
A016	3	5	3	3	2	4	5	4	-	-	-	-	0	3	-	-	-	-	-	-	-	-	-	-	-
A028	4	4	3	3	2	-	-	-	-	-	-	6	3	4	-	-	-	-	-	-	-	-	-	-	-
A031	3	4	3	3	2	-	-	-	-	-	-	-	3	-	-	-	-	-	-	-	-	-	-	-	-
A032	0	2	3	3	2	-	-	-	-	-	-	-	-	2	2	-	-	-	-	-	-	-	-	-	-
A033	2	2	3	3	2	-	-	-	-	-	-	-	-	3	-	6	-	6	-	1	6	3	-	-	7
A034	2	2	2	2	1	-	-	-	-	-	-	-	-	-	-	-	-	4	-	1	7	4	7	-	7
A035	2	4	-	-	-	-	-	-	-	-	-	-	0	-	-	-	-	-	5	2	3	-	-	-	-
A036	3	5	-	-	-	3	5	6	-	-	-	-	7	-	-	-	-	6	-	1	6	5	-	-	-
A037	1	2	2	2	1	-	-	-	-	-	-	-	-	-	-	-	-	-	-	-	-	-	-	-	-
A038	0	2	3	3	-	-	-	-	-	-	-	-	-	-	-	4	-	4	-	1	6	4	-	-	-
A039	1	2	-	-	0	-	-	-	-	-	-	-	-	-	-	-	-	3	-	1	3	2	-	-	-
A040	-	-	-	-	-	1	2	1	1	2	1	-	0	-	-	-	-	-	-	-	-	-	-	-	-
A041	3	3	-	-	-	-	-	-	-	-	-	-	-	-	-	-	-	3	2	3	2	-	-	-	-
A042	-	-	-	-	-	-	-	-	-	-	-	-	-	-	-	-	-	-	1	-	-	-	-	4	
A043	0	2	3	2	1	-	-	-	-	-	-	-	-	-	-	-	-	2	-	1	3	3	-	-	-
A044	2	2	-	-	-	-	-	-	-	-	-	-	-	-	-	-	-	-	1	6	4	-	-	-	
A072	-	-	-	-	1	-	-	-	-	-	-	-	-	-	-	-	7	-	1	7	7	-	-	-	
A073	4	6	5	5	1	-	-	-	-	-	-	-	-	-	-	-	-	3	6	6	-	-	-		
A074	3	4	-	-	-	-	-	-	-	-	-	-	-	-	-	-	-	1	6	5	2	-	-		
A076	1	2	-	-	-	-	-	-	-	-	-	0	3	-	-	6	-	1	6	5	5	-	-		
A077	2	6	0	0	1	-	-	-	-	-	7	-	6	2	-	-	-	-	-	-	-	-	-		
A078	2	6	0	0	1	-	-	-	-	-	6	0	5	-	-	2	-	-	-	-	-	-	-		
A079	0	2	3	3	2	-	-	-	-	-	-	-	3	-	-	-	-	-	-	-	-	-	-		
A080	-	-	-	-	-	-	-	-	-	-	-	-	-	-	-	-	-	-	-	-	-	-	-		
A081	5	6	6	5	1	-	-	-	-	-	-	-	6	-	-	-	-	-	-	-	-	-	-		
A082	0	0	-	-	-	-	-	-	-	-	-	-	1	-	-	6	-	1	6	5	-	-	-		

Table 11.2 (Continuation)

	A	B	C	D	E	F	G	H	I	J	K	L	M	N	O	P	Q	R	S	T	U	V	W	X	Y
A083	0	0	-	-	-	-	-	-	-	-	-	-	0	2	-	-	-	-	-	-	-	-	-	-	-
A085	-	-	-	-	2	-	-	-	-	-	-	-	-	-	-	-	-	-	1	6	6	-	-	-	
A086	1	2	-	-	-	-	-	-	-	-	-	-	-	-	-	-	-	7	-	1	7	6	-	-	-
A087	0	1	-	-	-	-	-	-	-	-	-	-	-	-	-	-	-	-	-	-	-	-	-	-	-
A088	2	4	2	2	2	-	-	-	-	-	-	6	0	3	-	3	-	6	-	1	6	3	-	-	-
A089	6	6	2	2	2	-	-	-	-	-	-	6	0	-	6	-	6	-	5	2	6	5	-	-	-
A090	3	3	1	1	2	-	-	-	-	-	-	-	-	-	-	-	-	4	-	1	6	7	-	-	-
A091	3	4	2	2	3	5	5	4	-	-	-	4	0	4	-	-	-	-	-	-	-	-	-	-	-
A092	5	5	4	4	2	5	5	4	-	-	-	5	0	-	5	-	-	-	-	-	-	-	-	-	-
A093	4	5	1	2	2	-	-	-	-	-	-	-	-	-	-	-	-	-	-	-	-	-	-	-	-
A094	4	6	2	2	2	4	5	4	4	4	5	5	0	4	4	-	-	-	-	3	6	6	4	-	-
A095	-	-	-	-	-	-	-	-	-	-	-	-	-	-	-	-	-	-	-	-	-	-	-	-	-
A096	4	6	4	3	2	-	-	-	-	-	-	-	0	5	5	-	-	6	-	1	6	7	-	-	-
A098	4	5	2	3	2	5	7	7	-	-	-	-	2	-	-	-	-	-	-	-	-	-	-	-	-
A099	4	2	2	2	2	-	-	-	-	-	-	4	0	3	4	-	-	-	-	-	-	-	-	-	-
A100	2	6	3	4	2	2	6	6	-	-	-	6	6	-	-	-	-	-	-	-	-	-	-	-	-
A102	2	3	-	-	-	4	6	6	-	-	-	-	0	2	0	3	-	7	-	1	7	7	4	-	-
A103	4	6	2	2	1	-	-	-	-	-	-	6	0	2	2	-	-	6	-	1	5	4	4	-	-
A104	-	-	-	-	2	-	-	-	-	-	-	-	-	2	-	4	-	5	-	-	-	-	-	-	-
A106	1	2	-	-	-	-	-	-	-	-	-	-	-	3	-	3	-	5	-	5	6	5	-	-	6
A112	2	6	2	2	2	-	-	-	-	-	-	-	-	-	-	-	-	-	-	9	6	5	-	-	-
A114	4	6	2	5	2	-	-	-	-	-	-	-	0	-	-	-	-	-	-	-	-	-	-	-	-
A116	5	6	3	4	2	-	-	-	-	-	-	-	-	5	-	6	-	7	-	-	-	-	-	-	-
A117	0	2	0	0	-	-	-	-	-	-	-	-	-	-	-	-	-	-	-	-	-	-	-	-	2
A118	3	4	3	3	2	-	-	-	-	-	-	-	-	-	-	-	-	6	-	1	6	6	-	-	-
A119	0	2	0	0	-	-	-	-	-	-	-	-	-	-	-	6	-	-	-	7	5	4	4	-	-
A120	0	0	-	-	-	-	-	-	-	-	-	-	-	-	-	-	-	6	-	1	6	5	4	-	6
A121	-	-	-	-	2	-	-	-	-	-	-	-	-	-	-	-	-	-	-	1	6	6	-	-	-
A122	3	4	2	2	2	-	-	-	-	-	-	-	0	-	-	-	-	-	-	2	7	6	-	-	6
A123	4	4	-	-	2	-	-	-	-	-	-	-	-	-	-	7	-	7	-	1	7	3	-	-	-
A124	2	5	0	2	2	5	6	6	-	-	-	-	0	-	7	-	-	-	-	-	-	-	-	-	-
A125	4	4	0	0	2	3	7	4	-	-	-	-	2	-	3	-	-	6	-	-	-	-	-	-	-

Table 11.2 (Continuation)

	A	B	C	D	E	F	G	H	I	J	K	L	M	N	O	P	Q	R	S	T	U	V	W	X	Y
A126	2	4	3	3	2	-	-	-	-	-	-	-	-	0	4	3	-	-	-	-	-	-	-	-	-
A127	4	4	2	2	2	4	5	-	-	-	-	-	-	0	-	-	-	3	-	4	-	-	-	-	-
A129	2	4	0	0	2	-	-	-	-	-	-	-	-	0	-	-	-	-	5	-	5	6	5	-	-
A130	4	5	3	3	2	-	-	-	-	-	-	-	-	2	5	4	-	-	-	-	-	-	-	-	-
A131	4	5	3	4	1	-	-	-	-	-	-	-	-	0	5	4	-	-	-	-	-	-	-	-	-
A132	3	5	3	3	1	3	5	-	4	-	-	-	0	5	-	6	-	7	-	1	6	4	-	-	-
A133	0	0	0	2	1	-	-	-	-	-	-	-	-	-	-	-	-	-	-	2	5	4	-	-	-
A134	0	2	0	0	2	-	-	-	-	-	-	2	0	2	-	-	-	-	-	-	-	-	-	-	-
A135	2	2	2	2	2	-	-	-	-	-	-	-	-	-	-	3	-	7	-	1	7	6	-	-	-
A136	2	2	2	2	1	-	-	-	-	-	-	-	0	3	2	-	3	-	-	2	7	5	-	-	-
A137	1	2	-	-	-	-	-	-	-	-	-	-	0	-	-	5	5	-	-	1	6	4	-	-	-
A138	4	5	-	-	-	-	-	-	-	-	-	-	0	5	4	5	5	-	-	-	-	-	-	-	-
A139	3	5	-	-	-	-	-	-	-	-	-	-	3	-	-	-	-	-	-	-	-	-	-	-	-
A140	3	2	2	2	-	-	-	-	-	-	-	-	-	-	4	-	-	-	-	-	-	-	-	-	-
A141	3	4	3	3	2	3	3	4	-	-	-	-	0	4	4	6	-	6	-	1	6	4	-	-	-
A142	4	5	3	3	2	-	-	-	-	-	-	5	0	4	-	4	-	5	-	5	5	4	-	-	-
A143	0	2	0	0	2	-	-	-	-	-	-	-	4	2	-	-	-	6	-	1	6	4	6	-	-
A144	3	5	2	2	-	-	-	-	-	-	-	-	0	-	2	2	-	5	-	1	5	4	-	-	-
A147	3	4	1	1	2	-	-	-	-	-	-	-	0	-	-	-	-	5	6	2	6	5	-	-	-
A148	5	5	4	3	1	-	-	-	-	-	-	-	6	-	-	-	-	-	-	-	-	-	-	-	-
A149	5	6	3	3	2	-	-	-	-	-	-	4	0	6	-	-	-	-	-	-	-	-	-	-	-
A150	3	2	2	2	2	-	-	-	-	-	-	-	1	2	-	-	4	-	-	-	-	-	-	-	-
A151	-	-	-	-	-	-	-	-	-	-	-	-	-	-	-	-	-	-	-	-	-	-	-	-	-
A152	3	3	2	2	2	-	-	-	-	-	-	5	0	2	2	-	3	-	6	2	6	4	-	-	-
A153	2	4	2	2	2	3	3	3	-	-	-	-	0	3	-	-	-	-	-	-	-	-	-	-	-
A154	3	6	3	3	2	-	-	-	5	6	6	7	0	4	3	4	-	4	-	-	-	-	-	-	-
A155	3	4	-	-	2	-	-	-	-	-	-	-	-	-	-	-	-	5	-	1	5	4	-	-	-
A156	4	4	3	6	-	-	-	-	-	-	-	-	2	-	2	-	-	-	-	-	-	-	-	-	-
A157	2	3	1	1	2	-	-	-	-	-	-	-	0	0	4	-	4	3	-	5	2	5	4	4	-
A158	4	6	3	3	2	-	-	-	-	-	-	-	-	5	-	-	-	-	-	-	-	-	-	-	-
A159	3	5	-	-	-	3	5	-	-	-	-	2	0	4	3	-	-	-	-	-	-	-	-	-	-
A160	4	6	2	2	2	-	-	-	-	-	-	-	0	5	-	-	-	-	-	-	-	-	-	-	-

Table 11.2 (Continuation)

	A	B	C	D	E	F	G	H	I	J	K	L	M	N	O	P	Q	R	S	T	U	V	W	X	Y
A161	3	5	2	2	2	7	7	-	-	-	-	-	2	3	5	5	-	7	-	1	7	7	5	-	-
A162	3	4	-	-	-	5	5	5	-	-	-	6	3	4	6	-	-	-	-	-	-	-	-	-	-
A163	3	6	2	2	2	-	-	-	-	-	-	-	-	-	-	-	-	-	-	-	-	-	-	-	-
A164	3	5	3	3	2	-	-	-	-	-	-	-	-	-	-	-	-	-	-	-	-	-	-	-	-
A165	0	0	-	-	-	-	-	-	-	-	-	-	-	-	-	-	-	-	-	-	-	-	-	-	-
A166	6	7	3	3	1	-	-	-	-	-	-	5	3	5	7	-	-	-	-	-	-	-	-	-	-
A167	3	4	3	3	1	-	-	-	7	5	-	4	0	2	4	-	-	-	-	-	-	-	-	-	-
A168	5	6	2	2	2	-	-	-	-	-	-	-	-	5	-	-	-	-	-	-	-	-	-	-	-
A169	3	4	2	2	1	4	5	-	-	-	-	-	-	5	-	-	-	-	-	1	6	7	-	-	-
A170	4	5	-	-	-	-	-	-	-	-	-	-	-	-	-	-	-	5	-	1	7	7	-	-	-
A172	3	4	-	-	-	-	-	-	-	-	-	-	-	-	-	-	-	7	-	1	6	4	-	-	-
A173	3	5	3	2	2	-	-	-	-	-	-	-	-	-	-	-	-	-	-	1	4	3	3	-	-
A174	2	3	0	0	2	-	-	-	-	-	-	-	0	-	2	4	-	5	-	1	6	6	3	-	-
A176	2	5	2	2	1	-	-	-	-	-	-	-	-	-	-	-	-	7	-	1	6	7	5	-	7
A177	4	6	2	2	1	2	5	-	-	-	-	-	4	4	-	-	-	-	-	-	-	-	-	-	-
A178	5	5	1	1	2	-	-	-	-	-	-	-	-	-	-	-	-	-	-	1	4	4	4	-	-
A179	2	6	2	4	1	-	-	-	-	-	-	2	0	3	4	7	-	7	-	1	5	7	5	-	5
A180	4	4	4	5	1	-	-	-	-	-	-	-	0	-	-	-	-	6	-	1	7	6	7	-	-
A181	4	4	3	3	-	-	-	-	-	-	-	-	-	-	-	-	-	-	-	1	6	6	-	-	-
A182	4	5	3	4	2	-	-	-	-	-	-	-	0	4	-	-	-	-	-	-	-	-	-	-	-
A183	4	5	0	0	1	-	-	-	-	-	-	-	-	4	4	-	-	-	-	-	-	-	-	-	-
A184	4	4	-	-	1	-	-	-	-	-	-	-	-	-	-	-	-	-	-	-	-	-	-	-	-
A186	3	5	4	4	2	-	-	-	-	-	-	-	-	-	-	-	-	-	6	2	4	4	-	-	-
A187	3	6	3	3	2	-	-	-	-	-	-	-	0	-	3	-	5	-	-	-	-	-	-	-	-
A188	4	5	2	2	2	-	-	-	-	-	-	5	2	6	-	-	-	-	-	-	-	-	-	-	-
A189	2	6	3	3	2	4	4	-	-	-	-	-	0	4	-	-	-	6	-	-	-	-	-	-	-
A192	5	5	2	2	2	-	-	-	-	-	-	-	-	-	-	-	-	7	-	1	7	7	-	-	-
A193	5	5	4	4	2	-	-	-	5	5	-	-	0	4	-	6	-	7	-	-	-	-	-	-	-
A194	2	4	1	2	1	-	-	-	-	-	-	-	-	4	-	5	-	-	-	1	5	6	-	-	-
A195	4	4	0	2	1	-	-	-	-	-	-	-	-	-	5	-	5	-	1	5	5	-	-	-	
A196	4	5	4	3	1	-	-	-	-	-	-	-	0	5	5	-	-	-	-	-	-	-	-	-	-
A197	5	6	4	4	1	-	-	-	-	-	-	0	0	-	4	5	-	6	-	-	-	-	-	-	-

Table 11.2 (Continuation)

	A	B	C	D	E	F	G	H	I	J	K	L	M	N	O	P	Q	R	S	T	U	V	W	X	Y
A198	4	5	4	4	1	-	-	-	-	-	-	-	4	0	4	-	5	-	7	-	1	7	7	-	-
A199	4	2	-	-	-	-	-	-	-	-	-	-	-	-	-	-	-	-	-	-	-	-	-	-	-
A200	4	7	3	3	1	-	-	-	-	-	-	-	-	-	-	-	-	-	-	-	-	-	-	-	-
A202	-	-	-	-	2	-	-	-	-	-	-	-	-	-	-	5	-	5	-	-	-	-	-	-	-
A203	4	4	2	2	-	-	-	-	-	-	-	-	0	-	-	-	-	-	-	1	6	5	6	-	-
A204	5	6	2	1	2	-	-	-	-	-	-	-	-	-	-	-	-	2	-	9	4	5	-	-	-
A205	4	5	1	1	2	-	-	-	-	-	-	-	0	5	5	-	-	-	-	-	-	-	-	-	-
A206	5	6	-	-	-	-	-	-	-	-	-	-	-	-	-	-	-	-	-	-	-	-	-	-	-
A207	-	-	-	-	-	-	-	-	-	-	-	-	-	-	-	-	-	4	-	1	4	4	-	-	-
A208	1	2	1	1	2	-	-	-	-	-	-	-	-	-	-	-	-	-	-	-	-	-	-	-	-
A209	0	0	0	0	-	-	-	-	-	-	-	-	-	-	-	-	-	-	-	-	-	-	-	-	-
A210	3	3	-	-	1	-	-	-	-	-	-	-	-	-	-	-	-	6	-	1	6	4	5	-	-
A211	4	5	4	4	1	-	-	-	-	-	-	-	-	-	-	-	-	-	-	-	-	-	-	-	-
A212	4	4	0	2	2	-	-	-	-	-	-	-	-	2	-	-	-	4	-	1	5	5	-	-	-
A213	2	2	2	2	2	-	-	-	-	-	-	-	0	4	-	-	-	-	-	1	6	4	6	-	-
A214	0	2	-	-	2	-	-	-	-	-	-	-	0	-	-	-	-	-	-	-	-	-	-	-	-
A215	-	-	-	-	-	-	-	-	-	-	-	-	-	-	-	-	-	-	-	-	-	-	-	-	-
A216	3	5	1	3	2	-	-	-	-	-	-	5	0	-	-	3	-	5	-	1	5	5	-	-	-
A217	5	5	-	-	-	-	-	-	-	-	-	-	4	-	-	-	-	-	-	-	-	-	-	-	-
A218	-	-	-	-	2	-	-	-	-	-	-	-	-	-	-	-	-	7	-	1	6	6	-	-	-
A219	-	-	-	-	-	-	-	-	-	-	-	-	-	-	-	-	-	6	-	1	5	5	-	-	-
A220	0	2	0	0	-	-	-	-	-	-	-	-	-	-	-	-	-	-	-	-	-	-	-	-	-
A221	5	6	3	7	2	4	6	6	-	-	-	-	-	5	0	6	-	7	5	-	-	-	-	-	-
B001	-	-	-	-	-	-	-	-	-	-	-	-	-	-	-	-	-	4	-	1	3	3	-	-	-
B002	0	0	0	0	1	-	-	-	-	-	-	-	-	4	-	-	-	6	-	1	5	4	-	-	-
B003	0	1	-	-	-	-	-	-	-	-	-	-	0	-	-	-	-	-	-	1	6	5	-	-	-
B004	2	2	-	-	2	2	2	2	-	-	-	-	2	-	2	-	-	-	-	-	-	-	-	-	-
B005	-	-	-	-	-	-	-	-	-	-	-	-	-	-	-	-	-	-	-	-	-	-	-	-	6
B006	0	2	3	3	-	-	-	-	-	-	-	-	-	-	-	-	-	4	-	4	5	-	-	-	-
B007	3	4	3	3	2	-	-	-	-	-	-	6	2	4	-	-	-	-	-	-	-	-	-	-	-
B008	-	-	-	-	-	-	-	-	-	-	-	-	-	-	-	-	-	-	-	1	3	2	-	-	-
B009	2	3	-	-	-	-	-	-	-	-	-	-	5	-	-	-	-	-	-	1	5	3	-	-	-

Table 11.2 (Continuation)

	A	B	C	D	E	F	G	H	I	J	K	L	M	N	O	P	Q	R	S	T	U	V	W	X	Y
B011	-	-	-	-	-	-	-	-	-	-	-	-	-	-	-	-	-	-	-	1	4	3	-	-	-
B012	-	-	-	-	-	-	-	-	-	-	-	-	-	-	-	-	-	-	-	1	6	5	-	-	-
B013	0	2	3	3	2	-	-	-	-	-	-	-	-	3	-	3	-	6	-	1	5	4	-	-	-
B014	-	-	-	-	2	-	-	-	-	-	-	0	-	-	-	-	-	7	-	1	7	5	-	-	-
B015	0	2	-	-	-	-	-	-	-	-	-	-	-	-	-	-	-	-	-	-	-	-	-	-	-
B016	3	5	2	2	2	-	-	-	-	-	-	-	-	-	-	-	-	-	-	-	-	-	-	-	-
B017	-	-	-	-	-	-	-	-	-	-	-	-	-	-	-	-	-	-	-	1	4	2	-	-	-
B018	4	5	2	3	2	-	-	-	-	-	-	-	-	-	-	-	-	-	-	-	-	-	-	-	-
B019	6	7	3	3	2	-	-	-	-	-	-	-	-	-	-	-	-	-	-	-	-	-	-	-	-
B020	4	4	3	3	2	-	-	-	-	-	-	-	-	4	3	-	-	-	-	-	-	-	-	-	-
B021	0	2	0	0	-	6	6	6	-	-	-	-	-	6	-	-	-	-	-	-	-	-	-	-	-
B023	0	2	-	-	-	-	-	-	-	-	-	-	0	3	3	-	-	-	-	-	-	-	-	-	-
B023	0	2	-	-	-	-	-	-	-	-	-	-	0	0	-	-	-	-	-	-	-	-	-	-	-
B024	0	0	0	0	1	-	-	-	-	-	-	-	0	-	-	-	-	-	-	1	4	2	-	-	-
B025	4	5	3	3	2	-	-	-	-	-	-	-	-	-	4	-	6	-	-	-	-	-	-	-	-
B026	-	-	-	-	-	-	-	-	-	-	-	-	-	-	-	-	-	6	-	1	6	4	-	-	-
B027	6	6	3	3	2	-	-	-	-	-	-	-	-	6	-	-	-	-	-	-	-	-	-	-	-
B028	3	2	0	0	-	-	-	-	-	-	-	-	0	-	-	-	-	-	-	-	-	-	-	-	-

Table 11.2. Immunostaining scores for p21 ras expression by case.

Table 11.3

A Normal epithelium
B Normal myoepithelium
C Lobular stromal cells
D Extralobular stromal cells
E Vascular smooth muscle
F Sclerosing adenosis: Epithelium
G Sclerosing adenosis: Myoepithelium
H Sclerosing adenosis: Stroma
I Radial scars: Epithelium
J Radial scars: Myoepithelium
K Radial scars: Stroma
L Cyst epithelium: Apocrine
M Cyst epithelium: Flattened
N Hyperplastic epithelium: Ductal without atypia
O Hyperplastic epithelium: Altered lobules
P Hyperplastic epithelium: Atypical ductal
Q Hyperplastic epithelium: Atypical lobular
R Ductal carcinoma in situ
S Lobular carcinoma in situ
T Invasive carcinoma: Type
U Invasive carcinoma cells
V Stromal cells of carcinoma
W Carcinoma cells within lymphatics
X Carcinome cells in venules
Y Carcinoma cells in lymph nodes

Table 11.3. Column headings for table 11.2.

JOURNAL OF PATHOLOGY, VOL. **155:** 185–190 (1988)

OPTIMAL PRESERVATION OF p21 *RAS* IMMUNOREACTIVITY AND MORPHOLOGY IN PARAFFIN-EMBEDDED TISSUE

J. J. GOING, A. R. W. WILLIAMS, A. H. WYLLIE, T. J. ANDERSON AND J. PIRIS

Department of Pathology, University of Edinburgh, Edinburgh, Scotland, U.K.

Received 12 February 1988
Accepted 26 February 1988

SUMMARY

Specific immunostaining of p21 *ras* protein by the well-characterized pan-*ras* antibody Y13-259 is achieved in paraffin sections of human and animal tissues fixed in periodate–lysine–paraformaldehyde–dichromate (PLPD). Intensity of staining is as good as in cryostat sections, with superior histological detail. Localization to plasma membrane is demonstrated in rodent cells genetically manipulated to express abundant p21 *ras* (the FHO5T1 cell line), both in preparations suspended in agar after culture *in vitro* and in those growing as tumour *in vivo*. Strong positive staining is observed in neoplasms of human breast and colon, tissues in which there is independent evidence of elevated *ras* gene expression. The superior morphology afforded by this technique allows clear characterization of p21 *ras* expression in small premalignant lesions for which other methods of detection of oncogene expression are not appropriate.

KEY WORDS—p21 *ras*, immunochemistry, fixation, monoclonal antibody Y13-259.

INTRODUCTION

The well-characterized monoclonal antibody Y13-259[1,2] reacts with an epitope, probably amino acids 70–81,[2] shared by the 21 kDa protein products of mutationally activated and non-mutated Harvey (Ha), Kirsten (Ki), and N-*ras* oncogenes. These proteins, collectively known as p21 *ras*, are GTP binding proteins located on the inner face of the plasma membrane[3,4] and are believed to be involved in transduction of extracellular signals.[5] Y13-259 has been used in several studies of *ras* oncogene expression, but in our experience and that of others[6,7] the epitope detected survives formaldehyde fixation poorly. Most but not all immunocytochemical studies with Y13-259 have used cryostat sections fixed in acetone.[6,8,9] Attempts to raise other monoclonal antibodies to *ras* peptides suitable for use in conventionally fixed, paraffin-processed tissues have not proved successful so far,[10] although polyclonal antisera with suitable immunoreactivity exist.[7]

In view of reports of *ras* mutation and hyperexpression in neoplasms of the human colon and breast, it is particularly important that immunocytochemical methods should exist for detection of p21 *ras* products with high specificity and good tissue localization. To be useful in the study of oncogene expression in premalignant lesions, such methods should be applicable to small tissue samples. Such samples are usually unsuited to biochemical analysis. In this paper, we report immunocytochemical demonstration of p21 *ras* using Y13-259 in paraffin sections of tissue fixed with periodate–lysine–paraformaldehyde (PLP) and its dichromate derivate (PLPD). These fixatives are known to allow demonstration of lymphocyte antigens in paraffin-embedded tissues, using antibodies hitherto reactive only in cryostat sections.[11] They appear to be particularly suited to demonstration of membrane-associated antigens. The validity and potential usefulness of these fixatives are demonstrated in animal cells known to express p21 *ras* at high levels, and in human colon and breast tissue.

Addressee for correspondence: Dr J. J. Going, Department of Pathology, University Medical School, Teviot Place, Edinburgh EH8 9AG, U.K.

0022–3417/88/070185–06 $05.00

MATERIALS AND METHODS

Fixatives

Stock 8 per cent paraformaldehyde was prepared by stirring 8 g/100 ml into deionized distilled water (DDW) at 70°C, adding 100 mg of sodium hydroxide for each 100 ml of solution, stirring until the solution cleared, and filtering. This solution is stable at room temperature. Stock 0·05 M phosphate buffer, pH 7·7, contains 0·0367 M dibasic sodium phosphate ($Na_2H\ PO_4$) and 0·0133 M monobasic sodium phosphate (NaH_2PO_4 in DDW. On the day of use, 200 ml batches of PLP were prepared by dissolving 2·74 g of anhydrous L-lysine monohydrochloride and 0·43 g of anhydrous sodium metaperiodate in a mixture of 50 ml of 8 per cent paraformaldehyde and 150 ml of phosphate buffer. This gives a solution with the composition described by McLean and Nakane[12] and a pH of 6·2, although their preparative method differed in detail. PLPD was prepared by dissolving 2·5 per cent w/v of potassium dichromate in PLP diluted with an equal volume of DDW. Other fixatives have included 2 per cent glutaraldehyde, 4 per cent neutral buffered formaldehyde, and Carson's fixative.[13]

Cell lines and experimental tumours

The CHL and FHO5T1 cell lines have been described previously.[14] Briefly, the FHO5T1 cell line was derived by transfection of an early passage embryonic Chinese hamster lung fibroblast strain (designated CHL) with the plasmid pHO5T1, which contains the mutationally activated human T24 Harvey-*ras* oncogene ligated to viral enhancing sequences. The resulting fully transformed FHO5T1 cell line is tumorigenic in immune-deprived mice. Quantitation of Ha-*ras* mRNA by dot-blot hybridization has shown 20–60 fold increased *ras* transcript in FHO5T1 cells and derived tumours, compared with parental untransformed CHL cells, and high levels of the p21 *ras* protein product have been confirmed by immunoblotting of FHO5T1 cell extracts.[15]

FHO5T1 and CHL cells were maintained in Dulbecco's modification of minimum Eagle's medium, containing 10 per cent newborn calf serum, penicillin, and streptomycin. Cell suspensions were prepared from monolayers by treatment with 0·02 per cent EDTA and 0·1 per cent trypsin Dulbecco's phosphate-buffered saline (PBS) and washing in PBS. Approximately 5×10^6 cells were fixed in PLPD for 15 min at 4°C, washed in PBS, and resuspended in 0·5 ml of 2 per cent low-melting-temperature agarose (FML Bioproducts) in PBS at 40°C. After setting, this pellet was post-fixed for up to 24 h in PLPD, washed in PBS, and processed to paraffin without raising the temperature higher than 56°C.

Subcutaneous tumours were engendered in immune-deprived mice by inoculation of FHO5T1 cells as described.[15] Samples of tumour tissue were sliced to 5 mm and placed immediately in PLPD. Fixation and subsequent processing were as for human tissues.

Human tissues

Colorectal and breast tissue were collected on ice from the operating room and taken directly to the laboratory, where 3–5 mm tissue blocks were placed in PLP and PLPD and allowed to fix at 4°C overnight. After fixation for 24–36 h, tissues were washed overnight in running tap water. Dehydration through graded alcohols, clearing in chloroform, and paraffin wax impregnation at 56°C were performed over 20 h. Three μm sections were dried at 56°C.

Immunocytochemistry

Rat monoclonal antibody Y13-259 was purified by ammonium sulphate precipitation from serum-free culture supernatant and dialysed enhaustively against PBS. Immunoglobulin concentration in this material was measured by radial immunodiffusion[16] using purified rat immunoglobulin (Sigma) as standard.

Dewaxed sections were rehydrated through graded alcohols to water and then rinsed in 10 mM Tris-buffered isotonic saline (TBS) at pH 7·6. A three-stage streptavidin–biotin–peroxidase complex (ABC)[17] immunostaining method was used. Y13-259 was applied to sections for 1 h in concentrations of 5, 25, 50, 100, and 200 μg/ml in TBS containing 10 per cent normal goat serum (TBS/NGS). Biotinylated goat anti-rat antibody (Sigma) 1/50 in TBS/NGS was applied for 30 min. These stages were each followed by two 5-min washes in TBS. Streptavidin–biotin–peroxidase (ABC) complex (Amersham International) 1/200 in TBS was applied for 15 min. After three 5-min TBS washes, sections were developed with diaminobenzidine–H_2O_2 in Tris-buffered 0·01 M imidazole (pH 7·6).

Negative controls included omission of Y13-259 from the first stage and its replacement with the

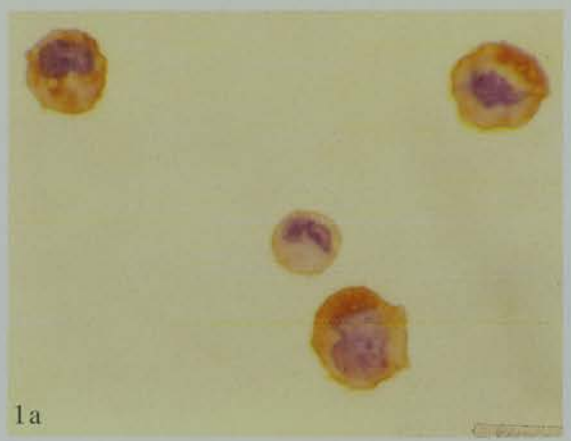

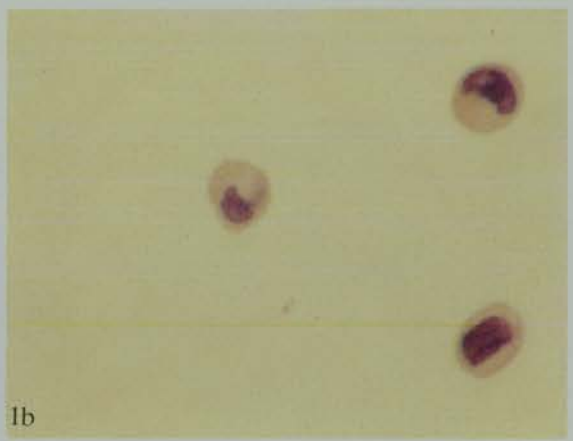

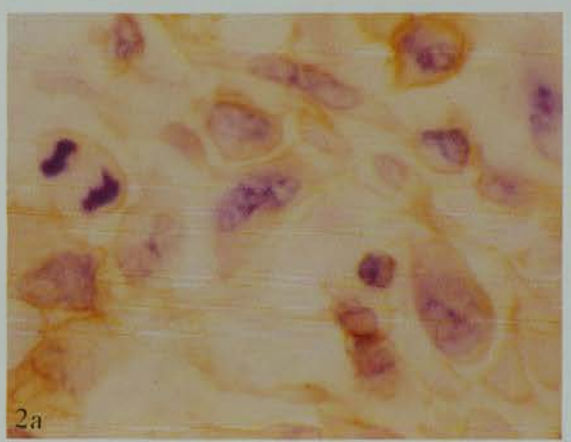

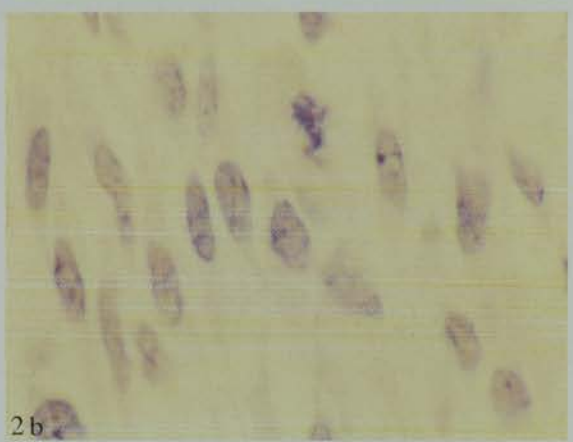

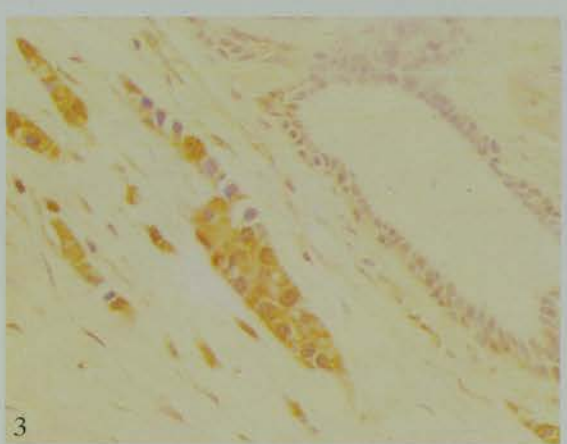

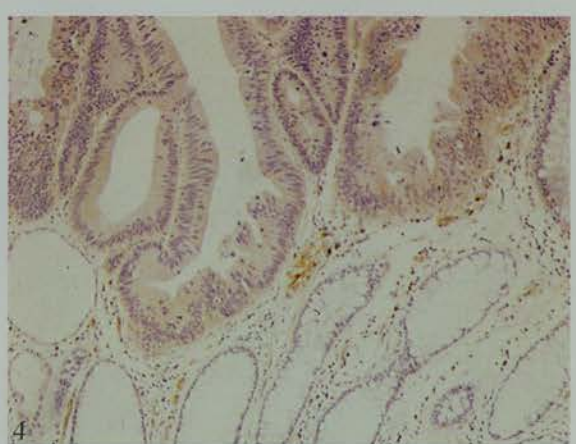

Fig. 1—(a) FHO 5T1 cells.(b) CHL cells. Both fixed in PLPD, embedded in agar and paraffin. Immunostaining with Y13-259, 50 μg/ml, ABC detection

Fig. 2—FHO 5T1 cells growing as a tumour in an immunosuppressed mouse. (a) Immunostaining with Y13-259, 50 μg/ml. (b) Y13-259 replaced by non-immune rat IgG, 50 μg/ml as primary antibody. Both ABC detection

Fig. 3—Human breast tissue fixed in PLPD, paraffin embedded. Invasive carcinoma cells adjacent to benign parenchyma show strong positive staining while benign epithelial elements do not. Immunostaining with Y13-259, 50 μg/ml, ABC detection

Fig. 4—Human colonic adenoma and adjacent normal mucosa fixed in PLPD, paraffin embedded. The adenoma shows staining while adjacent mucosa does not. Immunostaining with Y13-259, 100 μg/ml, ABC detection

same concentration of polyclonal rat immunoglobulins (Sigma) previously absorbed with acetone-extracted human liver powder.[18] A negative control of a different type was provided by the CHL cell line, which expresses p21 *ras* at barely detectable levels.

In some instances, ABC complex was replaced by light-microscopy grade streptavidin–colloidal gold complex (Janssens) diluted 1/50 in TBS. After three 5-min TBS washes, fixation for 15 min in 2 per cent glutaraldehyde in PBS, pH 7·6, 10 min in running tap water, and six 3-min washes in DDW, sections were exposed to 1–3 cycles of silver enhancement with Janssens' 'IntensE' kit according to the manufacturer's instructions. In an attempt to optimize sensitivity of this immunogold–silver staining (IGSS) protocol, some sections were immersed in Lugol's iodine and sodium thiosulphate before the first-layer antibody was applied, following described empirical procedures.[19,20]

RESULTS

Cell lines and experimental tumours

Immunostaining of PLPD-fixed agar and paraffin-embedded FHO5T1 cells with Y13-259 produced clear linear cell-membrane-associated immunostaining (Fig. 1a) which was absent from the parental CHL cells (Fig. 1b). Similar membrane staining was obtained in paraffin sections of PLPD-fixed FHO5T1 tumours growing in immune deficient mice (Fig. 2a). Replacement of Y13-259 with non-immune rat immunoglobulin at the same concentration abolished immunostaining (Fig. 2b). Faint cytoplasmic staining was also usually present, and it was our impression that this was accentuated and membrane localization diminished in tissues held at room temperature for 10 min prior to fixation in an attempt to reconstruct fixation conditions more likely to pertain for human operative specimens. Adjacent subcutaneous tissues of the host mice did not show staining. Similar results were obtained with ABC and IGSS detection systems. Although claimed to increase IGSS sensitivity, even brief pretreatment (5 s) with Lugol's iodine solution abolished all Y13-259 immunoreactivity, whatever detection system was used. Using the IntensE kit, it was possible by repeated application of freshly-mixed intensifying solution (up to three times) to develop stronger staining but only at the cost of increased background. No staining occurred when Y13-259 was omitted or replaced by non-immune rat immunoglobulin at the same concentration.

Human breast tissues

Tissues studied included normal parenchyma, benign but pathological tissue, and carcinomas. In general, after PLPD fixation, *in situ* and invasive carcinomas showed strong positive staining with Y13-259. Such staining was absent in negative controls. Frequently, staining of benign parenchymal elements in the same cases was either faint or absent. An example of this pattern is shown in Fig. 3. Unlike FHO5T1 cells and derived experimental tumours, staining seen in human material was usually cytoplasmic, with membrane accentuation in some instances. A proportion of nuclei showed immunostaining. This feature was not seen in FHO5T1 cells whether growing *in vivo* or *in vitro*. In normal breast parenchyma, more intense Y13-259 staining was associated with myoepithelial than with epithelial cells.

PLPD gave better preservation of morphology and immunoreactivity than PLP. In part, the better preservation of antigenicity probably reflects the lower concentration of paraformaldehyde in PLPD. Reducing the concentration of paraformaldehyde in PLP from 2 to 1 per cent gives stronger Y13-259 immunoreactivity in FHO5T1 cells but worse morphology. Carcinoma tissues fixed in Carson's fluid seldom showed staining with Y13-259 and never to the same extent shown by the same tissues fixed in PLPD.

Human colorectal tissues

Immunostaining with Y13-259 in colon was analogous to that observed in breast tissue. Normal colorectal mucosa showed very faint or absent staining, as did muscularis and connective tissue. In contrast, adenomas showed specific staining of tumour cells, a sharp transition occurring between negative normal mucosa and the strongly staining cells of the adenoma (Fig. 4). Staining was diffusely cytoplasmic in most cases, but as in the breast nuclear staining was occasionally observed. Specific membrane staining did not occur. Adenocarcinomas also showed specific staining of similar character, most frequently all cells showing diffuse cytoplasmic stain. In a few cases, heterogeneity of tumour cells was obvious, some cells being strongly stained whilst others were negative. Tumour stroma and muscle were negative or very faintly stained;

Campaign. J. J. G. is a Medical Research Council Training Fellow.

REFERENCES

1. Furth ME, Davis LJ, Fleurdelys B, Scolnick EM. Monoclonal antibodies to the p21 products of the transforming gene of Harvey murine sarcoma virus and of the cellular *ras* gene family. *J Virol* 1982; **43:** 294–304.
2. Lacal JC, Aaronson SA. Monoclonal antibody Y13-259 recognises an epitope of the p21-*ras* molecule not directly involved in the GTP-binding activity of the protein. *Mol Cell Biol* 1986; **6:** 1002–1009.
3. Willingham MC, Pastan I, Shih TY, Scolnick EM. Localisation of the *src* gene product of the Harvey strain of MSV to plasma membrane of transformed cells by electron microscopic immunocytochemistry. *Cell* 1980; **19:** 1005–1014.
4. Willumsen BM, Christensen A, Hubbert NL, Papageorge AG, Lowy DR. The p21-*ras* C-terminus is required for transformation and membrane association. *Nature* 1984; **310:** 583–586.
5. Mulcahy LS, Smith MR, Stacey DW. Requirement for *ras* proto-oncogene function during serum-stimulated growth of NIH 3T3 cells. *Nature* 1985; **313:** 241–243.
6. Williams ARW, Piris J, Spandidos DA, Wyllie AH. Immunohistochemical detection of the *ras* oncogene p21 product in an experimental tumour and in human colorectal neoplasms. *Br J Cancer* 1985; **52:** 687–693.
7. Ward JM, Pardue RL, Junker JL, Takahashi K, Shih TY, Weislow OS. Immunocytochemical localization of *ras* Ha p21 in normal and neoplastic cells in fixed tissue sections from Harvey sarcoma virus-infected mice. *Carcinogenesis* 1986; **7:** 645–651.
8. Candlish W, Kerr IB, Simpson HW. Immunocytochemical demonstration and significance of p21 *ras* family oncogene product in benign and malignant breast disease. *J Pathol* 1986; **150:** 163–167.
9. Kerr IB, Lee FD, Quintanilla M, Balmain A. Immunocytochemical demonstration of p21 *ras* family oncogene product in normal mucosa and in premalignant and malignant tumours of the colorectum. *Br J Cancer* 1985; **52:** 695–700.
10. Robinson A, Williams ARW, Piris J, Spandidos DA, Wyllie AH. Evaluation of a monoclonal antibody to *ras* peptide, RAP-5, claimed to bind preferentially to cells of infiltrating carcinomas. *Br J Cancer* 1986; **54:** 877–883.
11. Holgate CS, Jackson P, Pollard K, Lunny D, Bird CC. Effect of fixation on T and B lymphocyte surface membrane antigen demonstration in paraffin processed tissue. *J Pathol* 1986; **149:** 293–300.
12. McLean IW, Nakane PK. Periodate–lysine–paraformaldehyde fixative: a new fixative for immunoelectron microscopy. *J Histochem Cytochem* 1974; **22:** 1077–1083.
13. Carson FL, Martin JH, Lynn JA. Formalin fixation for electron microscopy: a reevaluation. *Am J Clin Pathol* 1973; **59:** 365–373.
14. Spandidos DA, Wilkie NM. Malignant transformation of early passage rodent cells by a single mutated human oncogene. *Nature* 1984; **310:** 469–475.
15. Wyllie AH, Rose KA, Morris RG, Steel CM, Foster E, Spandidos DA. Rodent fibroblast tumours expressing human *myc* and *ras* genes: growth, metastasis and endogenous oncogene expression. *Br J Cancer* 1987; **56:** 251–259.
16. Johnstone A, Thorpe R. Immunochemistry in Practice. Oxford: Blackwell, 1986: 125–127.
17. Hsu SM, Raine L. Protein A, avidin and biotin in immunohistochemistry. *J Histochem Cytochem* 1981; **29:** 1349–1353.
18. Nairn RC (ed.). Fluorescent Protein Tracing. Edinburgh: Churchill Livingstone, 1976; 371–372.
19. Holgate CS, Jackson P, Cowen PN, Bird CC. Immunogold–silver staining: New method of immunostaining with enhanced sensitivity. *J Histochem Cytochem* 1983; **31:** 938–944.
20. Springall DR, Hacker GW, Grimelius L, Polak JM. The potential of the immunogold–silver staining method for paraffin sections. *Histochemistry* 1984; **81:** 603–608.
21. Horan Hand P, Thor A, Wunderlich D, Muraro R, Caruso A, Schlom J. Monoclonal antibodies of predefined specificity detect activated *ras* gene expression in human mammary and colon carcinomas. *Proc Natl Acad Sci USA* 1984; **81:** 5227–5231.
22. Chesa PG, Rettig WJ, Melamed MR, Old LJ, Niman HL. Expression of p21 *ras* in normal and malignant human tissues: Lack of association with proliferation and malignancy. *Proc Natl Acad Sci USA* 1987; **84:** 3234–3238.
23. Furth ME, Aldrich TH, Cordon-Cardo C. Expression of *ras* proto-oncogene proteins in normal human tissues. *Oncogene* 1987; **1:** 47–58.
24. Chen Z-Q, Ulsh LS, DuBois G, Shih T. Post-translational processing of p21 *ras* proteins involves palmitylation of the C-terminal tetrapeptide containing cysteine-186. *J Virol* 1985; **56:** 607–612.
25. Grand RJA, Smith KJ, Gallimore PH. Purification and characterisation of the protein encoded by the activated human N-*ras* gene and its membrane localisation. *Oncogene* 1987; **1:** 305–314.
26. Bizub D, Heimer EP, Felix A, *et al.* Antisera to the variable region of *ras* oncogene proteins, and specific detection of H-*ras* expression in an experimental model of chemical carcinogenesis. *Oncogene* 1987; **1:** 131–142.
27. Page DL, Dupont WD, Rogers LW, Rados MS. Atypical hyperplastic lesions of the female breast: a long term follow-up study. *Cancer* 1985; **55:** 2698–2708.